UNIVERSITY OF
KWAZULU-NATAL

INYUVESI
YAKWAZULU-NATALI

MOLECULAR ANALYSIS OF HIV-1 RESISTANCE: BIOSYNTHESIS, KINETIC, AND THERMODYNAMIC STUDY OF RESISTANT HIV-PROTEASE (C-SA) MUTANTS

November 2018

Sibusiso Bonginkosi Maseko

210552840

MOLECULAR ANALYSIS OF HIV-1 RESISTANCE: BIOSYNTHESIS, KINETIC, AND THERMODYNAMIC STUDY OF RESISTANT HIV-PROTEASE (C-SA) MUTANTS

2018

Sibusiso Bonginkosi Maseko

210552840

A thesis submitted to the School of Pharmacy and Pharmacology, College of Health Science, University of KwaZulu-Natal, Westville, for the degree of Doctor of Philosophy in Health Science (Pharmaceutical chemistry).

This is the thesis in which the chapters are written as a set of discrete research publications, with an overall introduction and final summary. Typically, most of the chapters would be published in internationally recognized, peer-reviewed journals.

This is to certify that the content of this thesis is the original research work of Sibusiso Bonginkosi Maseko
As the candidate's supervisor, I have approved this thesis for submission.

Supervisor: Signed: ----------Name: **Prof. H. G. Kruger** Date: 30/11/2018

Co-Supervisor: Signed: ----------Name: **Prof. J. Lin** Date: 30/11/2018

Co-Supervisor: Signed: ----------Name: **Dr. G. E. M. Maguire** Date: 30/11/2018

CONTENTS

DEDICATION

This thesis is dedicated to my mother Mrs P Maseko, mom you are the best.

ABSTRACT

During the past three decades, acquired immunodeficiency syndrome (AIDS) has become one of the major socioeconomic and worldwide health challenges. The notorious causative agent of AIDS, namely Human immunodeficiency virus (HIV) has been studied in many research institutions around the globe. The high replicative rate of the virus and recombination of a variety of viral strains complicate the treatment of AIDS. The viral protease (PR) is vital for the propagation of the virus; and thus, is a major target in antiviral therapy.

The efficacy of HIV-1 protease inhibition therapies is often compromised by the emergence of mutations in the protease molecule that reduces the binding affinity of inhibitors while maintaining viable catalytic activity and affinity for natural substrates. The large-scale production of PR has been a problem for scientists due to the “manufactured” enzyme’s cytotoxicity, low yield, insolubility, and lowered activity. Two recently discovered mutants of HIV-1 C-SA (South African subtype C), I36T↑T, and E35D↑G↑S showed almost the same catalytic activity as the wild type enzyme. The first aim of this study was to establish a more efficient procedure to express and recover HIV-1 protease (C-SA) from inclusion bodies. Furthermore, to study the interaction of nine FDA approved protease inhibitors with the two mutants using both quantitative and molecular techniques.

Optimization of HIV-1 PR expression by means of various vectors, fusion tags, solubilisation methods is reported in this study. Furthermore, the kinetics, inhibition, vitality values and thermodynamics of the mutants against the nine FDA approved

protease inhibitors (PIs) is reported. The study also reports necessary conditions to crystalize the variants for structure elucidation.

The highest expression of HIV PR was achieved when the pET32a vector (Trx tag) was employed. A total of 19.5 mg of fusion protein was refolded of which 5.5 mg of active protease was obtained after cleavage with a high specific activity of 2.81 µmoles/min/mg. Darunavir and nelfinavir exhibited the weakest binding affinity, 155- and 95- fold decreases respectively, towards the I36T↑T variant. The thermodynamic data showed less favourable Gibbs free binding energies for the protease inhibitors to this mutant than to the wild type. Nelfinavir and atazanavir were the weakest inhibitors against the E35D↑G↑S as seen from the IC_{50}, with values of 1401±3.0 and 685±3.0 nM respectively. Again, binding of all the drugs was less favourable for this mutant.

This study gives solutions to the difficulty faced when expressing HIV-1 protease. The study reported the best technique to recover HIV-1 protease from inclusion bodies as seen from the yield and specific activity. Insertion mutations in the I36T↑T mutant results in the protease being resistant to most the PIs. Again, the E35D↑G↑S double insertion was found to be multidrug resistant. With respect to the mutant (I36T↑T), APV, LPV and RTV should be prescribed to patients as they are more effective inhibitors. Only APV and RTV can still be prescribed for patients harbouring the E35D↑G↑S mutant. This calls for the design or modification of the current medicines to fight these drug resistant forms. Future studies will focus on the design and synthesis of new inhibitors for these mutants.

DECLARATION

I, Sibusiso Bonginkosi Maseko, declare that;

1. The research reported in this thesis, except where otherwise indicated, is my original work.
2. This thesis has not been submitted for any degree or examination at any other university.

3. This thesis does not contain other persons' data, pictures, graphs or other information, unless specifically acknowledged as being sourced from other persons.

4. This thesis does not contain other persons' writing, unless specifically acknowledged as being sourced from other researchers. Where other written sources have been quoted, then:

    a. Their words have been re-written, but the general information attributed to them has been referenced

    b. Where their exact words have been used, then their writing has been placed in italics and inside quotation marks and referenced.

5. This thesis does not contain text, graphics or tables copied and pasted from the internet, unless specifically acknowledged, and the source being detailed in the thesis and in the reference's sections.

A detail contribution to publications that form part and/or include research presented in this thesis is stated (including publications submitted, accepted, in press and published).

Sibusiso Bonginkosi Maseko

Signed:……

Date: 30/11/2018

LIST OF PUBLICATIONS

1. Optimized procedure for recovering HIV-1 protease (C-SA) from inclusion bodies

   Authors: **Sibusiso B Maseko**, Deidre Govender, Thavendran Govender, Tricia Naicker, Johnson Lin, Glenn E.M. Maguire, Gert Kruger

   Under review, The Protein Journal 29 October 2018

   Sibusiso B Maseko: Performed the experiments and wrote the paper

   Deidre Govender: Helped in some of the experiments for her training and wrote corresponding parts of the paper.

   Thavendran Govender, Tricia Naicker, Johnson Lin, Glenn E.M. Maguire and Gert Kruger supervised the project.

2. I36T↑T mutation in South African subtype C (C-SA) HIV-1 protease significantly alters protease-drug interactions. Biological Chemistry 05/2017; 398(10)., DOI:10.1515/hsz-2017-0107
   Published, Biological Chemistry

   Authors: **Sibusiso B Maseko**, Eden Padayachee, Thavendran Govender, Yasien Sayed, Gert Kruger, Glenn E.M. Maguire, Johnson Lin

   Sibusiso B Maseko: Performed the experiments and wrote the paper

   Eden Padayachee: Helped in some of the experiments and in writing the paper

Thavendran Govender, Yasien Sayed, Gert Kruger, Glenn E.M. Maguire, Johnson Lin and supervised the project

3. Kinetic and Thermodynamic Characterization of HIV-Protease inhibitors against E35D↑G↑S mutant in the South Africa HIV-1 Subtype C Protease**.**

Submitted, The Protein Journal 29 June 2018

Authors: **Sibusiso B Maseko**, Eden Padayachee, Thavendran Govender, Yasien Sayed, Glenn EM Maguire, Johnson Lin, Gert Kruger

Sibusiso B Maseko: Performed the experiments and wrote the paper

Eden Padayachee: Helped in some of the experiments and in writing the paper

Thavendran Govender, Yasien Sayed, Gert Kruger, Glenn E.M. Maguire, Johnson Lin and supervised the project

OTHER RELATED PUBLICATIONS

1. Investigation of the binding free energies of FDA approved drugs against subtype B and C-SA HIV PR: ONIOM approach. Journal of molecular graphics & modelling 06/2017; 76., DOI: 10.1016/j.jmgm.2017.06.026

Z.K. Sanusi, T. Govender, G.E.M. Maguire, **S.B. Maseko**, J. Lin, H.G. Kruger, B. Honarparvar

2. . Purification and Characterization of Exo-Inulinase from Paenibacillus sp. d9 Strain. The Protein Journal 12/2017; 37(3):1-12., DOI:10.1007/s10930-017-9752-8

S. Jeza, **S. B. Maseko**, J. Lin

3. An insight to the molecular interactions of the FDA approved HIV PR drugs against L38L↑N↑L PR mutant. Journal of Computer-Aided Molecular Design 02/2018; 32(27)., DOI:10.1007/s10822-018-0099-9

Zainab K. Sanusi, Thavendran Govender, Glenn E. M. Maguire, **Sibusiso B. Maseko**, Johnson Lin, Hendrik G. Kruger, Bahareh Honarparvar

4. Exploring the flap dynamics of the South African HIV subtype C protease in presence of FDA-approved inhibitors: MD study. Chemical Biology & Drug Design 07/2018; 92(5)., DOI:10.1111/cbdd.13364

Siyabonga I. Maphumulo, Amit K. Halder, Thavendran Govender, **Sibusiso Maseko**, Glenn E. M. Maguire, Bahareh Honarparvar, Hendrik G. Kruger

ACKNOWLEDGEMENTS

I firstly want to thank my Father in heaven for being with me every second of every day. Knowing that I'm never alone and that He'll help with whichever task I undertake, makes me work harder to make a success of the opportunities He gives me.

I want to thank my wonderful family for being supportive and always being there to listen to and encourage me when I needed it most.

I want to thank all my lab friends (Sphelele Jeza, Kayleen, Annie, Eniola, Deidre, Nokwanda, Ntokozo, Annie, Jimmoh) for creating a convivial lab atmosphere

I also want to thank my supervisors, Prof. Gert Kruger, Prof. Johnson Lin, Prof. Thavi Govender and Dr Glenn Maguire for their continuous support.

Last but not least, I would like to thank my special friend Miss Nozinhle Dlamini for her support and encouragement.

LIST OF ABBREVIATIONS

AIDS	Acquired Immune Deficiency Syndrome
APV	Amprenavir
ATV	Atazanavir
DRV	Darunavir
CRF	circulating recombinant forms
DNA	Deoxy ribonucleic acid
Gag	group-specific antigen
gp120	surface glycoprotein
gp41	trans-membrane glycoprotein
HIV	Human immune virus
IDV	Indinavir
IN	integrase
LPV	Lopinavir
Nef	negative regulatory factor
NFV	Nelfinavir
NNRTIs	non-nucleoside reverse transcriptase inhibitors

NRTIs	nucleoside reverse transcriptase inhibitors
PI	Protease Inhibitors
Rev	regulator of virion protein expression
RNA	ribonucleic acid
RT	reverse transcriptase
RTV	Ritanavir
SQV	Saquinavir
TNF	tumor necrosis factor
TPV	Tipranavir
Vpr	viral protein R
Vpu	viral protein U

LIST OF FIGURES

Chapter one

Chapter Two

Chapter Four

Chapter 5

LIST OF TABLES

Chapter 1

Chapter 2

Chapter 3

Chapter 4

CHAPTER ONE

General Introduction and Overview

1.1 Background

During the past three decades, Acquired Immunodeficiency Syndrome (AIDS) has had a profound influence on socioeconomic and worldwide health challenges[1]. The Human Immunodeficiency Virus (HIV) which is the virus that causes AIDS has been broadly studied throughout many research institutions around the globe [2]. Research into genotypic characterization of the virus and antiretroviral (ARV) drug development are in are at the forefront of progress against this illness. Studying the virus at this molecular level is a prerequisite and knowledge acquired from various studies has aided in drug development [3]. There are approximately 35 million people living with the virus and 71% are in sub-Saharan Africa [4]. In South Africa, a population of about 7.1 million persons are living with HIV/AIDS with the province of KwaZulu-Natal having the highest prevalence [5]. Amid long-term treatment, statistics on ARV are inadequate. In addition, statistics from sub-Saharan countries are further inadequate due to the cost of HIV research studies and numerous socioeconomic hurdles [6, 7]. This results in a heavy health burden, since many reports on drug resistance and genetic variation of HIV are increasing [8]. Figure 1 illustrate the live cycle of HIV-1 and as well as the major ART target areas.

Reverse transcription of the viral genetic material (RNA) to DNA by the enzyme viral reverse transcriptase (RT) is required for the virus to thrive within a human host (Figure 1). Mutations present themselves often within the viral proteins which are antiviral drug

targets, due to the inability of RT enzymes to proof-read effectively and the elevated replication rate of HIV.

Therefore, challenges to manufacture effective antiviral compounds continue to escalate [9].

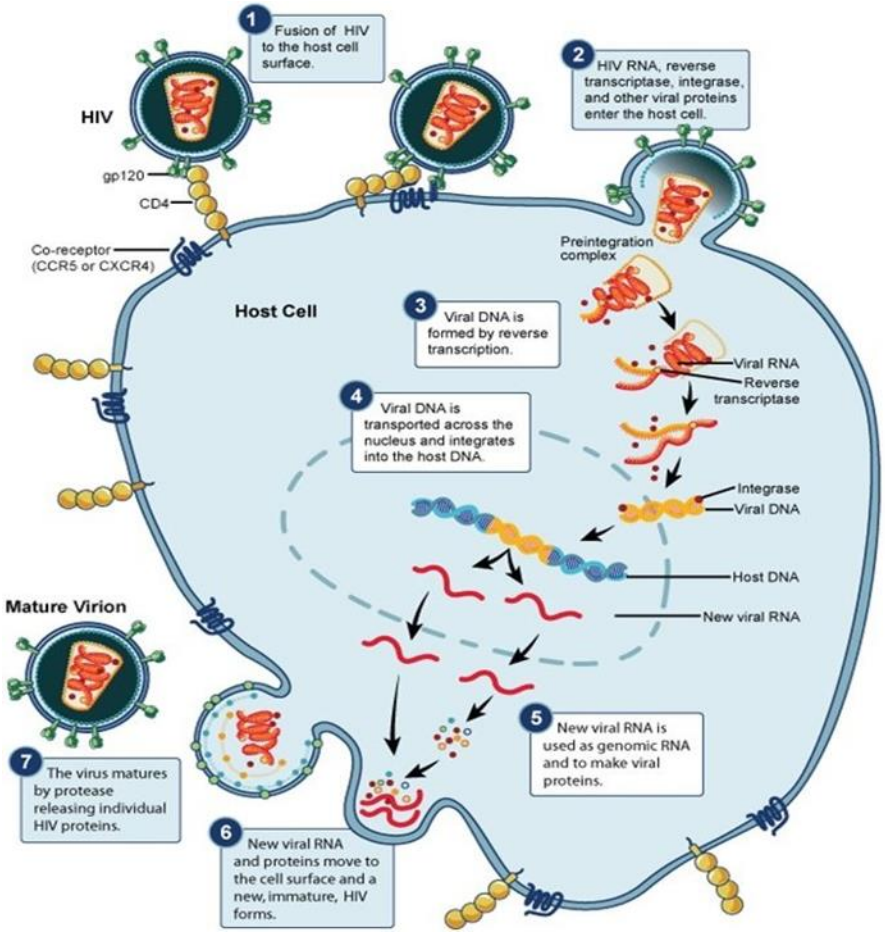

Figure 1: The HIV life cycle and the major targets of HIV-1 drug therapy. Stages in the life cycle are number 1-7 [10]. (Open access)

Presently, there are six classes of anti-HIV drugs, namely; non-nucleoside RT inhibitors (NNRTIs), nucleoside RT inhibitors (NRTIs), protease inhibitors (PIs), integrase inhibitors, fusion inhibitors and entry inhibitors. Both RT and PIs are favoured in treatment administrations and wide-ranging data are accessible which encompasses drug

resistance profiles of each therapeutic [4, 11]. Information regarding novel classes of inhibitors are lacking but diminished efficacies due to drug resistance mutations (DRMs) appear to be imminent. Attempts to generate a potent HIV vaccine are in the pipeline and in the interim, major studies on HIV epidemiology are dependent on the data from RT and PIs. Essentially, compared to other classes of ART, greater mutations are selected in response to PIs [12]. Proteases, including HIV-1 are encoded on the viral *pro* gene for all retroviruses.[13]. Along the replication cycle of HIV, gene products *gag* and *gag-pol* are translated as polyproteins [14, 15]. Thereafter, the virally encoded protease processes these proteins to obtain both structural proteins and crucial viral enzymes such as the protease itself [16, 17].

For almost 20 years, numerous studies on the structure and activity of HIV protease, protease drug-resistant variants and its interactions with inhibitors have been pursued. One ultimate goal is to eradicate the challenge of ever increasing HIV drug resistance [18]. Approximately 25 differing antiretroviral drugs (ARVs) are presently employed to combat HIV and AIDS [19]. The current prescribed AIDS therapy employs a cocktail of drugs from varying classes in what is termed a highly active antiretroviral therapy (HAART) [20]. The HIV protease serves as a target to nine of the 25 drugs. These drugs belong to the previously stated class of protease inhibitors [21]. The study focuses more on HIV-1 protease and its inhibition, these are discussed in detail in the following sections.

1.2 HIV Protease and Inhibition [9, 16, 20]

HIV-1 protease is normally a homo dimeric protein with 99 amino acids per monomer (Figure 2). The protease is responsible for an autoproteolytic release of the protease from the gag-pol fusion precursor protein and a subsequent processing of the gag and

pol proteins to yield the viral structural proteins. This makes the enzyme a major target for HIV therapy. A ribbon structure of the enzyme is shown in figure 2.

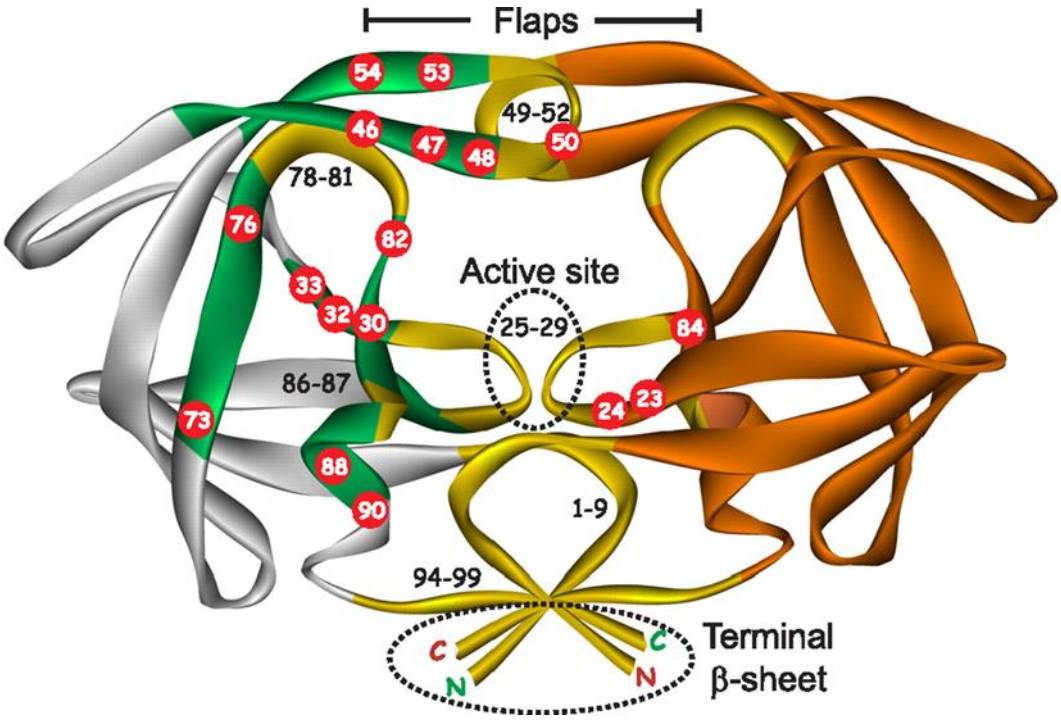

Figure 2: Structure of HIV-1 protease indicating the positions of extremely conserved regions (gold and black lettering), regions of natural variability in protease among the HIV-1 groups (M,N,O,and P (gray), and naturally conserved regions where key drug resistant mutations (DRMs) are selected under drug pressure (green). Numbered red circles indicate the positions of major DRMs [22]. (open access)

In 1995, when therapy became an option to use drugs to block the viral enzymes, protease and transcriptase, the initial PI emerged into clinical practice [11]. Incorporating PIs into antiviral therapy resulted in primary clinical advantages which include; extensive viral suppression, control and decreased morbidity and mortality for HIV infected individuals [23]. Inspired by the efficacy of the antiviral PIs, more studies were evoked to produce the next generation of inhibitors [18]. Unfortunately, the rise of drug resistance to PIs impaired the effectiveness of the therapeutic measures against HIV infections [24].

Novel HIV infections that convey drug resistant viruses into drug naïve patients reduce antiviral options and therefore the management of HIV infection is complex [10-12]. More mutations are provoked by PIs compared to any other class of ARV, due to their use over the years. Within the PI class, drug resistance results in cross resistance to other drugs. The number of mutations and the type of mutation induced by PI determines the extent of cross resistance [13].

Currently, ritonavir is employed as a pharmokinetic booster alone. Ritanavir is responsible for boosting lopinavir/r, atazanavir/r, amprenavir/r and saquinavir/r which have poor pharmacokinetics and poor availability and are used as a first line therapy against HIV infection. Unboosted nelfinavir, atazanavir and amprenavir are subprime alternative selections for first line treatment [25]. Recovery therapy for drug resistant mutants makes use of boosted lopinavir/r, tipranavir/r and darunavir/r. Despite ritanavir boosted PIs, mutations still arise, and a PI may not be clinically effective due to their presence. With regards to these challenges, it is imperative to study the mechanism of PI drug resistance at a molecular level. The acquired knowledge could be a tool to design the next generation of inhibitors with enhanced efficacy against not only the wild-type HIV but also against drug resistant strains [18]. A summary of the nine FDA inhibitors is shown in Table 1. Table one also shows common mutations and common side effects that normally arise when these PIs are employed.

Table 1: Summary of common major drug resistant mutations and side effects that arise from the use of PIs [26-31].

Protease Inhibitor	Major Drug resistant mutations	Common Side Effect
Atazanavir	I50V, I84V and N88S	Nausea, Diarrhoea, rash, stomach ache, lipodystrophy, liver toxicity diabetes, liver function, hyperbilirubinemia, headache, insomnia, vomiting, heartburn
Darunavir	I47V, I50V, I54ML, L76V and I84V	Diarrhoea, Nausea, rash, stomach pain, vomiting, headache, fever, lipodystrophy, liver toxicity, diabetes
Lopinavir	V32I, I47VA, L76V, and V82AFTS	Lipodystrophy raised liver enzymes, nausea, vomiting, abdominal pa vomiting, heartburn, raised lipids, liver toxicity,
Ritonavir	Now rarely given as sole inhibitor.	Raised lipid levels
Tipranavir	I47V, Q58E, I74P, V82LT, N83D, and I84V	Nausea, diarrhoea, vomiting, abdominal pain, tiredness,Headache, fever, lipid increases, flatulence, liver, abnormalities, rash, lipodystrophy, diabetes, liver toxicity
Amprenavir	I50V and I84V	Burning or prickling sensation in arms or legs, fatigue, dry or itchy skin, increased thirst, increased hunger, increased urination, increased cholesterol and triglycerides
Indinavir	M46IL, V82AFT, and I84V	Blood in the urine, sharp back pain just below the ribs
Nelfinavir	D30N, L90M	Diarrhoea, Intestinal gas, redistribution or accumulation of body fat
Saquinavir	G48V, L90M	Diarrhoea, nausea, vomiting, stomach pain, or tiredness

With so much that has been said about the viral enzymes, recent focus has been directed towards the capsid as a new target for ART. A novel capsid-targeting HIV drug was recently reported at a scientific meeting [32]. The new drug, GS-CA1, has shown highly antiviral potency in human peripheral blood mononuclear cells (EC_{50} = 140 pM) and is

effective against all HIV classes. The drug is reported to be effective for up to 10 weeks, and clinical trials are reported to start in 2018 [33].

Two mutants of the HIV-1 South African subtype C (C-SA) were recently discovered [26]. The mutants did not respond well to all available protease inhibitors however, they responded to the subsequent reverse transcriptase inhibitors (RTIs): efavirenz, d4t (stavudine) and 3TC (lamivudine). This study encompasses these mutants in order to assess their functional characteristics for therapeutic measures. The first mutant possesses a single amino acid substitution, and an insertion at position 36, *i.e.* I36T↑T, with respect to the wild-type HIV-1 C-SA protease. The other mutant comprise of 101 amino acid residues per monomer and is designated as E35D↑G↑S (the upward arrows preceding an amino acid indicate that glycine and serine are inserted in position 35, respectively) [34].

1.3 Cloning, Expression, Purification, and Characterization of Proteins [26, 27, 29]

The preparation of many identical DNA molecules comprising fragments from various sources lies at the core of recombinant DNA technology [35]. The formation of such molecules, called recombinant molecules, involves the incorporation of the sequence of interest into a vector capable of replication upon introduction into a host cell. When the vector replicates within the host, so too does the sequence of interest (the insert). Gene expression can result in protein production [36]. This occurs after DNA has been transcribed to messenger RNA (mRNA) [37], which is then translated into polypeptide chains. These undergo post-translational modification, giving rise to proteins [38]. Proteins are usually the targets of drug design. To study the drug-protein interactions or

just the characterization of a protein, it must be free from contaminants. This brings forth the need for thorough purification. The purification of proteins involves a series of processes to separate one or a few proteins from a complex mixture, usually cells, tissues or whole organisms [39]. Chromatographic techniques are normally used to achieve this. Depending on the nature of the protein one can decide which method to use [40]. After purification the protein of interest must be characterized. Protein characterization involves creating a fingerprint or profile of a protein's physical, biological, and chemical properties [41]. In recombinant DNA technology biological properties are used to characterize the protein (usually an enzyme) [42]. One major aspect of drug discovery is to understand enzyme kinetics. This makes it easier to synthesize or design drugs. Enzyme kinetics, inhibition and thermodynamics is discussed in detail in the following section.

1.4 Kinetics and Thermodynamics [43, 44]

One of the most important features of enzymology is enzyme catalysis [43]. Fast reaction rates and specificity are characteristics of enzyme catalysis. Enzyme specificity is defined as catalysis of unique or reactants by the enzyme while disregarding others. In principle, enzymes (like most other catalysts) are responsible for lowering the Gibbs energy of activation by reducing the number of degrees of freedom of the reaction [45]. An intermediate is formulated with the reactants in the first step (pre-complex) in which the reactants are pre-organized in such a privileged position so that the rate of effective collisions is increased, followed by the release of the product(s). Despite the catalytic mechanisms and kinetic energetics of the reaction, an enzyme cannot affect the relative enthalpies or the Gibbs energies for the reactants and products. Only the rate of reaction

is increased until equilibrium, however the thermodynamic equilibrium constant is not affected. The equations used in enzyme kinetics are discussed in detail next.

1.5. Enzyme Inhibition [34, 46]

Many drugs are designed to block/inhibit enzymes and help stop disease progression. Inhibition decreases the rate of enzyme catalysed reactions. Inhibitors are classified as either reversible or irreversible [47]. For reversible inhibition, an equilibrium occurs between the enzyme and the inhibitor. On the other hand, irreversible inhibition increases progressively over time. The focus in this study is reversible inhibition as the FDA approved protease inhibitors are employ this mechanism of action. Reversible inhibition is further divided into three categories, competitive, non-competitive, and uncompetitive (Figure 3) [48]. These are defined in terms of Michaelis-Menten equation as follows:

Competitive

$V_0 \quad \frac{Vmax[S]}{Km\left(1+\frac{I}{Ki}\right)+[S]}$ (only K_m changes) (equation 1)

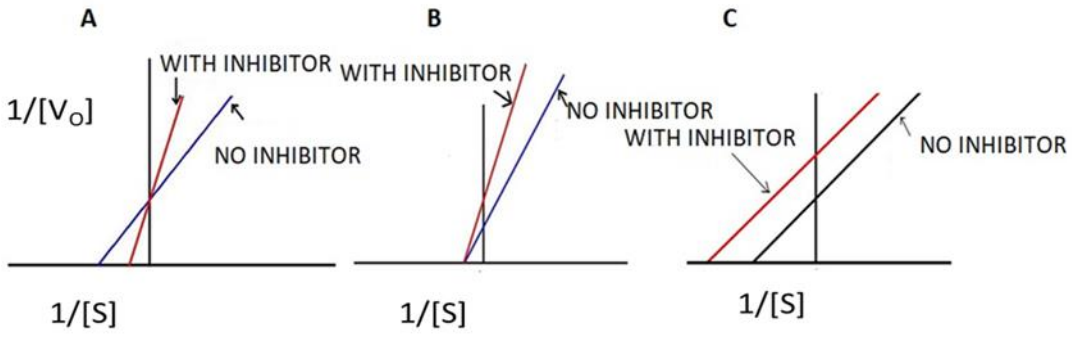

Figure 3: Illustration of reversible Enzyme inhibition. A, Competitive, Non-competitive and C Uncompetitive inhibition.

Non-competitive

$$V_0 = \frac{Vmax}{\frac{(1+\frac{I}{Ki})}{Km+[S]}}[S] \qquad (V_{max} \text{ changes}) \qquad \text{(equation 2)}$$

Uncompetitive

$$v_0 = \frac{\frac{v_{max[S]}}{\left(1+\frac{I}{K_I}\right)}}{\frac{K_M}{1+\frac{1}{K_I}}} + [S] \qquad \text{Both } V_{max} \text{ and } K_m \text{ changes} \qquad \text{(equation 3)}$$

The next sections discuss the techniques used in enzymology. The section gives deeper insight on both quantitative and molecular techniques used to study protein-protein, or protein drug interactions.

1.6 Techniques used in Enzyme Kinetics and Inhibition[42, 45, 41, 45]

There are various techniques that have been developed over the years for enzyme kinetics and inhibition studies. Scientists often look for easy, quick, sensitive, reliable techniques when doing this type of research. The most conventional technique employed is through the use light, *i.e.* Spectrophotometers or spectrofluorimeters. Further to that, more modern techniques include Isothermal Titration Calorimetry (ITC), Surface Plasmon Resonance (SPR), and Microscale Thermophoresis (MST).

1.6.1 Spectrophotometry/Spectrofluorimetry[42,44]

Spectrophotometry can be used to determine enzyme kinetics and inhibition. The enzyme is mixed with the substrate or drug, formation of products usually give rise to a change in the absorbance signal. During inhibition, in many examples, the enzyme-substrate interactions renders a decrease in absorbance. The decrease is monitored with increasing drug concentration from which the inhibition constant K_i is determined [49]. The inhibition constant is the linked to the Gibb's free energy by equation 11:[48]

$$\Delta G = -RT\ln K_i \qquad \text{(equation 4)}$$

Fluorescence quenching is also used to study the interaction of biomolecules in solution. It can be defined as a process which reduces the fluorescence intensity of a given molecule. Various number of processes can lead to quenching, these include: excited state energy transfer, complex formation and collision between enzyme and substrate. Fluorescence data can be evaluated using the Stern-Volmer equation,

$$F_0/F = 1 + K_q \tau o[Q] = 1 + K_{sv}[Q] \qquad \text{(equation 5)}$$

Where F_0 and F are the fluorescence signals with and without a quencher (Q) respectively. K_q is the quenching rate constant of the bio-molecule, K_{SV} is the Stern-Volmer quenching constant, and τo (10^{-8} s) is the average lifetime of the fluorescent substance without any quencher. When small molecules bind independently to a set of equivalent sites on a macromolecule, the equilibrium between free and bound molecules is given by the equation:

$$\log[(F_0-F)/F] = \log K_b + n\log[Q] \qquad \text{(equation 6)}$$

Where K_b an n are the binding constant and number of binding sites respectively. The thermodynamic parameters existing in the system can be determined using the Van't Hoff equation:

$$\ln K_b = (\Delta H/RT) + (\Delta S/R) \quad \text{(equation 7)}$$

Here, K is analogous to the Stern Volmer quenching constant K_{sv} at corresponding temperature. A plot of lnK vs 1/T enables the determination of the thermodynamic parameters (ΔH and ΔS) from slopes and intercepts respectively. The Gibs' free energy can the determined from the relationship:

$$\Delta G = \Delta H - T\Delta S. \quad \text{(equation 8)}$$

Even though fluorescence is still widely used, it is now rapidly being replaced by more sensitive techniques such as ITC, MST and SPR.

1.6.2 Isothermal Titration Calorimetry (ITC) [50]

Researchers have been using this technique to determine binding affinities (K_d),binding stoichiometry (n) and enthalpy changes (ΔH) of the interaction between two or more molecules in solution [50]. This is then used to calculate the other thermodynamic parameters, Gibbs's free energy (ΔG) and change in entropy (ΔS) from the relationship [51]: Figure 4 shows the graphical presentation of ITC and a typical ITC experiment.

$$\Delta G = -RT\ln K_a$$

$$\Delta G = \Delta H - T\Delta S$$

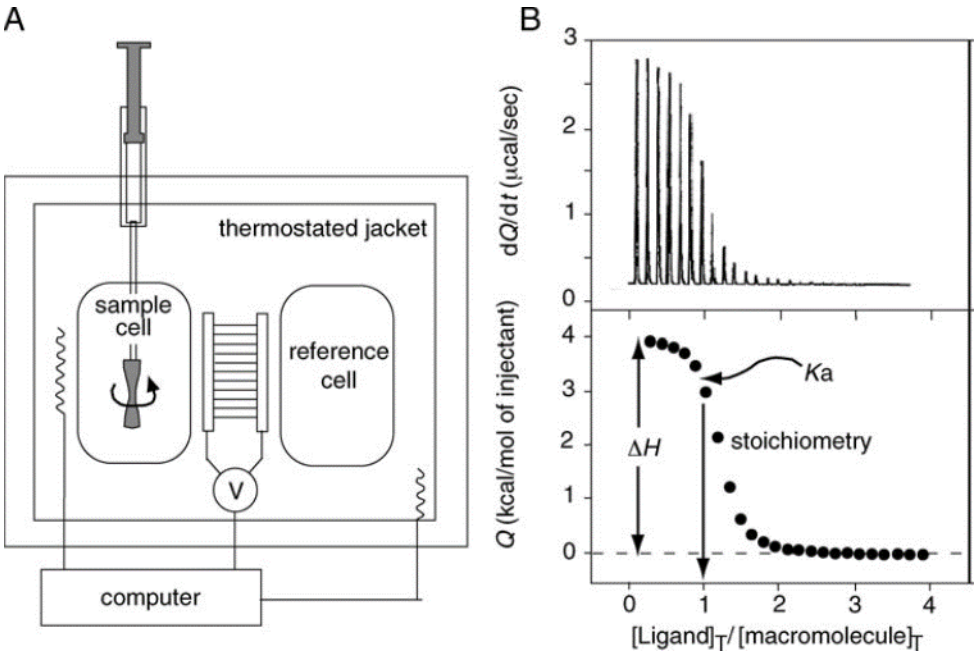

Figure 4: (**A**) Schematic presentation of the ITC instrument. (**B**) Example of a typical ITC binding experiment [41]. (open access)

Another label free technique used to assess binding of ligands to analytes (proteins) is Surface Plasmon Resonance. This discussed in detail in the next section.

1.6.3 Surface Plasmon Resonance Spectroscopy (SPR)[41, 42, 43]

In the field of drug discovery, SPR is a powerful technique as it is primarily used to study ligand binding interactions with proteins [52, 53]. The technique is free from labelling and permits measurement of real time quantitative binding affinities and kinetics for proteins associated with ligand molecules [54]. SPR employs an optical protocol for the measurement of an alteration in refractive index of the medium near a metal surface. This technique involves the generation of surface plasmons on thin metal films and the internal reflection of light at a surface solution to generate an electromagnetic film or an evanescent wave that expands a short distance (approximately 300 nm) into the solution (see Figure 5). BIAcore™ technology are the major developers of SPR.

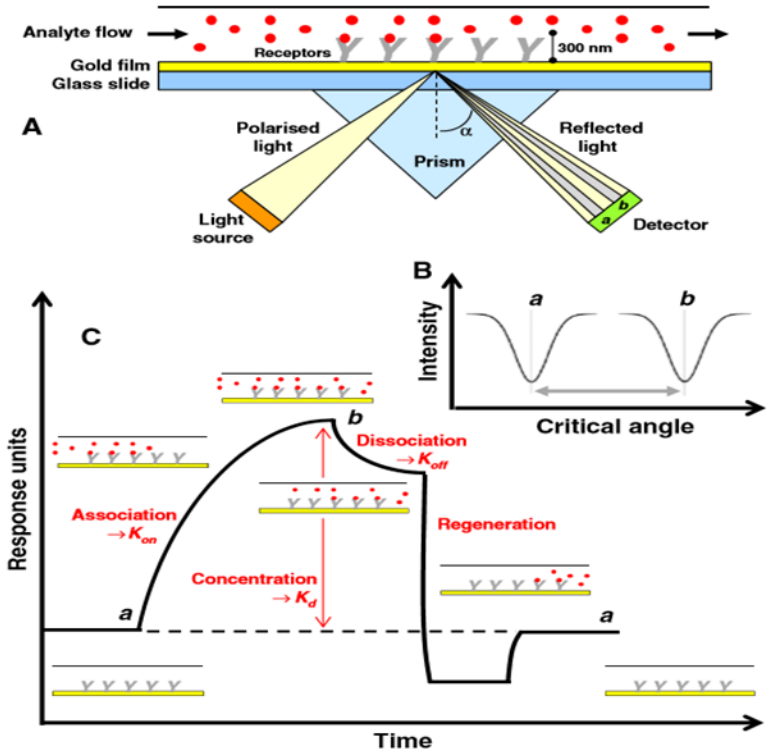

Figure 5: Graphical presentation of the basic SPR for determining the interaction of an analyte to a receptor molecule. A, SPR experimental set up based on BIAcore™ technology, B, and C , Typical binding experiment in SPR [54]. (Open access)

As mentioned before both SPR and ITC are label free. In Microscale Thermophoresis the analyte must have a fluorescent label. This is discussed in the next section.

1.6.4 Microscale Thermophoresis (MST)[44 ,45]

MST functions by measuring biomolecular interactions quantitatively and is centred on the direct movement of small molecules within a temperature gradient (thermophoresis) The movement is dependent on the charge, size, conformation, or hydration shell of the

molecule. Therefore, it has been described as the most sensitive technique employed thus far. The technique involves an infrared laser that stimulates a temperature gradient. The assigned movement of the molecules through a temperature gradient is monitored and quantified via the attachment of fluorophores (Figure 6) [55].

Within MST experiments, the change in temperature, ΔT in space conduces to the deficiency of solvated biomolecules in the domain of increased temperature, measured by the Soret coefficient S_T: $C_{hot}/C_{cold} = \exp(-S_T \Delta T)$. With constant buffer conditions, thermophoresis examines the size, charge and solvation entropy of the molecule. The change in temperature of protein and protein-ligand varies significantly [56], due to the ligand impelling changes in size, charge and solvation energy. The advantage of MST is that despite the insignificant alteration of size or charge of protein by ligand binding, it can monitor the binding-induced changes in the solvation entropy [55]. Furthermore, MST allows rapid and quick analysis of high affinity interactions with K_{ds} down to 1 pM and can be used as an analysis tool for binding modes, stoichiometries and protein folding and unfolding [57].

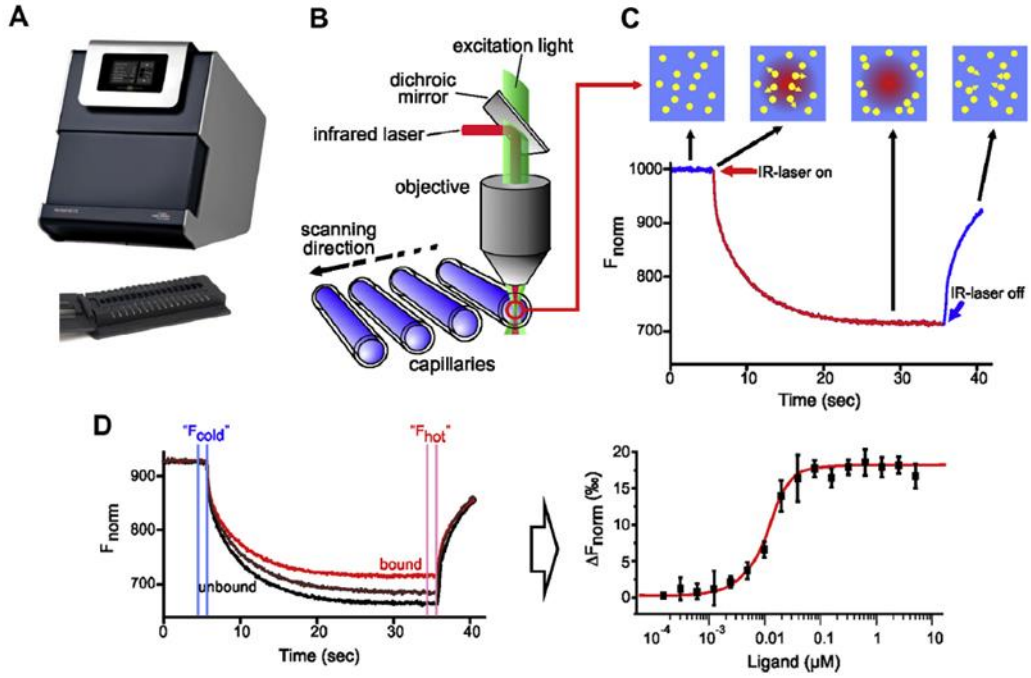

Figure 6: Graphical illustration of MST instrumentation and experiment. A, MST instrument, B, An illustration of MST optics. A model of MST signal. D, A presentation of MST binding experiment [57] (open access).

All the techniques discussed thus far fall under quantitative analysis. The next sections will focus on molecular analysis. A brief overview of two techniques under molecular techniques, Protein crystallography and Nuclear Magnetic Resonance Spectroscopy (NMR) are presented next.

1.7 Protein Crystallography [58, 59]

X-ray crystallography is the main method used to solve the 3D structure of proteins. X-ray was discovered by Wilhen Conrad Rontager in 1895 [55]. The first 3D structure of was solved using this technique in 1958. X-ray crystallography accounts for 87 % of protein 3D structures reported so far [56]. The steps in protein crystallography are illustrated in figure 7. Although crystallography of proteins is well understood, it still difficult to predict conditions in which a protein will crystalize. Thus, the approach is still

to coarse-screen a wide range of chemical conditions such as buffer type, temperature, pH, protein concentration (normally 3 to 20 mg/ml), detergents if , precipitants (organic solvents, salts, and polymers), presence or absence of divalent cations, and additives, in the hope of obtaining a few hits [60]. Screens are also available commercially, where 96 conditions are available in a 96 well plate format. Recently there have been advances where by crystallization robots are used aliquot nanolitre volumes into crystallization trays. The trays are then kept at constant temperatures where images are taken daily by crystal recognition software. Current 3rd generation synchrotron sources together with quick and reliable X-ray detectors has revolutionized macromolecular crystallography for the collection of diffraction data. The availability of software such as Collaborative Computational Project Number 4 (CCP4) and PHENIX [61, 62] now help in solving structures from data reduction through phasing and electron density map calculation, map interpretation, structure refinement and even depositing to PDB (Protein Data Bank) [60]. Crystallography is very important in the design of new protease inhibitors (structure based design) [63]. Protein crystallography remains the most widely used technique for structural elucidation.

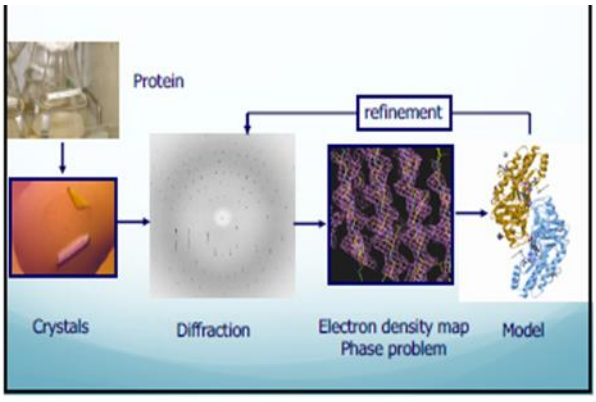

Figure 7: Steps in protein X-ray structure elucidation [60]

The section below discusses the other technique used in molecular analysis of proteins.

1.8 Protein Labelling and NMR Spectroscopy [59, 60, 61, 62, 63]

Labelling of proteins with isotopes is a very important way to simplify overlapped spectra by either diluting the NMR active nuclei or allowing the resonances to be separated in multiple dimensions. ^{15}N labelling of proteins is the easiest and most cost-effective form of protein labelling. This is achieved by expressing the proteins bacteria grown in minimal media, with ^{15}N NH_4Cl or $NH_4(SO4)_2$ as the sole nitrogen source [64, 65]. Spectra of the proteins prepared this way are then recorded using a standard solution-NMR HSQC (heteronuclear single quantum coherence**)** experiment. An HSQC experiment is a 2D experiment which was first described as ^{1}H to ^{15}N system but also involves ^{1}H and ^{13}C [66]. It involves the transfer of magnetization from the proton to the second nucleus (^{13}C or ^{15}N). In this type of experiment protein folding can be assessed [67]. Furthermore, if the protein is comparatively small, less than 150 amino acids, the ^{1}H and ^{15}N NOESY and ^{15}N-TOCSY experiments can be used to assign the backbone resonances [68]. ^{15}N labelled proteins are also used for titration with ligands or other protein with which it forms complexes [69]. This is useful as kinetic parameters (inhibition constants) and thermodynamics of the inhibitor can be determined. This is useful as it helps researchers to modify the ligands in cases of drug resistant mutations. This makes ^{15}N labelling and NMR spectroscopy a powerful tool in pharmaceutical research

1.9 Aims and Objectives

The overall aim of this study was to establish a more efficient procedure to express and recover South African Subtype C (C-SA) HIV-1 Protease from inclusion bodies. Furthermore, to study the interaction of nine FDA approved protease inhibitors with the two mutants using both quantitative and molecular techniques.

1. Introductory background of the study.
2. To optimize the expression, solubilization, recovery of HIV-1 protease from inclusion bodies by exploring the use of different fusion tags and solubilization methods.
3. To assess the effect of the I36T↑T mutant on protease inhibitor binding, by means of enzyme kinetics, inhibition and fluorescence quenching.
4. To assess the effect of the E35D↑G↑S mutant on protease inhibitor binding, by means of enzyme kinetics, inhibition and fluorescence quenching.
5. To find necessary conditions crystalize the mutants optimize expression in ^{15}N minimal media
6. Overall conclusion of the research outcome.

1.10 Thesis Outline

The thesis is presented in a paper format in which each chapter is dedicated to addressing one or two research questions. In the first and the last chapters, a general introduction and an overall conclusion are provided, respectively, for the entire study. The outline is therefore highlighted.

Chapter 1: Introductory background, and where the main direction of the study is highlighted.

Chapter 2: Optimized procedure for recovering South African Subtype C (C-SA) HIV-1 Protease from inclusion bodies.

Chapter 3: I36T↑T Mutation in South African Subtype C (C-SA) HIV-1 Protease Significantly Alters Protease-Drug Interactions

Chapter 4: Kinetic and Thermodynamic Characterization of HIV-Protease inhibitors against E35D↑G↑S mutant in the South Africa HIV-1 Subtype C Protease.

Chapter 5: Crystallization and ^{15}N labelling of the Wildtype and the two Mutant HIV-1 Proteases for Structural Studies

Chapter 6: Overall conclusion on the research outcome

1.11 References

1. Tellier, S., et al., *Basic Concepts and Current Challenges of Public Health in Humanitarian Action*, in *International Humanitarian Action*. 2018, Springer. p. 229-317.
2. Ssemwanga, D., et al., *Update on HIV-1 acquired and transmitted drug resistance in Africa*. 2015.
3. Naicker, P. and Y. Sayed, *Non-B HIV-1 subtypes in sub-Saharan Africa: impact of subtype on protease inhibitor efficacy.* Biological chemistry, 2014. **395**(10): p. 1151-1161.
4. Organization, W.H., *Global update on HIV treatment 2013: results, impact and opportunities.* 2013.
5. UNAIDS., *http://www.unaids.org/en/regionscountries/countries/southafrica.* 2017.
6. Barth, R.E., et al., *Virological follow-up of adult patients in antiretroviral treatment programmes in sub-Saharan Africa: a systematic review.* The Lancet infectious diseases, 2010. **10**(3): p. 155-166.
7. Nucita, A., et al., *A global approach to the management of EMR (electronic medical records) of patients with HIV/AIDS in sub-Saharan Africa: the experience of DREAM software.* BMC medical informatics and decision making, 2009. **9**(1): p. 42.
8. Resch, S., et al., *Economic returns to investment in AIDS treatment in low and middle income countries.* PloS one, 2011. **6**(10): p. e25310.
9. Wright, C.F., et al., *Beyond the consensus: dissecting within-host viral population diversity of foot-and-mouth disease virus by using next-generation genome sequencing.* Journal of virology, 2011. **85**(5): p. 2266-2275.
10. Mbogo, R., *Intra-Host stochastic models for HIV dynamics and management*. 2013.
11. De Clercq, E., *Anti-HIV drugs: 25 compounds approved within 25 years after the discovery of HIV.* International journal of antimicrobial agents, 2009. **33**(4): p. 307-320.
12. Shafer, R.W. and J.M. Schapiro, *HIV-1 drug resistance mutations: an updated framework for the second decade of HAART.* AIDS reviews, 2008. **10**(2): p. 67.
13. Kohl, N.E., et al., *Active human immunodeficiency virus protease is required for viral infectivity.* Proceedings of the National Academy of Sciences, 1988. **85**(13): p. 4686-4690.
14. Robins, T. and J. Plattner, *HIV protease inhibitors: their anti-HIV activity and potential role in treatment.* JAIDS Journal of Acquired Immune Deficiency Syndromes, 1993. **6**(2): p. 162-170.
15. Hellen, C.U., H.G. Kraeusslich, and E. Wimmer, *Proteolytic processing of polyproteins in the replication of RNA viruses.* Biochemistry, 1989. **28**(26): p. 9881-9890.
16. Park, J.H., et al., *Binding of Clinical Inhibitors to a Model Precursor of a Rationally Selected Multidrug Resistant HIV-1 Protease Is Significantly Weaker Than That to the Released Mature Enzyme.* Biochemistry, 2016. **55**(16): p. 2390-2400.
17. Moyer, C.L., E.S. Besser, and G.R. Nemerow, *A Single Maturation Cleavage Site in Adenovirus Impacts Cell Entry and Capsid Assembly.* Journal of virology, 2016. **90**(1): p. 521-532.

18. Weber, I.T. and J. Agniswamy, *HIV-1 protease: structural perspectives on drug resistance.* Viruses, 2009. **1**(3): p. 1110-1136.
19. Flexner, C., *HIV drug development: the next 25 years.* Nature Reviews Drug Discovery, 2007. **6**(12): p. 959-966.
20. Ferradini, L., et al., *Scaling up of highly active antiretroviral therapy in a rural district of Malawi: an effectiveness assessment.* The Lancet, 2006. **367**(9519): p. 1335-1342.
21. Mastrolorenzo, A., et al., *Inhibitors of HIV-1 protease: current state of the art 10 years after their introduction. From antiretroviral drugs to antifungal, antibacterial and antitumor agents based on aspartic protease inhibitors.* Current medicinal chemistry, 2007. **14**(26): p. 2734-2748.
22. Louis, J.M., et al., *Inhibition of autoprocessing of natural variants and multidrug resistant mutant precursors of HIV-1 protease by clinical inhibitors.* Proceedings of the National Academy of Sciences, 2011. **108**(22): p. 9072-9077.
23. Gazzard, B., *British HIV Association guidelines for the treatment of HIV-1-infected adults with antiretroviral therapy 2008.* HIV medicine, 2008. **9**(8): p. 563-608.
24. Wainberg, M.A. and G. Friedland, *Public health implications of antiretroviral therapy and HIV drug resistance.* Jama, 1998. **279**(24): p. 1977-1983.
25. Naggie, S. and C. Hicks, *Protease inhibitor-based antiretroviral therapy in treatment-naive HIV-1-infected patients: the evidence behind the options.* Journal of Antimicrobial Chemotherapy, 2010. **65**(6): p. 1094-1099.
26. Chetty, S., et al., *Multi-drug resistance profile of PR20 HIV-1 protease is attributed to distorted conformational and drug binding landscape: molecular dynamics insights.* J Biomol Struct Dyn, 2016. **34**(1): p. 135-51.
27. Aoki, M., et al., *Mechanism of Darunavir (DRV)'s High Genetic Barrier to HIV-1 Resistance: A Key V32I Substitution in Protease Rarely Occurs, but Once It Occurs, It Predisposes HIV-1 To Develop DRV Resistance.* mBio, 2018. **9**(2): p. e02425-17.
28. Karade, S., et al., *HIV drug resistance following a decade of the free antiretroviral therapy programme in India: A review.* International Journal of Infectious Diseases, 2018. **66**: p. 33-41.
29. Wensing, A.M., et al., *2017 Update of the Drug Resistance Mutations in HIV-1.* Topics in antiviral medicine, 2017. **24**(4): p. 132-133.
30. Wensing, A.M., N.M. van Maarseveen, and M. Nijhuis, *Fifteen years of HIV Protease Inhibitors: raising the barrier to resistance.* Antiviral research, 2010. **85**(1): p. 59-74.
31. Agbowuro, A.A., et al., *Proteases and protease inhibitors in infectious diseases.* Medicinal research reviews, 2017.
32. Tse, W., et al. *Discovery of novel potent HIV capsid inhibitors with long-acting potential*. in *Conference on Retroviruses and Opportunistic Infections*. 2017.
33. Carnes, S.K., J.H. Sheehan, and C. Aiken, *Inhibitors of the HIV-1 capsid, a target of opportunity.* Current Opinion in HIV and AIDS, 2018. **13**(4): p. 359-365.
34. Maseko, S.B., et al., *Purification and characterization of naturally occurring HIV-1 (South African subtype C) protease mutants from inclusion bodies.* Protein expression and purification, 2016. **122**: p. 90-96.

35. Botstein, D., et al., *Sterile host yeasts (SHY): a eukaryotic system of biological containment for recombinant DNA experiments.* Gene, 1979. **8**(1): p. 17-24.
36. Kallioniemi, O.P., et al., *Association of C-erbB-2 protein over-expression with high rate of cell proliferation, increased risk of visceral metastasis and poor long-term survival in breast cancer.* International journal of cancer, 1991. **49**(5): p. 650-655.
37. Childs, G., R. Maxson, and L.H. Kedes, *Histone gene expression during sea urchin embryogenesis: Isolation and characterization of early and late messenger RNAs ofStrongylocentrotus purpuratus by gene-specific hybridization and template activity.* Developmental biology, 1979. **73**(1): p. 153-173.
38. Jacobson, M.F. and D. Baltimore, *Polypeptide cleavages in the formation of poliovirus proteins.* Proceedings of the National Academy of Sciences of the United States of America, 1968. **61**(1): p. 77.
39. Scopes, R.K., *Protein purification: principles and practice*. 2013: Springer Science & Business Media.
40. Harrison, R., *Protein purification process engineering*. Vol. 18. 1993: CRC Press.
41. Uriel, J., *CHARACTERIZATION OF ENZYMES IN SPECIFIC IMMUNE-PRECIPITATES.* Annals of the New York Academy of Sciences, 1963. **103**(2): p. 956-979.
42. Langer, R. and D.A. Tirrell, *Designing materials for biology and medicine.* Nature, 2004. **428**(6982): p. 487-492.
43. Jencks, W.P., *Catalysis in chemistry and enzymology*. 1987: Courier Corporation.
44. Borchardt, R.T., et al., *Catechol O-methyltransferase. 8. Structure-activity relationships for inhibtion by 8-hydroxyquinolines.* J Med Chem, 1976. **19**(4): p. 558-60.
45. Leuthardt, A. and J.L. Roesel, *Cloning, expression and purification of a recombinant poly-histidine-linked HIV-1 protease.* FEBS letters, 1993. **326**(1-3): p. 275-280.
46. Rabi, S.A., et al., *Multi-step inhibition explains HIV-1 protease inhibitor pharmacodynamics and resistance.* J Clin Invest, 2013. **123**(9): p. 3848-60.
47. Maseko, S.B., et al., *I36T↑ T mutation in South African subtype C (C-SA) HIV-1 protease significantly alters protease-drug interactions.* Biological Chemistry, 2017.
48. Mosebi, S., et al., *Active-site mutations in the South African human immunodeficiency virus type 1 subtype C protease have a significant impact on clinical inhibitor binding: kinetic and thermodynamic study.* Journal of virology, 2008. **82**(22): p. 11476-11479.
49. Cleland, W., *The kinetics of enzyme-catalyzed reactions with two or more substrates or products: II. Inhibition: nomenclature and theory.* Biochimica et Biophysica Acta (BBA)-Specialized Section on Enzymological Subjects, 1963. **67**: p. 173-187.
50. Velázquez-Campoy, A., et al., *Isothermal Titration Calorimetry*, in *Current Protocols in Cell Biology*. 2001, John Wiley & Sons, Inc.
51. Freire, E., O.L. Mayorga, and M. Straume, *Isothermal titration calorimetry.* Analytical Chemistry, 1990. **62**(18): p. 950A-959A.

52. Pattnaik, P., *Surface plasmon resonance.* Applied biochemistry and biotechnology, 2005. **126**(2): p. 79-92.
53. Szabo, A., L. Stolz, and R. Granzow, *Surface plasmon resonance and its use in biomolecular interaction analysis (BIA).* Current opinion in structural biology, 1995. **5**(5): p. 699-705.
54. Patching, S.G., *Surface plasmon resonance spectroscopy for characterisation of membrane protein–ligand interactions and its potential for drug discovery.* Biochimica et Biophysica Acta (BBA)-Biomembranes, 2014. **1838**(1): p. 43-55.
55. Jerabek-Willemsen, M., et al., *Molecular interaction studies using microscale thermophoresis.* Assay and drug development technologies, 2011. **9**(4): p. 342-353.
56. Zillner, K., et al., *Microscale thermophoresis as a sensitive method to quantify protein: nucleic acid interactions in solution*, in *Functional Genomics*. 2012, Springer. p. 241-252.
57. Jerabek-Willemsen, M., et al., *MicroScale Thermophoresis: Interaction analysis and beyond.* Journal of Molecular Structure, 2014. **1077**: p. 101-113.
58. Su, X.-D., et al., *Protein Crystallography from the Perspective of Technology Developments.* Crystallography reviews, 2015. **21**(1-2): p. 122-153.
59. Bolinska, A., *Synthetic versus analytic approaches to protein and DNA structure determination.* Biol Philos, 2018. **33**(3): p. 26.
60. Garman, E.F., *Developments in x-ray crystallographic structure determination of biological macromolecules.* Science, 2014. **343**(6175): p. 1102-1108.
61. Afonine, P.V., et al., *Joint X-ray and neutron refinement with phenix. refine.* Acta Crystallographica Section D: Biological Crystallography, 2010. **66**(11): p. 1153-1163.
62. Winn, M.D., et al., *Overview of the CCP4 suite and current developments.* Acta Crystallographica Section D, 2011. **67**(4): p. 235-242.
63. Wong-Sam, A., et al., *Drug Resistance Mutation L76V Alters Nonpolar Interactions at the Flap–Core Interface of HIV-1 Protease.* ACS omega, 2018. **3**(9): p. 12132-12140.
64. Gronenborn, A.M., et al., *A powerful method of sequential proton resonance assignment in proteins using relayed 15N-1H multiple quantum coherence spectroscopy.* FEBS letters, 1989. **243**(1): p. 93-98.
65. Mitri, E., et al., *15 N isotopic labelling for in-cell protein studies by NMR spectroscopy and single-cell IR Synchrotron Radiation FTIR Microscopy: a correlative study.* Analyst, 2018.
66. Bodenhausen, G. and D.J. Ruben, *Natural abundance nitrogen-15 NMR by enhanced heteronuclear spectroscopy.* Chemical Physics Letters, 1980. **69**(1): p. 185-189.
67. Saio, T. and F. Inagaki, *Structural Study of Proteins by Paramagnetic Lanthanide Probe Methods*, in *Experimental Approaches of NMR Spectroscopy*. 2018, Springer. p. 227-252.
68. Hiroaki, H. and D. Kohda, *Protein–Ligand Interactions Studied by NMR*, in *Experimental Approaches of NMR Spectroscopy*. 2018, Springer. p. 579-600.
69. Becker, W., et al., *Investigating protein-ligand interactions by solution NMR spectroscopy.* ChemPhysChem, 2018.

CHAPTER TWO

Optimized Procedure for Recovering HIV-1 Protease (C-SA) from Inclusion Bodies

Sibusiso B Maseko[a], Deidre Govender[a], Thavendran Govender[a], Tricia Naicker[a], Johnson Lin[b], Glenn E.M. Maguire[ac], Gert Kruger[a. *]

[a]Catalysis and Peptide Research Unit, School of Health Sciences, University of KwaZulu-Natal, Durban 4001, South Africa

[b] School of Life Sciences, University of KwaZulu-Natal, Durban 4001, South Africa

[c] School of Chemistry and Physics, University of KwaZulu-Natal, Durban 4001, South Africa

[*]Corresponding author, Kruger@ukzn.ac.za

Key words, HIV-1 protease, Thioredoxin, Fusion tags, inclusion bodies, refolding

Abstract

HIV-1 is an infectious virus that causes acquired immunodeficiency syndrome (AIDS) and it's one of the major causes of the deaths worldwide. The production of HIV-1 protease (PR) at large scale has been a problem to scientists due to its cytotoxicity, low yield, insolubility, and low activity. HIV-1 C-SA protease has been cloned, expressed, and purified previously, however, with low recovery (0.25 mg/L). Herein we report an optimal expression and solubilisation procedure to recover active HIV-1 C-SA protease enzyme from inclusion bodies. The HIV protease was expressed in seven different vectors (pET11b, pET15b, pET28a pET32a, pET39b, pET41b and pGEX 6P-1). The highest expression was achieved when the pET32a vector (Trx tag) was employed. A total of 19.5 mg of fusion protein was refolded of which 5.5 mg of active protease was obtained after cleavage. The free protease had a high specific activity of 2.81 µmoles/min/mg. Interestingly the Trx-fusion protein also showed activity closer (1.24 µmoles/min/mg) to that of the free protease suggesting that pET32a vector (Trx tag) expressed in BL21 (DE3) pLysS provides a quicker way to obtain HIV-1 protease.

1 Introduction

HIV-1 infection is mainly transmitted through direct contact to infected bodily fluids. About 39 million people in the world are living with HIV [1]. If HIV is left untreated, the virus can progress to full blown AIDS, and has resulted to about 25.8 million deaths [2-4]. HIV/AIDS is a disease people must possibly will have to live with for the rest of their lives [1, 5]. However, due to the nature of the virus new mutations always develop leading to drug resistance [6]. It is therefore of key importance to know the clinical effectiveness of existing drugs against new mutants.

The HIV protease (PR) structure and its drug-resistant variants have been studied for nearly 20 years in order to combat the challenges of AIDS antiviral therapy and the evolution of HIV drug resistance [7]. Currently about 25 different antiretroviral drugs (ARV) have been approved for HIV [8]. The prescribed HIV treatment incorporates a combination of drugs from different classes in highly active antiretroviral therapy (HAART) [9]. Among the approved drugs, nine of them target HIV protease [10]. Recombinant HIV-1 PR is used for screening new inhibitors. Scientists have been trying to optimize the production of this protein and to explore other hosts for the expression of the PR enzyme. These includes the used different promoters and fusion tags, or codon optimization and various bacterial host strains and the use of different expression media [11, 12]. Volente *et al* recently made developments in the production optimization of this enzyme. The employed the use of the use Glutathione S Transference tag fusion tag and managed about 2 mg/L of culture [20]. The recovery was a bit lower that the 4mg/L recently reported by Nguyen *et al* [19].

We have previously reported [13] a procedure where we cloned, expressed, and purified C-SA HIV protease. The vector that was used in that case was pGEX-6P-1 [13]. The protease was characterized and verified by LC-MS sequencing. Though the purity was high, recovery was low (0.25 mg/L), which then prompted us to further optimise expression and purification.

In this study were report a procedure that gives the highest recovery of HIV-1 C-SA protease from inclusion bodies. This protease was cloned with seven different vectors and the best vectors were chosen.

2 Materials and Methods

2.1 Materials

All reagents were purchased from Sigma Aldrich, unless stated different. All pET vectors, enterokinase kit and *E. coli* BL21 were purchased from Novagen (USA). PGEX-6P1 and Gstrap columns were purchased from GE Health Care. (Sweden). HRV 3C protease and His-Pur cartridges were bought from Thermo Fisher Scientific.

2.2 Cloning of HIV-1 protease and protein expression

The HIV-1 protease gene (having Q7K to avoid autocatalysis) from previous work [13] was amplified with specific primers and cloned to the respective vectors. For pET11b, 15b and 28b NdeI and XhoI restriction sites were used. For pET32b, 39b and 41b NcoI and XhoI sites were, and lastly BamHI and XhoI were used for pGEX 6P-1. The amplified genes and their respective vectors were then restricted and purified. These were then ligated and transformed into BL21 (DE3) pLysS using a heat shock method [13, 14]. Transformed cells were plated in antibiotic selection plates and grown overnight at 37°C. Positive clones were screened using colony PCR and further by restriction digestion and plasmid DNA sequencing. The *E. coli* cells harbouring HIV-1 plasmids were grown at 37ºC in LB medium with antibiotics (100 µg/ml ampicillin and 25 µg/ml chloramphenicol for pET11b, 32b (His and Trx-tag), 15b (His-tag) and pGEX 6P-1 (GST-tag), 34 µg/mL kanamycin and 25 µg/ml chloramphenicol for pET28b (His-tag), pET41b (His and GST-tag) and pET39b (His and DbsA-tag). The overnight culture was diluted 100-fold in Luria broth containing the respective antibiotics and grown for approximately 3 hours at 37ºC.

When optical density at 600 nm of the culture reached 0.4-0.5, IPTG was added to a final concentration of 1.0 mM. The cultures were grown for 4 hours, cells harvested by centrifugation at 5 000 x *g*, 30 minutes, 4ºC and stored at -20ºC.

2.3 Inclusion body isolation and solubilization optimization

The pellet was re-suspended in 50 mM Tris pH 8 containing 1 mM phenlymentanesulfonlyl fluoride (PMSF), thereafter sonicated on ice to liberate the cell contents, followed by centrifugation at 14000 *x g*. The pellet comprised of the expressed proteins as inclusion bodies was washed again with the same buffer but this time with 1% triton. The final pellet was re-suspended in 10 mL of three different solubilisation conditions. Two of these were mild solubilisation procedures, and they comprised of the following, procedure one had 50 mM Tris, pH12, 2M urea, the second one contained 50 mM Tris pH 8, 3 M urea and 30% trifluoroethanol. The third solubilization procedure (denaturing) had 50 mM Tris pH 8, 8 M urea and 2 mM dithiothreitol (DTT). These three homogenized samples were then allowed to stand at room temperature for 1 hour. The proteins solubilized under mild conditions were then quickly refolded by 10-fold dilution with refolding buffer (50 mM Tris, pH 8, 5% sucrose and 2 mM DTT).

2.4 Purification

GST (Protease expressed in pGEX 6P-1) fusion protein was purified as described previously [13]. Briefly, purification was done using an AKTA purifier 100-950 (GE Health Care). Partial purification was carried out using a Hitrap QFF (5 mL) anion exchange column (GE Health Care) and the GST-HIV-PR was eluted using a 0 – 1 M NaCl gradient.

The bound proteins were then desalted using a Hiprep desalting column (GE Health Care, USA). Further purification was performed using a GSTrap affinity column (GE Healthcare, USA). The GST tag was then removed by overnight digestion at 4 ºC with precision protease (Thermo Scientific). All contents were loaded back into the GSTrap affinity column and HIV-1 PR was collected in the unbound fraction, then refolded and stored at -70 ºC.

Fusion proteins from pET32a and pET39b were also purified by affinity chromatography, but using a His Pur Cobalt column, 5 mL, (Thermo Scientific). The column was first equilibrated with a 10-column volume of equilibration/wash buffer (50 mM Na_2PO_4, pH 7.5, 300 mM NaCl, 5 mM imidazole. Samples (20 mL) were then loaded onto the column using a sample pump. The column was washed with 5 column volumes of the same buffer. Bound proteins were then eluted using elution buffer (50 mM Na_2PO4, pH 7.5, 300 mM NaCl, 150 mM imidazole). Purity of the eluted fraction was verified by SDS PAGE. The samples were then refolded by removing urea slowly by dialysis. The fusion proteins were then cleaved using enterokinase cleavage capture kit (Novagen) according to the manufacture's protocol. Following cleavage, the enterokinase was removed from the mixture using the same kit. The remaining mixture was now containing Trx and HIV-PR was then loaded back to the His-Pur cobalt column. Free pure HIV-PR was collected in the flow through. The purified protease was confirmed by SDS-PAGE, Western blot and LC-MS-TOF (Central Analytical Facility, University of Stellenbosch); data provided in the supplementary materials. Protein quantification for pure free HIV-PR was achieved by measuring absorbance at 280 nm and the concentration was calculated using Beer-

Lamberts law. The extinction coefficient used was 24 480 $M^{-1}cm^{-1}$. Absorbance at 340 nm was subtracted from the 280 nm absorbance to account for protein aggregation.

2.5 Enzyme activity

The enzyme activities of the fusion protein and the free HIV-PR were measured following the breakdown of the HIV-1 fluorogenic substrate, Abz-Arg-Val-Nle-Phe(NO_2)-Glu-Ala-Nle-NH_2 as previously reported [13, 15]. Hydrolysis of the HIV-1 fluorogenic substrate was monitored by a decrease in absorbance at 300 nm. The specific activity for both the fusion protein and free PR were calculated. All enzyme catalytic activity assays were done using a Jasco V-630 spectrophotometer. The effect of pH and temperature on the purified enzyme was also determined.

3 Results

3.1 Cloning of HIV-1 protease and protein expression

The HIV-PR genes were successfully cloned to the seven vectors (Figures S1, S2 and S3). The HIV-PR was then expressed in each different vector as either fused or non-fused protein. All the vectors used have a T7 promoter except for pGEX 6P-1 which uses a tac promoter. A summary of the expression results is presented in Table 1. The best results were obtained when pET32b was used (Figure S4). The expression was higher for pGEX 6P-1 compared to pET39b, which was also high. Vectors pET11b, 15b, 28b and 41 showed the lowest expression of the HIV-PR. Expression in these vectors was only detected through western blot as nothing was visible with SDS-PAGE.

3.2 Inclusion body isolation, solubilization and purification

Inclusion bodies from the three selected vectors were solubilized using the three procedures as described in the methods section. A summary of the solubilisation results is shown in Table 2. The fusion proteins were then purified using affinity chromatography as described in the methods section. High recovery was obtained after refolding from pET32a. There was high aggregation (seen as white precipitate) observed from the other two vectors. Again, pET32a gave the highest concentration of free PR (approx. 5.5 mg/L) after cleavage. A summary of the recovered PR is also presented in Table 2. As pET32a rendered the best results, further characterization was performed using proteins from this vector. Figure 1 shows a chromatogram of Trx fusion protein and protein profile. The protein fusion protein was purified with a single step purification procedure.

Table 2*:* Optimizing expression of HIV-PR in seven different vectors

Vector	Promoter	Tag	Comment
pET11b	T7 Promoter	No tag	Low expression level. Difficult in purification
pET15b	T7 Promoter	His-N-Terminus	Very low expression, only detected through western blot
pET28b	T7 Promoter	His N and C Terminus	Very low expression, only detected through western blot (Figure S4)
pET32b	T7 Promoter	Trx, His N and C terminus	High Expression level. High purification yield. Highly recovery after refolding
pET39b	T7 Promoter	DbsA N terminus, His N and C terminus	Fair Expression. High Purification yield. Low recovery after refolding
pET41b	T7 Promoter	GST N terminus, His N and C terminus	Low expression level. Only detected through Western blot (Figure S6)
pGEX-6P-1	Tac Promoter	GST N Terminus	High Expression Level. Low recovery due to aggregation

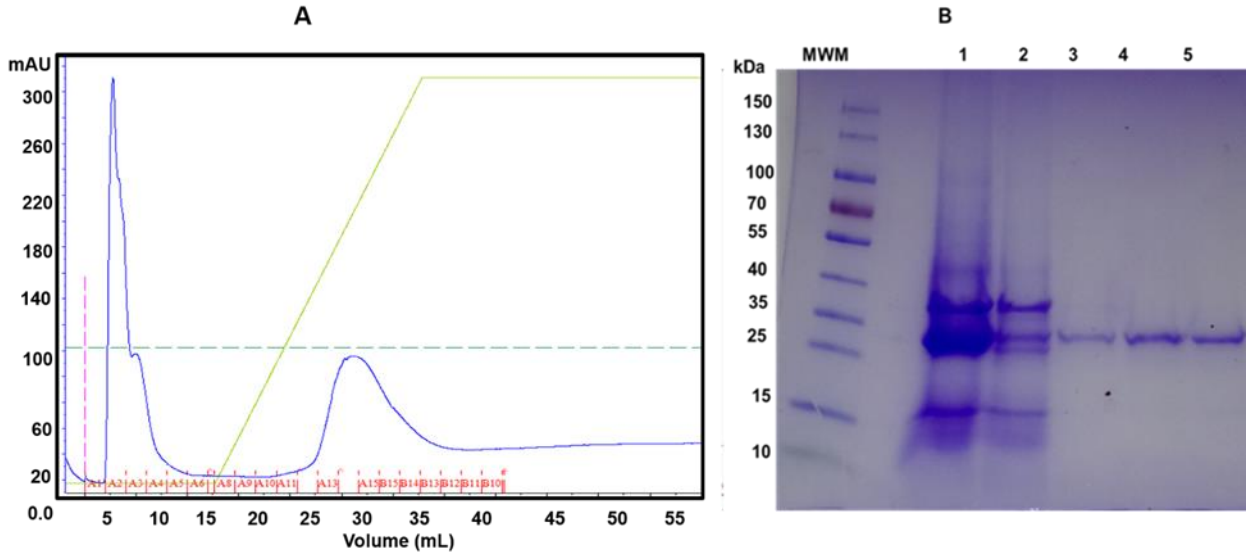

Figure 1: Purification of Thioredoxin (Trx) fusion protein using affinity chromatography. The solubilized inclusion bodies were loaded onto a His Pur cobalt column previously equilibrated with 50 mM $NaPO_4$, 300 mM, NaCl and 5 mM imidazole. Unbound proteins were washed out with 2 column volumes of the same buffer and bound proteins were eluted with same buffer but with 0-250 mM imidazole gradient. The y-axis represents absorbance at 280nm, x-axis represent the fractions collected. The green line represents imidazole gradient. Purity was verified using SDS-PAGE. A; chromatogram showing bound and unbound fractions. B; SDS-PAGE of the collected fractions, MMW; Molecular weight marker; 1 crude protein, 2 unbound protein, 3 (A13), 4 (A15), 5 (B14) are bound proteins.

3.3 Enzyme activity

We also assessed whether the fusion protein (Trx-HIV-PR) has activity against the synthetic substrate. These results are presented in Figure 3. The experiment was performed using constant substrate concentration and increasing enzyme concentration. The fusion protein showed almost the same activity as the free PR though slightly lower. The free HIV PR had a specific activity of 2.81 µmoles/min/mg compared to 1.24 µmoles/min/mg for the fusion protein.

Table 3: Protein recovery from the three solubilisation procedures.

Vector	Solubilizing method	Total fusion protein from 1L	Fusion protein refolded (%)	Total HIV-PR (mg) in 1L
pET32a (His and Trx)	50 mM Tris, pH 8,8 M Urea	23.0 mg	44	4.10
	50 mM Tris, pH 12, 2 M Urea	22.8 mg	49	5.50
	50 mM Tris, pH 8,30% TFE, 3M Urea	20.2 mg	49	4.30
pET39b (His and DbsA)	50 mM Tris, pH 8, 8 M Urea	4.0 mg	10	0.20
	50 mM Tris, pH 12, 2 M Urea	3.4 mg	16	0.30
	50 mM Tris, pH 8,30% TFE, 3M Urea	3.2 mg	13	0.22
pGEX 6P-1 (GST)	50 mM Tris, pH 8,8 M Urea	12.0 mg	2	0.15
	50 mM Tris, pH 12, 2 M Urea	10.0 mg	5	0.20
	50 mM Tris, pH 8,30% TFE, 3M Urea	9.0 mg	5	0.23

The free HIV-PR obtained after enterokinase cleavage showed a single band of 11 kDa on SDS-PAGE, Figure 2. These was also confirmed by the LC-MS-TOF results (Table S1)

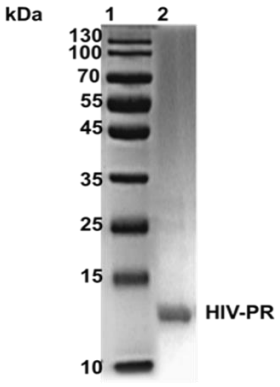

Figure 2: SDS-PAGE of free HIV-PR. This was achieved after dialysis of the fusion protein, which was the cleaved using enterokinase. Lane 1 Molecular weight marker, Lane 2 HIV-PR.

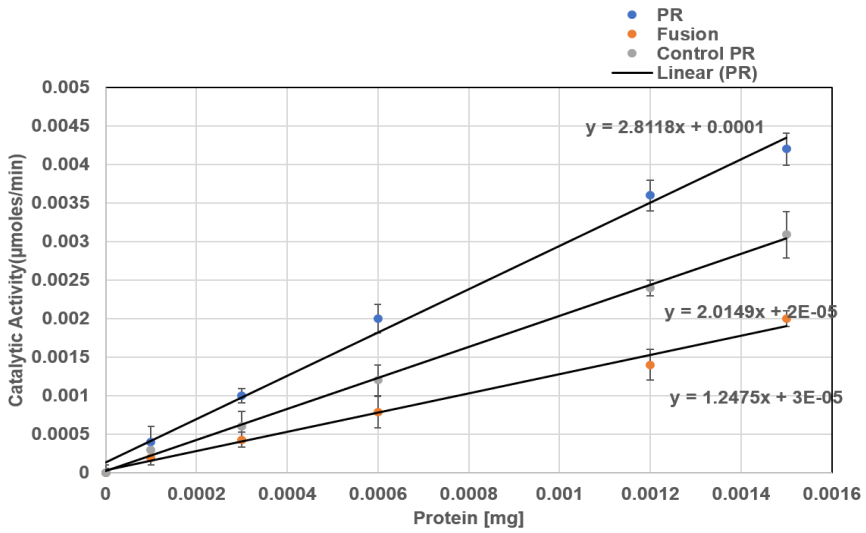

Figure 3: Comparing activities of Trx-fusion protein, free HIV-PR and control PR purified previously [13]. This was determined following the hydrolysis of the synthetic substrate (Abz-Arg-Val-Nle-Phe-(NO_2)-Glu-Ala-Nle-NH_2) in 50 mM sodium acetate and 100 mM NaCl (pH 5) and 37°C (n = 3).

To confirm whether the purified protease possesses the same properties as reported in literature, the optimum pH and temperature were determined. The optimum pH and temperature pH were found to be 5 and 37°C respectively. This is presented graphically in Figure 4.

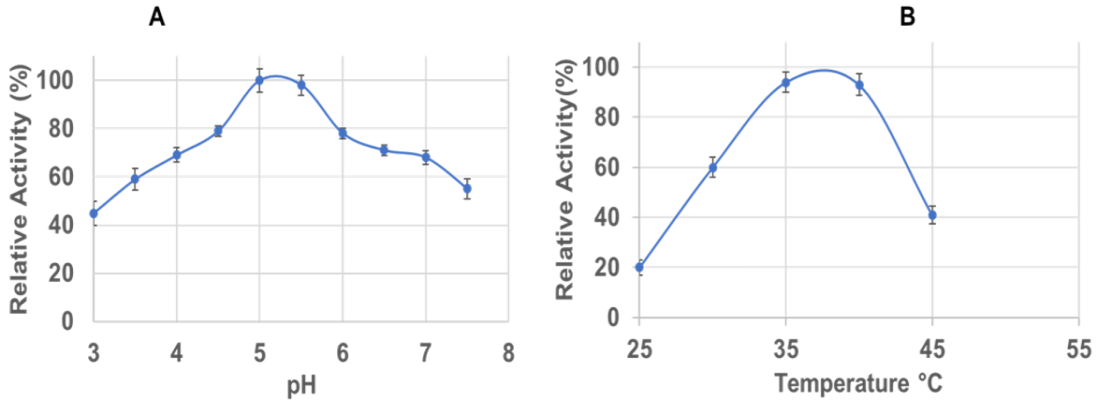

Figure 4: Determination of optimum pH and optimum temperature for the free HIV-PR. The experiment was performed using the synthetic substrate (250 µM) and 2 µM of enzyme at varying pH and temperature. A; optimum pH, B; optimum temperature. The optimum pH and temperature pH were found to be 5 and 37°C respectively (n = 3).

4 Discussion

HIV-1 protease production at large scale is difficult because of its cytotoxicity, insolubility, low yield, and low activity [16, 17]. Over the past 20 years, scientists have attempted to overcome this problem by using several expression systems containing different promoters, fusion tags with by using various hosts and media [18]. In this study, we employed several vectors and three solubilisation procedures. Four of the seven vectors used showed very low expression. This could be due to cytotoxicity of the PR which was not suppressed by the fusion tags on the vectors. The protease was fairly expressed as a DbsA fusion protein as seen from Table 2. Again, recovery was also low when the three solubilisation procedures in this study were used. These results are in agreement with what was reported by Nguyen *et al.* [19]. The expression in the pGEX 6-P1 vector was very high, PR was expressed as a GST fusion protein. Since the protein was expressed as inclusion bodies, refolding was required before loading to the Gstrap column. In this case, 90% of the protein was lost due to aggregation. GST is reported to form disulfide bonds which makes refolding difficult. Cleavage with the precision protease was also not effective. The overall yield was 0.25 mg/L, which was low. Volente *et al.* also reported high expression in pGEX-6P-1 but low recovery yield [20].

Table 2 indicates that the highest expression and recovery was obtained when Trx (pET32a) fusion tag was employed. This is the highest recovery of HIV-1 protease reported from inclusion bodies. The recovery is a 22-fold increase of what we have previously reported for HIV-1 C-SA [13]. This procedure appears to solve the difficulties associated with expression, purification, and recovery of HIV-1 PR and will also be applicable to other strains. The recovery of HIV-PR we are reporting is better than the

reported for subtype B (2.0 mg/L) by Volente *et al.* and 4.0 mg/L from Nguyen *et al.* [19, 20]. Again, the PR have better specific activity (2.81µmoles/min/mg) compared to 1.19 µmoles/min/mg reported by the former [17], and even better than the method we previously reported (2.02 µmoles/min/mg) [13].

Trx is an intracellular thermostable *E .coli* protein with a molecular weight of 12 kDa and is highly soluble [21]. Trx has been reported to increase solubility in recombinant protein expression by taking advantage of its intrinsic oxido-reductase activity which aid in the reduction of disulfide bonds through thio-disulfide exchange [21]. This explains the high recovery even when either of the three solubilisation procedures were used. There was very low aggregation when the protein samples were refolded. Interestingly the Trx fusion protein had almost the same activity as the free HIV-1 PR. Trx is also useful in crystallization of certain target proteins [22]. Its rigid connection to the target protein blocks conformational heterogeneity facilitating crystallization [21]. This will provide an easy and rapid way of crystallizing new HIV-PR mutants.

5 Conclusion

We have shown in this study that Trx is the best fusion tag for the expression of HIV-1 protease. This brings a solution to the issue of aggregation observed in other expression systems. Another interesting result is that the fusion protein possesses almost the same activity as the free HIV-PR. Again, the fusion, in theory, should allow for crystallization of new HIV-1 PR mutants.

Compliance with Ethical Standards

This study was funded by the National Research Foundation (NRF) (Grant number 106803)

Ethical approval: This article does not contain any studies with human participants or animals performed by any of the authors.

Conflict of interest

The Authors declare they have no conflict of interest

6 References

1. Ayres, J.R.D.C.M., et al., *Vulnerability, human rights, and comprehensive health care needs of young people living with HIV/AIDS.* American Journal of Public Health, 2006. **96**(6): p. 1001-1006.
2. Zanakis, S.H., C. Alvarez, and V. Li, *Socio-economic determinants of HIV/AIDS pandemic and nations efficiencies.* European Journal of Operational Research, 2007. **176**(3): p. 1811-1838.
3. Emlet, C.A., S.S. Gusz, and J. Dumont, *Older adults with HIV disease: challenges for integrated assessment.* Journal of Gerontological Social Work, 2003. **40**(1-2): p. 41-62.
4. DeVaughn, S., et al., *Aging with HIV-1 Infection: Motor Functions, Cognition, and Attention–A Comparison with Parkinson's Disease.* Neuropsychology review, 2015. **25**(4): p. 424-438.
5. Skinner, D. and S. Mfecane, *Stigma, discrimination and the implications for people living with HIV/AIDS in South Africa.* SAHARA: Journal of Social Aspects of HIV/AIDS Research Alliance, 2004. **1**(3): p. 157-164.
6. Nunez Aguilar, E., *HIV-1 Protease Inhibitors From Marine Brown Alga: A Literature Review.* McNair Research Journal SJSU, 2017. **13**(1): p. 4.
7. Weber, I.T. and J. Agniswamy, *HIV-1 protease: structural perspectives on drug resistance.* Viruses, 2009. **1**(3): p. 1110-1136.
8. Flexner, C., *HIV drug development: the next 25 years.* Nature Reviews Drug Discovery, 2007. **6**(12): p. 959-966.
9. Ferradini, L., et al., *Scaling up of highly active antiretroviral therapy in a rural district of Malawi: an effectiveness assessment.* The Lancet, 2006. **367**(9519): p. 1335-1342.
10. Mastrolorenzo, A., et al., *Inhibitors of HIV-1 protease: current state of the art 10 years after their introduction. From antiretroviral drugs to antifungal, antibacterial and antitumor agents based on aspartic protease inhibitors.* Current medicinal chemistry, 2007. **14**(26): p. 2734-2748.
11. Leuthardt, A. and J.L. Roesel, *Cloning, expression and purification of a recombinant poly-histidine-linked HIV-1 protease.* FEBS letters, 1993. **326**(1-3): p. 275-280.
12. Louis, J.M., et al., *Autoprocessing of the HIV-1 protease using purified wild-type and mutated fusion proteins expressed at high levels in Escherichia coli.* European journal of biochemistry, 1991. **199**(2): p. 361-369.
13. Maseko, S.B., et al., *Purification and characterization of naturally occurring HIV-1 (South African subtype C) protease mutants from inclusion bodies.* Protein expression and purification, 2016. **122**: p. 90-96.
14. Van der Rest, M., C. Lange, and D. Molenaar, *A heat shock following electroporation induces highly efficient transformation of Corynebacterium glutamicum with xenogeneic plasmid DNA.* Applied Microbiology and Biotechnology, 1999. **52**(4): p. 541-545.
15. Maseko, S.B., et al., *I36T↑ T mutation in South African subtype C (C-SA) HIV-1 protease significantly alters protease-drug interactions.* Biological Chemistry, 2017.

16. Buchner, J., I. Pastan, and U. Brinkmann, *A method for increasing the yield of properly folded recombinant fusion proteins: single-chain immunotoxins from renaturation of bacterial inclusion bodies.* Analytical biochemistry, 1992. **205**(2): p. 263-270.
17. Kim, S.-K. and N. Rajapakse, *Enzymatic production and biological activities of chitosan oligosaccharides (COS): A review.* Carbohydrate polymers, 2005. **62**(4): p. 357-368.
18. Forstner, M., L. Leder, and L.M. Mayr, *Optimization of protein expression systems for modern drug discovery.* Expert review of proteomics, 2007. **4**(1): p. 67-78.
19. Nguyen, H.-L.T., et al., *An efficient procedure for the expression and purification of HIV-1 protease from inclusion bodies.* Protein Expression and Purification, 2015. **116**: p. 59-65.
20. Volontè, F., L. Piubelli, and L. Pollegioni, *Optimizing HIV-1 protease production in Escherichia coli as fusion protein.* Microbial Cell Factories, 2011. **10**(1): p. 53.
21. Costa, S., et al., *Fusion tags for protein solubility, purification and immunogenicity in Escherichia coli: the novel Fh8 system.* Frontiers in microbiology, 2014. **5**.
22. Sugiki, T., T. Fujiwara, and C. Kojima, *Latest approaches for efficient protein production in drug discovery.* Expert opinion on drug discovery, 2014. **9**(10): p. 1189-1204.

CHAPTER THREE

I36T↑T Mutation in South African Subtype C (C-SA) HIV-1 Protease Significantly Alters Protease-Drug Interactions

Sibusiso B Maseko[a], Eden Padayachee[a], Thavendran Govender[a], Yasien Sayed[b], Gert Kruger[a*], Glenn E.M Maguire[ac], Johnson Lin[d.]

[a]Catalysis and Peptide Research Unit, School of Health Sciences, University of KwaZulu-Natal, Durban 4001, South Africa

[c] Protein Structure-Function Research Unit, School of Molecular and Cell Biology, University of the Witwatersrand, 2050, South Africa

[c] School of Chemistry and Physics, University of KwaZulu-Natal, Durban 4001, South Africa

[d] School of Life Sciences, University of KwaZulu-Natal, Durban 4001, South Africa

Corresponding Author: Kruger@ukzn.ac.za

Key words: Enzyme kinetics, InhibitorIC_{50}, Thermodynamics, Vitality value

Abstract

The efficacy of HIV-1 protease inhibition therapies is often compromised by the emergence of mutations in the protease molecule that reduces the binding affinity of inhibitors while maintaining viable catalytic activity and affinity for natural substrates. In the present study, we used a recombinant HIV-1 C-SA protease and a recently reported variant for inhibition (K_i, IC_{50}) and thermodynamic studies against nine clinically used inhibitors. This is the first time that binding free energies for C-SA PR and the mutant are reported. This variant protease harbours a mutation and insertion (I36T↑T) at position 36 of the C-SA HIV-1 protease and did not show a significant difference on the catalytic effect of the HIV-1 protease. However, the nine clinically-approved HIV PR drugs used in this study demonstrated weaker inhibition and lower binding affinities toward the variant when compared to the wild-type HIV-1 protease. All the protease inhibitors, except Amprenavir and Ritonavir exhibited a significant decrease in binding affinity ($p < 0.0001$). Darunavir and Nelfinavir exhibited the weakest binding affinity, 155- and 95- fold decreases respectively, toward the variant. Vitality values for the variant protease, against the seven selected protease inhibitors, confirm the impact of the mutation and insertion on the South African HIV-1 subtype C protease. This information has important clinical application for thousands of patients in Sub-Saharan Africa.

1 Introduction

The protease (PR) enzyme is encoded in the gene of all retroviruses, including HIV-1 [1]. During the replication cycle of HIV, *gag* and *gag-pol* gene products are translated as polyproteins [2, 3]. These proteins are subsequently processed by the virally-encoded protease to yield structural proteins of the virus core, together with essential viral enzymes, including the protease itself [4, 5].

The importance of HIV-1 protease in the viral life cycle has made it one of the essential targets of antiviral therapy [6]. Protease inhibitors (PIs) were introduced into clinical practice in 1995-1996 and together with the application of highly active antiretroviral therapy (HAART) caused a decreased mortality and prolonged the life of infected individuals. However, the selection pressure of a virostatic leads to rapid selection of mutations in viral enzymes that are resistant to a specific inhibitor. Viral protease variants that are resistant to PIs have been observed in more than half of the 99 residues of the HIV-1 protease [7]. The rapid development of PR variants resistant to protease inhibitors may be explained by the natural variability (i.e. polymorphisms) that occur in the virus and the dynamic nature of viral replication present in infected patients [8, 9]. There are two different mutation types that take place in the HIV-1 protease [10]. The first occurs in the active site of the PR and is termed a primary resistance mutation and directly influences the binding of a PI[11]. The second type is referred to as a secondary resistance mutation and occurs at sites distal from the binding cleft. The latter type influences PI binding indirectly by impacting on subdomain flexibility of the PR molecule or mutations that occur outside the PR coding region. Mutations of this type alter the amino acid processing sites

of the Gag-Pol polyprotein and increase the capability of variant PRs to process viral polyproteins at the sites[10].

Structure-based design of drug molecules is of great importance in the search for potential novel drugs[12]. Resistance of HIV to antiretroviral drugs is one of the most common causes for therapeutic failure in people infected with the virus [13]. Thus far, no single antiretroviral drug combination can completely shut down viral replication and the emergence of HIV drug resistance usually follow these treatments [14]. Evolving knowledge of drug resistance is crucial to effectively develop novel therapeutics for patients infected with HIV [15]. In our study, we assessed the effect of a mutation at codon 36 and an insertion (at the same position) [16] in the South African subtype C (C-SA) HIV-1 PR on the binding capacity of the nine commonly used PIs. The mutation and insertion present in this PR is indicated as I36T↑T, where the upward arrow preceding the amino acid threonine indicates an amino acid insertion after codon 36 and is referred to as the variant PR in this paper and is shown in figure 1. The variant was discovered in a HIV-1 positive mother who participated in a PMTCT (Prevention of Mother-To-Child Transmission) cohort. The patient received treatment with the following reverse transcriptase inhibitors (RTIs): efavirenz, d4t (stavudine) and 3TC (lamivudine). Interestingly, the patient was completely drug-naïve with respect to protease inhibitors [16]

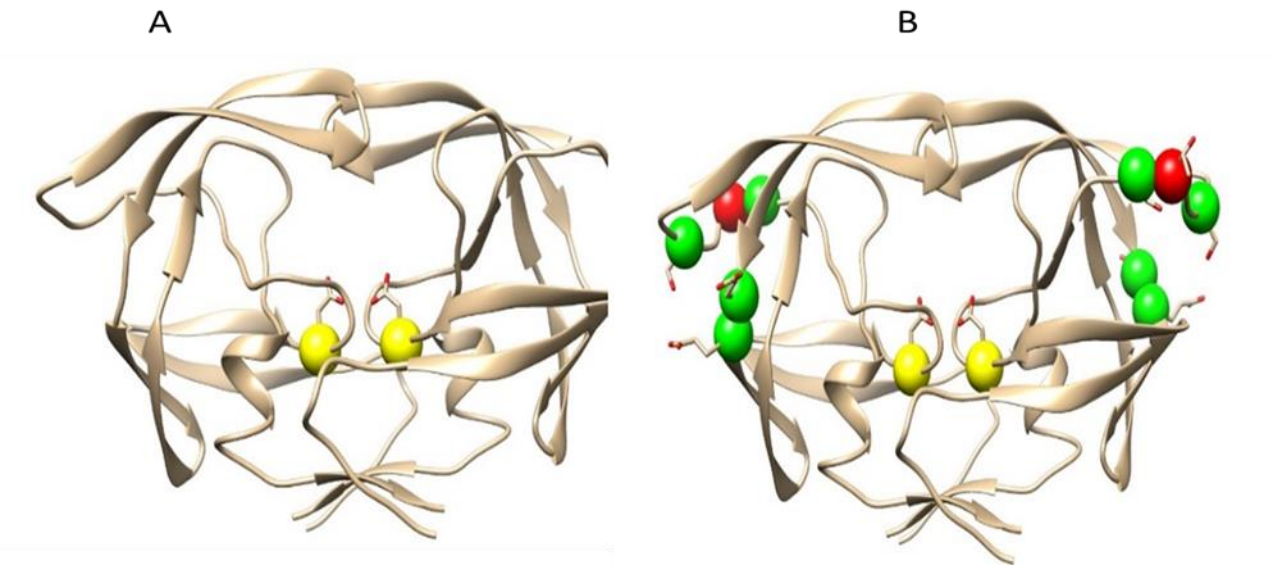

Figure 8. A ribbon representation of the wild type C-SA HIV protease (A) and I36T↑T variant (B). Shown in yellow is the aspartic residues (Asp 25/25'). The insertion is shown in red. The green spheres are other amino acid mutations found in this variant protease. The figures were created using UCSF Chimera version 1.9 [17].

The variant protease together with the wild type C-SA HIV protease were cloned, purified and characterized [18]. The purified variant protease possessed similar catalytic ability as the wild type [18]. We have previously reported a computational model of the I36T↑T variant protease [16]. Our model predicted that all of the protease inhibitors exhibited reduced Gibb's free binding energies for the variant I36T↑T than the wild type PR [16]. To confirm the findings from our computational model, the Gibbs free binding energies of all nine commercially approved protease inhibitors compounds were for the first time experimentally determined for C-SA and I36T↑T.

2 Results and Discussion

2.1 Enzyme kinetics

A summary of the enzyme kinetic parameters of HIV-1 protease wild type and variant is shown in Table 1. The variant PR, I36T↑T, showed a decreased (K_m) toward the synthetic substrate (Abz-Arg-Val-Nle-Phe(NO_2)-Glu-Ala-Nle-NH_2) [19] and increased catalytic efficiency (higher k_{cat}/K_m) compared to the wild type PR (Table 1). The greater catalytic efficiency when compared to the wild type PR, is attributed to the higher turnover number (k_{cat}).

Table 1: Enzyme kinetic parameters of the wild type C-SA protease and the I36T↑T variant protease using a synthetic substrate (Abz-Arg-Val-Nle-Phe (NO_2)-Glu-Ala-Nle-NH_2) (n = 3).

Parameter	Wild type	I36T↑T
K_m (μM)	129.0± 3.0	103.0±3.0
k_{cat} (s^{-1})	1.08±0.00	1.29±0.01
k_{cat}/K_m ($\mu M^{-1}s^{-1}$)	0.008±0.000	0.013±0.003

This will result in faster replication cycles as processing of viral proteins occur at an increased rate and thus increased viral load that could lead to a more rapid progression to AIDS. This data is consistent with our previous study and follows the same trend [19].

The K_i values of PIs against the wild type calculated from Equation 2 are shown in Table 2. From the table, the PIs can be divided into three groups (more effective, effective, less effective). ATV, IDV, APV, RTV and the DRV were the most effective ones against the wildtype and all had Ki values of less than 200 pM. ATV showed the tightest binding of

all the inhibitors with a K_i value of 78±5 nM. NFV and SQV can be classified as effective and had K_i values of 330±82 and 350±14 respectively.

Table 2: A summary of K_i and IC_{50} values for the wild type C-SA PR (n = 3).

Protease Inhibitor	K_i (pM)	IC_{50} (pM)
ATV	78 ± 5	81± 4
IDV	140 ±1	1,070 ± 8
APV	160± 4	1,070 ± 4
RTV	170 ± 5	3,400± 6
DRV	190±6	3,000±1
NFV	330±8	2,000 ± 41
SQV	350 ±10	790 ± 1
LPV	470 ± 14	780 ± 5
TPV	510 ± 32	1,600 ± 21

LPV and TPV were the less effective inhibitors against the wild type. Overall, the inhibitors had a better binding against the wild type C-SA protease. IC_{50} values (Table 2) for all the inhibitors were less than 4000.0 pM against the wild type confirming the observed K_i values. Both the K_i and IC_{50} values are within the same range as reported for C-SA and other HIV-1 proteases [20-22]. A summary of the K_i values for the variant protease is shown in table 3. Again, from the table, the PIs can be classified into three groups, (effective, somewhat effective, and not effective). APV, RTV and LPV are classified as effective. They had K_i values of 160±3, 190±2, 560±1 pM respectively. IDV and ATV were somewhat effective and had K_i values of 980±2 and 1,300±88 pM respectively. TPV, SQV, DRV and NFV were not effective against the variant. All these inhibitors had K_i values above 20,000 pM.

Table 3: A summary of K_i and IC_{50} values the variant protease. The ratio of variant to wild type is shown in parenthesis (n = 3).

Protease inhibitor	K_i (pM)	IC_{50} (pM)
APV	160±3 (1)	1,300±30 (1)
RTV	190±2 (1)	5,900±80 (1.7)
LPV	560±1(1.2)	7,100±2 (9)
IDV	980±2 (6.8)	8,150±74 (7.6)
ATV	1,340±88 (17.2)	19,400±60 (24)
TPV	20,560±30 (40.2)	114,100±300 (73.6)
SQV	21,900±30 (63)	154,100±300 (196.6)
DRV	29,300±10 (155)	161,100±700 (53.9)
NFV	30,900±41(95)	196,900±340 (99)

Almost all the inhibitors showed a decreased binding to the variant when compared to the wild type. A ratio of K_i values (variant/wild type) is shown in brackets in Table 3. The trend observed against the wild type is different from that of the variant. APV and RTV showed a decrease in binding affinity but it was not significant when compared to the wild type ($p = 0.4353$ and $p = 0.5898$). A 17-fold increase in K_i was observed when ATV was also used against the variant than that of the wild type, (Table 3). NFV and DRV showed the weakest binding of all the PIs used in the experiment with a 95- and 155-fold decrease respectively when compared to the wild type.

IC_{50} values for all the inhibitors against the variant are shown in Table 3. The variant protease also showed increased IC_{50} values when compared to wild type. RTV and APV were better inhibitors against the variant and their IC_{50} values were close to the wild type (Table 3). Again, DRV and NFV exhibited the highest IC_{50} values against the variant compared to the other drugs with 54- and 99-fold changes, respectively (Table 3). A

graphical presentation of DRV IC_{50} is shown in Figure 2. The variant protease required a higher concentration of DRV (161,100±700 pM) to reduce the catalytic activity to less than 50 % than the wild type (3,000±100 pM).

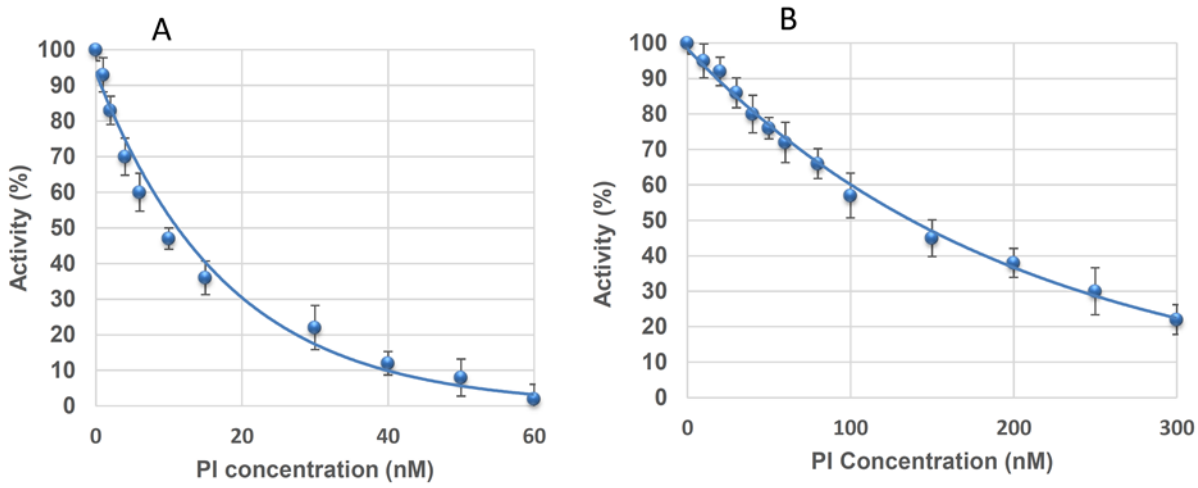

Figure 2: Graphical presentation of IC_{50} determination using DRV. The experiment was performed at 37 °C using 50 nM of enzyme, 250 µM substrate, and increasing concentration of inhibitor (0 - 60 nM for wild type and 0 - 300 nM for the mutant. The experiments were done in triplicates and results were presented as mean ± standard deviations. A, wild type and B the mutant I36T↑T (n = 3).

All the IC_{50} values were much higher than the respective Ki values which are expected according to the literature [23]. IC_{50} always is higher than Ki, because IC_{50} = Eo/2 + Ki (app). Kuzmič *et al*., 2000 also emphasize that K_i values on the biochemical assays provide the intrinsic molecular measure of potency of the inhibitors, however, IC_{50} values cannot and IC_{50} values are perfectly good for cell-based assays. Therefore, emphasis should be given to K_i values. In this study though, IC_{50} values follow the same trend as observed from the K_i values and can as well be grouped the same way as the K_i values.

The vitality values which predict the therapeutic effect of a given protease inhibitor toward the variant against the wild type were calculated based on Equation 3 and the results are shown in Figure 3. A large vitality value indicates that the variant is resistant to that

specific drug. High vitality values were observed when DRV and NFV were used, with 2.28 and 2.27 log vitality respectively.

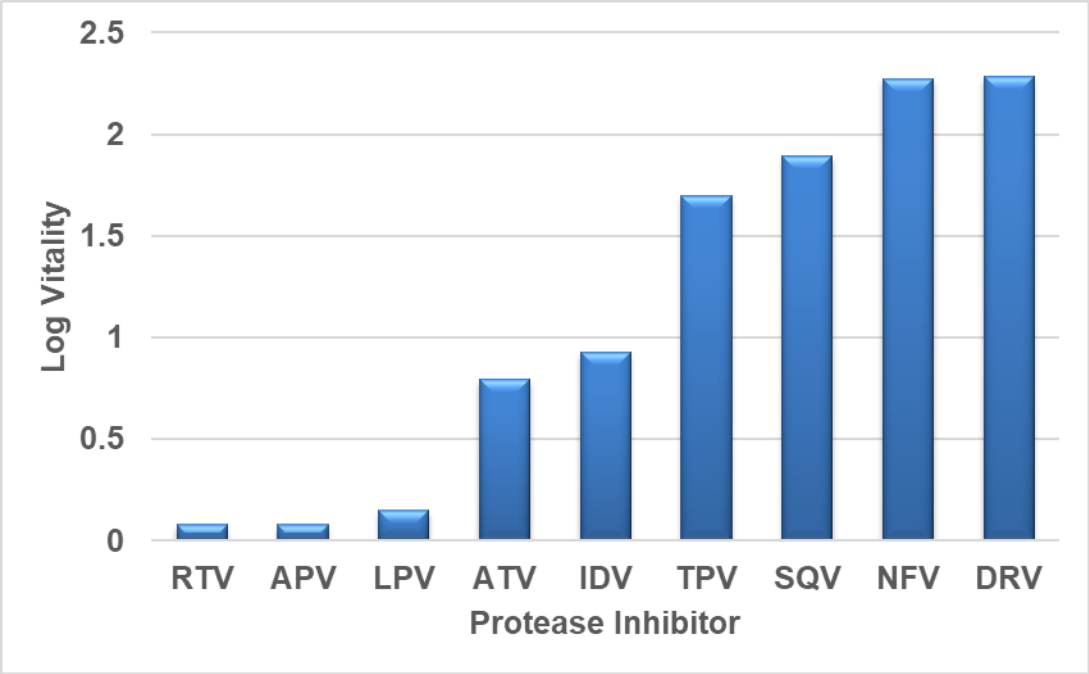

Figure 3: Vitality values for the I36T↑T protease in comparison to the wild type C-SA HIV-1 protease with respect to the seven inhibitors.

TPV and SQV had log vitality values of 2.05 and 1.89 respectively. Thus, the above drugs (TPV, SQV, DRV and NFV) should not be prescribed to patients with this variant PR. The log vitality value of IDV was found to be 0.93 which was the fifth highest. ATV was the closest to IDV and had a log vitality value of 0.780. These drugs may still be prescribed for the variant PR. The last three drugs, RTV, APV and LPV are suitable drugs for clinical treatment of the variant PR as they have log vitality values of 0.079, 0.079 and 0.149, respectively.

2.2 Quenching and Thermodynamics

Inhibitor binding thermodynamics of variant I36T↑T were compared to those of WT protease employing kinetics and fluorescence quenching. The tryptophan fluorophore molecules [24] within HIV-1 protease, especially those that are close to the active site behave as intrinsic quenchers and decrease the quantum yield of fluorescence. The two tryptophan residues of HIV-1 protease are not uniformly exposed to water; Trp-6 is closer to the active than Trp-42 (Figure S1), as can be judged from the three-dimensional structure of the enzyme [24] and we expect that residue to be more affected by the inhibitors.

In this study, the addition of each inhibitor to the HIV-1 proteases resulted in fluorescence quenching with linear Stern-Volmer plots (Figure 4), and allows for the estimation of Stern-Volmer quenching constants (K_{sv}) from the slope of the linear regression (Eq.4) [25]. The greater the quenching, the larger the K_{sv} value. The Stern Volmer quenching constants follow the same trend as the kinetic data for both the wild type and mutant. ATV was the best inhibitor for the wildtype with K_{sv} value of 114 μM^{-1}. APV was the best inhibitor for the variant with a K_{sv} value of 81 μM^{-1}. TPV was revealed as the weakest binding result against the wild type, and SQV was the poorest for the mutant. Differentiation between static and dynamic quenching is temperature dependent and because the values of K_{sv} increased with increasing temperature, this pointed (as expected) towards a dynamic quenching mechanism (Figure 4), (Table 4).

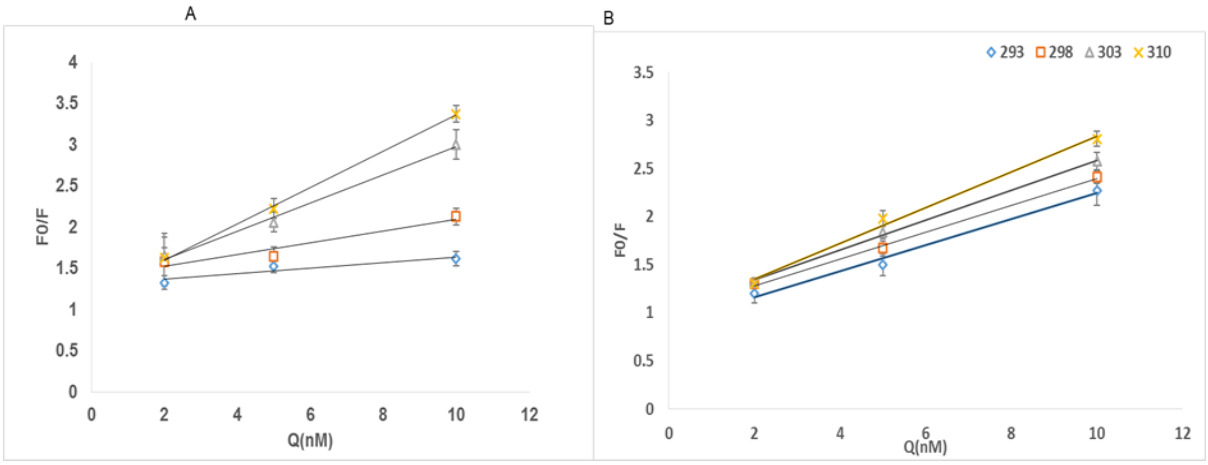

Figure 4: Examples of Stern-Volmer plots for fluorescence quenching of WT (A) and the variant I36T↑T in 50 mM sodium acetate buffer (pH 5) containing NaCl (1 M) in a final volume of 100 µl when treated with Amprenavir at different temperatures,[293 K];[298 K];[303 K];[310 K] (n = 3).

Table 4: Stern-Volmer quenching constants (K_{sv}) at 298 K for both wild type (WT) and variant (36T↑T) interacting with nine PIs (n = 3).

	K_{sv} (μM^{-1}) at 298K	**K_{sv} (μM^{-1}) at 298 K**
Protease Inhibitor	**WT**	**I36T↑T**
ATV	110±2	70±2
IDV	95±5	750±2
APV	87±2	81±2
RTV	83±1	41±1
DRV	82±9	51±3
NFV	76±2	56±2
SQV	69±4	22±5
LPV	57±12	29±9
TPV	48±10	37±4

To elucidate the interactive forces between the nine inhibitors and the wild type and variant HIV protease, temperature-dependent thermodynamic parameters for the

interaction between the ligand and enzymes were calculated per the Van't Hoff equation (Equation 5) and shown in Figure 5.

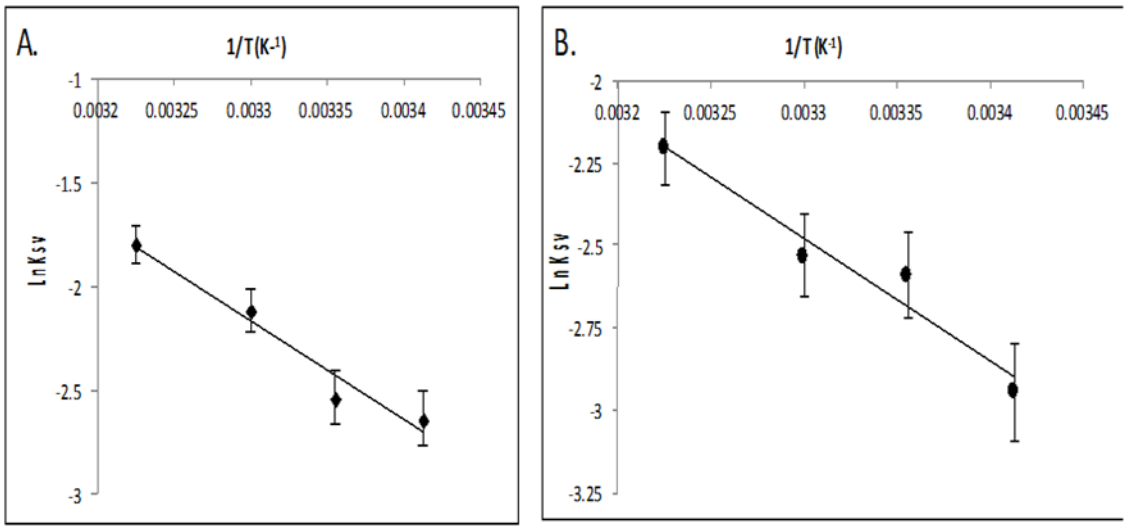

Figure 5: Examples of Van't Hoff plots for the determination of thermodynamic data (ΔH and ΔS) for the interaction of the protease inhibitor, Amprenavir, with HIV-1 protease at different temperatures. (A) Wild Type (B) Variant I36T ↑T (n = 3).

A summary of the thermodynamic parameters (ΔG, ΔH, -TΔS) are shown in table 5. The inhibitors are listed in alphabetical order. The thermodynamic data for the wildtype follow the same trend as the kinetic data, within the previous groupings. ATV was the best inhibitor against the wild type with ΔG value of -14.4±1.7 kcal/mol followed IDV with a ΔG value of 14.0±1.3 kcal/mol. LPV and TPV were the worst inhibitors against the wild type with ΔG values of -13.2±2.1 and -13.2±1.0 kcal/mol respectively. All the reactions were entropy driven as judged from the large negative values. The ΔH was positive in all but one of the inhibitors, TPV.

Table 5: A summary of experimental thermodynamic parameters for the nine commercially available HIV PR inhibitors (n = 3).

		PARAMETER		
DRUG	**PROTEASE**	**∆G (kcal/mol)**	**∆H (kcal/mol)**	**-T∆S(kcal/mol)**
APV	**WT**	-13.9±2.0	4.4±1.9	-18.3±2.0
	I36T↑T	-13.9±1.8	13.3±2.0	-27.2±2.8
ATV	**WT**	-14.4±1.7	7.4±0.5	-21.7±0.6
	I36T↑T	-12.6±1.0	20.4±2.4	-33.0±2.4
DRV	**WT**	-13.8±0.7	10.5±0.2	-24.3±7.4
	I36T↑T	-10.7±0.7	3.7±0.7	-14.3±0.8
IDV	**WT**	-14.0±1.3	4.3±0.8	-18.2±0.9
	I36T↑T	-12.8±1.2	10.4±0.7	-23.2±0.8
LPV	**WT**	-13.2±2.1	19.8±4.0	-33.0±4.3
	I36T↑T	-13.1±1.3	12.0±2.0	-25.7±2.4
NFV	**WT**	-13.5±3.0	1.4±0.1	-14.9±1.1
	I36T↑T	-10.7±0.9	4.8±0.3	-15.5±1.8
RTV	**WT**	-13.9±0.3	9.5±2.1	-23.4±2.1
	I36T↑T	-13.8±0.8	7.4±1.5	-21.1±1.5
SQV	**WT**	-13.4±1.4	7.0±1.0	-20.4±1.0
	I36T↑T	-10.9±1.3	15.0±2.3	-25.7±2.0
TPV	**WT**	-13.2±1.0	-6.1±0.2	-7.2±0.9
	I36T↑T	-10.9±0.2	-9.0±0.1	-1.9±0.1

Table 5 also shows the thermodynamic data for the variant, also in alphabetical order. The data is also in agreement with the kinetic data and can be grouped as was in the previous data. APV was the best inhibitor against the variant with a ∆G value of -13.9±1.8 kcal/mol. NFV was the worst inhibitor against the variant with a ∆G value -10.7±0.9 kcal/mol. The reaction was also entropy driven for the inhibitors except for TPV. TPV had an entropy value -1.9±0.0 that was the least of all the inhibitors. The ∆H was positive for all the inhibitors except once again for TPV.

For both the wild type and the variant ΔG was negative. The ΔG values were more negative for the wild type compared to the variant, meaning all nine inhibitors were more effective against the wild type enzyme. This was expected as the kinetic data showed that the inhibitors bind tighter to the wild type than the variant.

Significantly, the values for APV remained very close for both the wild type and variant. The range of experimental results obtained here were close to those reported for C-SA protease and other HIV-1 strains [26, 27]. The observed trend of all nine inhibitors is in agreement with our computational model data [16].

For PR in HIV it has been reported that the substrate is more amenable to changes induced by mutations at the active site being able to maintain significant affinity [28, 29]. However, inhibitor results associated with such mutations, have yielded poor responses [30, 31] , rendering most of the PIs ineffective.

In this study, the changes are in the hinge region as shown in Figure 1 and are not in the active site. Drug resistance is usually demonstrated when the IC_{50} values increase to over 20,000 pM. From our results APV, RTV, LPV and IDV appear to be able to maintain their efficacy for the C-SA and mutant variant. TPV, DRV are reported to have a best binding affinity against HIV-1 subtype B PR with ΔG values -14.6 and -15.0 kcal/mol respectively [26]. In our study, they generally showed the worst results with values of -13.2 and -13.8 kcal/mol respectively but they followed the same trend. SQV, NFV and ATV also fall within the potential drug resistant parameters. In previous work protease resistance to SQV has been shown to result from G48N and L90M mutations, which are non-active site mutations [31, 32]. These mutations are not present in the variant we are studying (I36T↑T) yet we still observed poor binding to SQV.

We propose that the decreased binding affinity for all inhibitors is the result of a conformational change to the binding pocket. This change has been brought about by a long-range effect of the alterations in the hinge region of the enzyme. In our study ATV was the best inhibitor against the wild type (14.3±1.7 kcal/mol), interestingly this is the same value reported for subtype B [26]. APV was found to be effective against subtype B, C-SA and the mutant to almost equal degree, implying that it is still a viable drug.

3 Conclusion

Several experimental techniques were employed to assess the effect of a mutation and an insertion in HIV-1 C-SA protease. The enzyme kinetic data revealed that the variant enzyme maintained its proteolytic capacity. Thermodynamic data showed a reduction in Gibb's energy, meaning the mutant enzyme binding to inhibitors was less favourable, indicating that in a clinical environment the efficacy of currently available PIs would be significantly reduced. All inhibitors exhibited good activities and should be prescribed for patients infected with C-SA. With respect to the mutant, APV, LPV and RTV should be prescribed to patients as they are more effective inhibitors. The changes for this variant occur in the hinge region of the enzyme, it would be of interest to compare these results to variants that arise from mutations in the binding site, but this is the first full evaluation of the nine FDA approved protease inhibitors for this sub-species.

4 Materials and Methods

4.1 Protein overexpression and purification

Protein overexpression was performed as described previously [18]. Briefly, HIV-1 C - SA PR and the variant I36T↑T PR were cloned into pGEX-6P-1 (GE Health Care, USA) vector and expressed in *E. coli* BL21 (DE3) cells harbouring a pLysS plasmid (Novagen, USA). The bacterial cells were harvested by centrifugation after a four hour IPTG induction period. The cells were re-suspended in ice-cold buffer A (10 mM Tris-HCl, 5 mM EDTA, 1 mM PMSF, pH 8) and ruptured by sonication. The lysate was centrifuged at 14 000 x *g*. The pellet was washed with buffer A containing 1% Triton X-100 and centrifuged at the same speed for 20 minutes. The pellet, containing inclusion bodies, and re-suspended in buffer B (10 mM Tris-HCl, 5 mM EDTA, 8 M urea, 5 mM DTT, pH 8) and kept at room temperature for 1 hour. The presence of a glutathione transferase (GST) - tagged protein was verified by SDS-PAGE and western blot analyses using GST antibodies. Protein purification was carried out using an AKTA purifier 100-950 (GE Health Care) Partial purification was carried out using a 5 mL Hitrap QFF cation exchange column (GE Health Care) and the protein of interest was eluted using a 0 – 1 M NaCl gradient. The eluted samples were desalted with using a Hitrap desalting column (GE Health Care, USA) Further purification was performed using a GSTrap affinity column (GE Healthcare, USA). The GST tag was then removed by overnight digestion at 4 ºC with precision protease (Thermo Scientific). All contents were loaded back onto the GSTrap affinity column and HIV-1 PR was collected in the flow through, refolded and stored at -70 ˚C until further use. All protease inhibitors were acquired from Aspen Pharmacare.

4.2 Enzyme kinetics studies

The enzymatic activity of the wild type and variant HIV-1 C-SA PRs was measured by following the hydrolysis of the HIV-1 fluorogenic substrate, Abz-Arg-Val-Nle-Phe(NO_2)-Glu-Ala-Nle-NH_2 as previously reported [18]. Hydrolysis of the HIV-1 fluorogenic substrate was characterized by a decrease in absorbance at 300 nm. The catalytic properties (K_m, k_{cat}, and k_{cat}/K_m) of the PRs were calculated. The enzyme kinetics parameters were determined under Michaelis-Menten reaction conditions (see Equation 1) and Lineweaver-Burk plots were constructed from the data. All enzyme catalytic activity assays were performed on a Jasco V-630 spectrophotometer.

$$\mathbf{V = V_{max}[S]/(K_m + [S])} \qquad \text{(Equation 1)}$$

In equation 1, [S] is the substrate concentration, K_m is the Michaelis constant and V_{max} is the maximum velocity of the enzyme.

4.3 Inhibition studies

The reaction rates were obtained at 37 °C by measuring the rate of fluorogenic substrate hydrolysis using 50 nM of each purified PR (wild type and variant) in 50 mM sodium acetate, 0.1 M NaCl, pH 5.0 in the presence of the chromogenic substrate (0 - 250 µM). Nine FDA approved PIs were used in this study, Atazanavir (ATV) Indinavir (IDV), Amprenavir (APV), Ritonavir (RTV), Darunavir (DRV), Nelfinavir (NFV), Saquinavir (SQV), Lopinavir (LPV), Tipranavir (TPV). The inhibitor concentrations used were 0 - 10 nM. The K_i values were estimated using a competitive inhibition equation (Equation 2) according to Williams *et al.* [33].

$$V = \frac{Vmax[S]}{Km\left(1+\frac{[I]}{Ki}\right)+[S]} \qquad \textbf{(Equation 2)}$$

[I] is the inhibitor concentration, K_m is the Michaelis constant, K_i is the inhibition constant, V and V_{max} are the velocity and the maximum velocity of the enzyme, respectively.

4.4 Determination of the vitality values

In order to compare the relative selective advantage of the variant I36T↑T PR over the wild type PR, in the presence of an inhibitor and based on their catalytic efficiency values, the vitality value (V) was determined using Equation 3 [34]. This value predicts the therapeutic effect, or advantage, of a given protease inhibitor over another.

$$\textbf{Vitality (V)} = (K_i \,.\, k_{cat}/K_m)_{MUT}/(K_i \,.\, k_{cat}/K_m)_{WT} \qquad \textbf{(Equation 3)}$$

4.5 Thermodynamic studies

Thermodynamic studies were performed according to Padayachee and Whiteley, 2013 [25]. Spectrofluorometric studies were conducted on a Jasco V-630 spectrofluorometer (Jasco International Co., LTD, Japan). These studies enabled us to determine whether any tertiary structural changes were induced in each HIV-1 PR. The reaction was followed by monitoring the interaction between each protease inhibitor and each purified enzyme. Tryptophan residues were selectively excited at 295 nm thus serving as a local probe of the immediate environment of tryptophan residues in the HIV-1 PR molecules. The emission wavelength of the tryptophan residues was monitored at 482 nm. The inhibitor concentration (1 μL) was increased incrementally and added to HIV-1 PR (5 μL)

in solution. The initial stock of inhibitor concentration (2 μM) was made up in 50 mM sodium acetate, 0.1 M NaCl, pH 5 (protease assay buffer) in a final reaction volume of 100 μL. The solution with enzyme and inhibitor was incubated for 1 minute, after which the change in fluorescence was monitored. A decrease in fluorescence at increasing concentrations of inhibitor (2, 5, 10 nM), was indicative of inhibitor quenching by the tryptophan fluorophores on the enzyme. All fluorescence quenching experiments were performed at four different temperatures (293 K, 298 K, 303 K and 310 K). Various thermodynamic parameters were calculated using Equations 4 and 5, which are derived from the Stern Volmer and Van't Hoff graphical plots, respectively, as shown in the following equations:

$$F_0/F = 1 + K_{sv}[Q] \qquad \textbf{(Equation 4)}$$

$$\ln K_{sv} = -(\Delta H/RT) + (\Delta S/R) \qquad \textbf{(Equation 5)}$$

where F_0 and F are the florescence intensities in the absence and presence of a quenching agent; respectively, K_{sv} is the Stern-Volmer constant, [Q] is the concentration of quencher (drug), ΔH is the enthalpy, ΔS is entropy, R is the gas constant and T is the absolute experimental temperature in kelvin (K).

The nine but one (TPV) FDA-approved PIs used in this study are all competitive inhibitors [21]. For pure competitive inhibition, the K_i of a drug is equal to the K_d, The Gibbs free binding energy (ΔG**)** is, therefore, calculated from Equation 6 [34].

$$\Delta G = RT\ln K_i \qquad \textbf{(Equation 6)}$$

4.6 Statistical analyses

The results are presented as the mean ± standard deviation. The significance value was set to 0.05 and data were analysed using an unpaired t-test. GraphPad Prism 7 software program was used in the data analysis [35].

CONFLICT OF INTEREST

The authors declare that they have no competing interests.

ACKNOWLEDGEMENTS

We thank the NRF, University of KwaZulu-Natal, University of the Witwatersrand, Aspen Pharmacare and MRC (SA) for financial support. The protease sequence was supplied by Professor Lynn Morris (Head: HIV Research, National Institute for Communicable Diseases, South Africa).

5 References

1. Kohl, N.E., et al., *Active human immunodeficiency virus protease is required for viral infectivity.* Proceedings of the National Academy of Sciences, 1988. **85**(13): p. 4686-4690.
2. Robins, T. and J. Plattner, *HIV protease inhibitors: their anti-HIV activity and potential role in treatment.* Journal of Acquired Immune Deficiency Syndromes, 1993. **6**(2): p. 162-170.
3. Hellen, C.U., H.G. Kraeusslich, and E. Wimmer, *Proteolytic processing of polyproteins in the replication of RNA viruses.* Biochemistry, 1989. **28**(26): p. 9881-9890.
4. Park, J.H., et al., *Binding of Clinical Inhibitors to a Model Precursor of a Rationally Selected Multidrug Resistant HIV-1 Protease Is Significantly Weaker Than That to the Released Mature Enzyme.* Biochemistry, 2016. **55**(16): p. 2390-2400.
5. Moyer, C.L., E.S. Besser, and G.R. Nemerow, *A Single Maturation Cleavage Site in Adenovirus Impacts Cell Entry and Capsid Assembly.* Journal of virology, 2016. **90**(1): p. 521-532.
6. Potempa, M., et al., *The triple threat of HIV-1 protease inhibitors*, in *The Future of HIV-1 Therapeutics*. 2015, Springer. p. 203-241.
7. Mascolini, M., *HIV DART 2008: Novel Agents, Strategies, and Assays to Control HIV.* 2009.
8. Santoro, M.M. and C.F. Perno, *HIV-1 genetic variability and clinical implications.* ISRN Microbiology, 2013. **2013**.
9. Fraser, C., et al., *Virulence and pathogenesis of HIV-1 infection: an evolutionary perspective.* Science, 2014. **343**(6177): p. 1243727.
10. Hayashi, H., et al., *Dimerization of HIV-1 protease occurs through two steps relating to the mechanism of protease dimerization inhibition by darunavir.* Proceedings of the National Academy of Sciences, 2014. **111**(33): p. 12234-12239.
11. Velazquez-Campoy, A., et al., *Structural and thermodynamic basis of resistance to HIV-1 protease inhibition: implications for inhibitor design.* Current Drug Targets-Infectious Disorders, 2003. **3**(4): p. 311-328.
12. Honarparvar, B., et al., *Integrated approach to structure-based enzymatic drug design: molecular modeling, spectroscopy, and experimental bioactivity.* Chemical reviews, 2013. **114**(1): p. 493-537.
13. Wensing, A.M., et al., *2015 Update of the Drug Resistance Mutations in HIV-1.* Topics in Antiviral Medicine™, 2015: p. 132.
14. Blanco-Heredia, J., et al., *Identification of Immunogenic Cytotoxic T Lymphocyte Epitopes Containing Drug Resistance Mutations in Antiretroviral Treatment-Naïve HIV-Infected Individuals.* PloS one, 2016. **11**(1): p. e0147571.
15. Zhan, P., et al., *Anti-HIV Drug Discovery and Development: Current Innovations and Future Trends: Miniperspective.* Journal of medicinal chemistry, 2015. **59**(7): p. 2849-2878.
16. Lockhat, H.A., et al., *Binding Free Energy Calculations of Nine FDA-approved Protease Inhibitors Against HIV-1 Subtype C I36T↑ T Containing 100 Amino Acids Per Monomer.* Chemical biology & drug design, 2016.

17. Pettersen, E.F., et al., *UCSF Chimera--a visualization system for exploratory research and analysis.* J Comput Chem, 2004. **25**(13): p. 1605-12.
18. Maseko, S.B., et al., *Purification and characterization of naturally occurring HIV-1 (South African subtype C) protease mutants from inclusion bodies.* Protein Expression and Purification, 2016. **122**: p. 90-96.
19. Maseko, S.B., et al., *Purification and characterization of naturally occurring HIV-1 (South African subtype C) protease mutants from inclusion bodies.* Protein expression and purification, 2016. **122**: p. 90-96.
20. Altman, M.D., et al., *HIV-1 protease inhibitors from inverse design in the substrate envelope exhibit subnanomolar binding to drug-resistant variants.* Journal of the American Chemical Society, 2008. **130**(19): p. 6099-6113.
21. Ali, A., et al., *Molecular basis for drug resistance in HIV-1 protease.* Viruses, 2010. **2**(11): p. 2509-2535.
22. Mosebi, S., et al., *Active Site Mutations in the South African HIV-1 Subtype C Protease Impact Significantly on Clinical Inhibitor Binding: a Kinetic and Thermodynamic Study.* Journal of Virology, 2008.
23. Kuzmič, P., et al., *High-throughput screening of enzyme inhibitors: automatic determination of tight-binding inhibition constants.* Analytical biochemistry, 2000. **281**(1): p. 62-67.
24. Szeltner, Z. and L. Polgár, *Conformational stability and catalytic activity of HIV-1 protease are both enhanced at high salt concentration.* Journal of Biological Chemistry, 1996. **271**(10): p. 5458-5463.
25. Padayachee, E. and C. Whiteley, *Etiology of Alzheimer's disease: Kinetic, thermodynamic and fluorimetric analyses of interactions of pseudo Aβ-peptides with neuronal nitric oxide synthase.* Neuropeptides, 2013. **47**(5): p. 321-327.
26. Muzammil, S., et al., *Unique thermodynamic response of tipranavir to human immunodeficiency virus type 1 protease drug resistance mutations.* Journal of virology, 2007. **81**(10): p. 5144-5154.
27. Yanchunas, J., et al., *Molecular basis for increased susceptibility of isolates with atazanavir resistance-conferring substitution I50L to other protease inhibitors.* Antimicrobial agents and chemotherapy, 2005. **49**(9): p. 3825-3832.
28. Luque, I., et al., *Molecular basis of resistance to HIV-1 protease inhibition: a plausible hypothesis.* Biochemistry, 1998. **37**(17): p. 5791-5797.
29. Mittal, S., et al., *Hydrophobic core flexibility modulates enzyme activity in HIV-1 protease.* Journal of the American Chemical Society, 2012. **134**(9): p. 4163-4168.
30. Hornak, V. and C. Simmerling, *Targeting structural flexibility in HIV-1 protease inhibitor binding.* Drug discovery today, 2007. **12**(3): p. 132-138.
31. Clemente, J.C., et al., *Comparing the accumulation of active-and nonactive-site mutations in the HIV-1 protease.* Biochemistry, 2004. **43**(38): p. 12141-12151.
32. Hong, L., et al., *Crystal structure of an in vivo HIV-1 protease mutant in complex with saquinavir: Insights into the mechanisms of drug resistance.* Protein Science, 2000. **9**(10): p. 1898-1904.
33. Kožíšek, M., et al., *Characterisation of mutated proteinases derived from HIV-positive patients: enzyme activity, vitality and inhibition.* Collection of Czechoslovak chemical communications, 2004. **69**(3): p. 703-714.

34. Kožíšek, M., et al., *Molecular analysis of the HIV-1 resistance development: enzymatic activities, crystal structures, and thermodynamics of nelfinavir-resistant HIV protease mutants.* Journal of molecular biology, 2007. **374**(4): p. 1005-1016.
35. Motulsky, H., *Analyzing data with GraphPad prism*. 1999: GraphPad Software Incorporated.

CHAPTER FOUR

Kinetic and Thermodynamic Characterization of HIV-Protease inhibitors against E35D↑G↑S Mutant in the South Africa HIV-1 Subtype C Protease.

Sibusiso B Maseko[a], Eden Padayachee[a], Thavendran Govender[a], Yasien Sayed[b], Glenn EM Maguire[a,c], Johnson Lin[d], Gert Kruger[a*]

[a] Catalysis and Peptide Research Unit, School of Health Sciences, University of KwaZulu-Natal, Durban 4001, South Africa

[b] Protein Structure-Function Research Unit, School of Molecular and Cell Biology, University of the Witwatersrand, 2050, South Africa

[c] School of Chemistry and Physics, University of KwaZulu-Natal, Durban 4001, South Africa

[d] School of Life Sciences, University of KwaZulu-Natal, Durban 4001, South Africa

Corresponding author: Kruger@ukzn.ac.za

Abstract

Resistance of HIV to antiretroviral drugs is one of the most common causes for therapeutic failure in people infected with HIV-1. Herein, we report the effect of nine FDA approved protease inhibitor drugs against a new HIV-1 subtype C mutant protease, E35D↑G↑S. The mutant has five mutations, ED35, I36G, two insertions at position 38 S and L, and D60E. Kinetics, inhibition constants, vitality, Gibbs free binding energies are reported. The E35D↑G↑S variant showed a decreased affinity for substrate and low catalytic efficiency compared to the wild type. There was a significant decrease in the binding of seven FDA approved protease inhibitors against the mutant ($p < 0.0001$). Amprenavir and ritonavir showed the least decrease, but still significant reduced activity in comparison to the wildtype (4 and 5 folds respectively, $p = 0.0021$ and 0.003 respectively). Nelfinavir and atazanavir were the worst inhibitors against the variant as seen from the IC_{50}, with values of 1401±3.0 and 685±3.0 nM respectively. The thermodynamics data showed less favourable Gibbs free binding energies for the protease inhibitors to the mutant than to the wild type.

1 Introduction.

The Human Immunodeficiency Virus (HIV) is a retrovirus from the Retroviride family and is responsible for Acquired Immune-Deficiency Syndrome (AIDS), which was first reported in 1981 [1]. This infection is controlled by the use of antiviral drugs which helps reduce the mortality and morbidity as well as promote increased patient life expectancy [2].

Protease inhibitors (PIs) are one class of antiviral drugs that target an essential viral enzyme, HIV-1 protease [3-5]. The role of HIV-1 protease in the processing of Gag and Gag-Pro-Pol polyproteins into building blocks for individual proteins essential for viral maturation, has made it one of the major targets for drug development [6]. There are currently nine FDA approved protease inhibitors [7], originally designed for type B HIV PR [8]. These inhibitors represent the most potent anti-AIDS drug reported to date and are essential components of the highly active antiretroviral therapy (HAART) [9]. HAART is credited with significantly lowering AIDS related deaths, and is currently implemented to the whole world as the standard care for HIV-AIDS treatment [9].

The emergence of drug resistant mutants in the HIV-PR has become a huge problem with the increased failure of HAART [10, 11]. Newly infected patients are infected with resistant strains, which are an added challenge in the treatment of HIV infections [12]. Herein we report the effect of a variant protease in the South African HIV-1 subtype C PR on the binding capacity of the nine commonly used PIs. The variant has the following mutations; ED35, I36G, two insertions at position 35 (S and L), and D60E and is referred to as E35D↑G↑S with the upward arrows showing positions of insertions[13]. The variant was discovered in a HIV-1 positive mother who participated in a PMTCT (Prevention of

Mother-To-Child Transmission) cohort. This mutant was discovered from different patient reported by Lockhat *et al.* and Maseko *et al.* 2017(Lockhat et al., 2016, Maseko et al., 2017). This mutant is also different from the I36TT mutant as bears to insertions compared to just one from the former. The patient received treatment with the following reverse transcriptase inhibitors (RTIs): efavirenz, d4t (stavudine) and 3TC (lamivudine). Interestingly, the patient was completely drug-naïve with respect to protease inhibitors [14].

The variant protease together with the wild type C-SA HIV protease were cloned, purified, and characterized[13]. The purified variant protease possessed weaker catalytic activity compared the wild type [13].

2 Results

2.1 Kinetic parameters

The kinetic Michaelis constant was found to be 128.6± 1.0 and 198.0±1.0 µM for the wild type (C-SA) and the mutant (E35D↑G↑S) respectively. The lower K_m for the wild type means that the wildtype exhibited higher affinity for the substrate than the mutant. The turnover numbers were determined from the slopes from Figure 2 and was found to be 1.067±0.003 and 0.446±0.001 s^{-1} for the wildtype and the mutant respectively. Again, the wildtype exhibits an increased catalytic efficiency (k_{cat}/K_m) compared to the mutant. This can be attributed by that fact that K_m for the wild type was lower than that of the mutant.

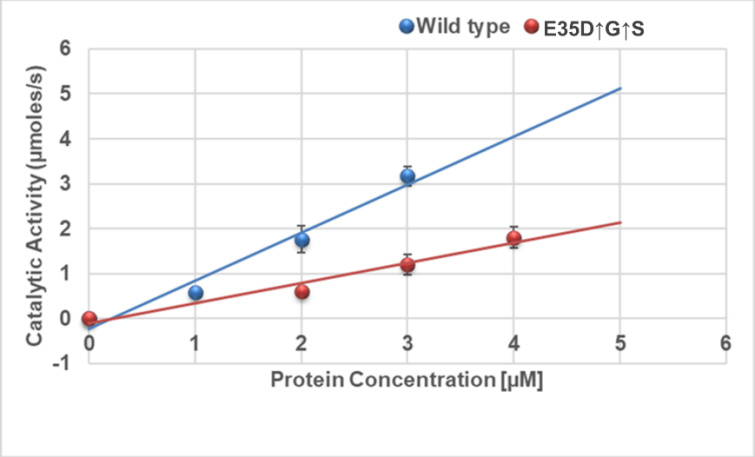

Figure 9: Determination of enzyme turn-over number. Linear curves for determining the turn-over number (k_{cat}) of the wild-type and the variant. Turn-over number was determined from the slopes of the plots. The experiments were performed at 37°C in 10 mM sodium acetate buffer, 0.1 M sodium chloride, pH 5.0, at substrate concentration of 250 µM. The experiments were conducted in triplicates and the data is reported as the mean ± SD (n = 3).

2.2 Inhibition studies.

A summary of the inhibition by the nine FDA approved PIs is shown in Figure 2. The figure shows the logarithmic K_i values for both the wild type and the mutant. For the wild

type, all the inhibitors exhibited negative log K_i values meaning all the inhibitors had K_i values less than 1.0 nM. ATV was the best inhibitor (log K_i = -1.11) against the wild type as seen from Figure 2. TPV was the poorest inhibitor (log K_i = -0.29) against the wild type. Overall, all nine inhibitors are effective against the wild type. For the mutant, only two inhibitors (APV and RTV) exhibited negative log K_i values. The other seven inhibitors showed weaker binding to the mutant, and the log K_i values of these seven inhibitors were positive. ATV, which showed the best inhibition (log K_i value of -1.11) against the wild type and yet the second weakest drug against the mutant with a log K_i value of 2.16. NFV was the worst inhibitor against the mutant with a log K_i value of 2.24. A graphical example of K_i determination is shown in figure S2.

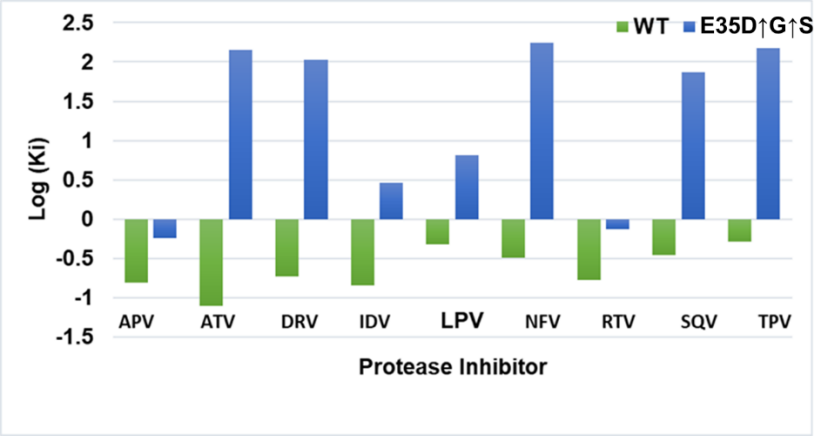

Figure 2: Inhibition constants of the wild type C-SA and the mutant in a logarithmic scale. The wild type (C-SA) is shown in green, and mutant (E35D↑G↑S) in blue (n = 3).

The IC_{50} values for the two enzymes are summarised in Table 1. IC_{50} values for the wild type are all better than 4.0 nM. This means that all the drugs are much more effective against the wild type than against the mutant. For the mutant APV and RTV were the only effective inhibitors with reasonable IC_{50} values (4.1±0.3 and 7.1±0.4 respectively). All the other inhibitors exhibited IC_{50} values above 30 nM. Again, ATV and NFV were the

worst inhibitors against the mutant with IC_{50} values of 685.0±3.0 and 1401.0±3.0 nM respectively. This data agrees with the K_i data.

Table 1. A summary of IC_{50} values for the wild type C-SA protease and the mutant (n = 3).

Inhibitor	WT IC_{50} (nM)	E35D↑G↑S IC_{50} (nM)	Fold Change (Mutant/WT)
APV	0.81±0.04	4.1±0.05	5
ATV	1.07±0.08	685.0±3.0	686
DRV	1.07±0.04	154.10±2.0	154
IDV	3.44±0.06	33.56±1.0	10
LPV	2.99±0.01	51.67±0.8	17
NFV	1.99±0.05	1401.0±3.0	704
RTV	0.78±0.01	7.1±0.40	9
SQV	0.77±0.05	114.10±1.2	148
TPV	1.55±0.02	202.70±2.6	130

2.3 Vitality

Log vitality values are shown in Figure for the E35D↑G↑S mutant protease with the corresponding inhibitor using the wild type as reference enzyme. The E35D↑G↑S mutant showed low vitality values for APV and RTV displaying log vitality values of 0.362 and 0.30 respectively. IDV and LPV had log vitality values close to 1.0. ATV showed the highest vitality value, meaning the mutant was resistant against ATV. DRV, SQV, NFV and TPV with all had log vitality values around two.

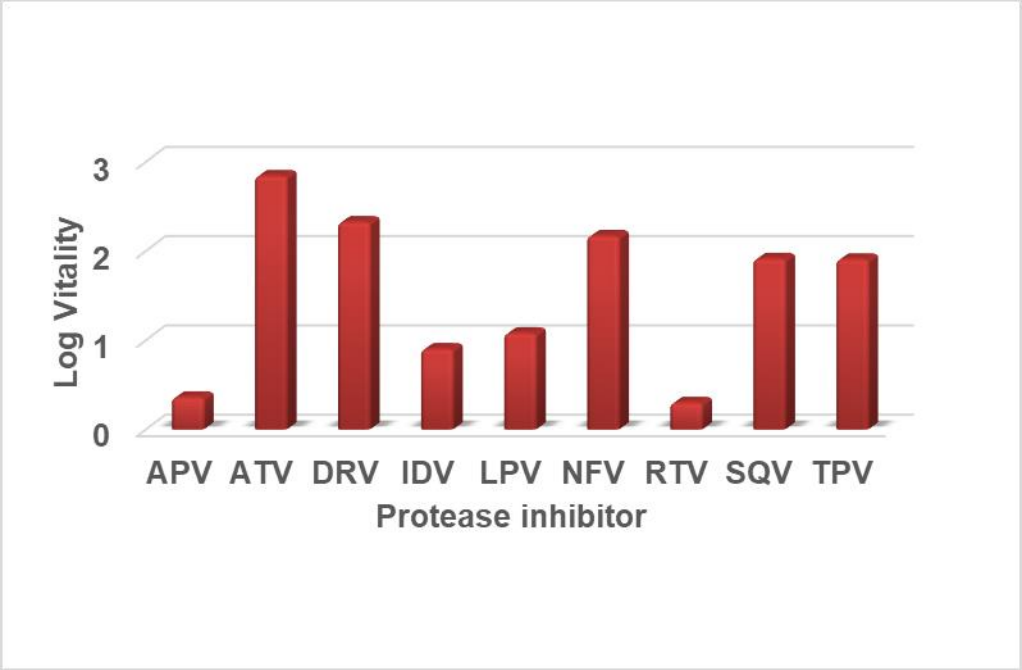

Figure 3: Log vitality values for the E35D↑G↑S mutant protease with respect to the nine inhibitors using wild type as a reference.

2.4 Quenching and thermodynamics

Thermodynamic parameters were calculated from the Stern Volmer and Van't Hoff plots (Figures S3 and S4). From these plots ΔH and ΔS values for each drug were calculated. ΔG values were calculated from the K_i values from Equation 3. A graphical presentation of the ΔG values for both the wild type and the mutant is shown in Figure 4. For the wild type, ATV was the best drug with a ΔG value of -14.35 kcal/mol. TPV displayed slightly weaker binding to the wild type with a ΔG value of -13.19 kcal/mol. All the thermodynamic reactions were entropy driven as judged from the big negative (favourable) values. The ΔH was positive (unfavourable) for all the inhibitors except for TPV.

For the variant, APV and RTV showed the best binding with ΔG values of -13.12 and -12.96 kcal/mol respectively. The other seven inhibitors showed weaker binding to the

mutant as seen from Figure 4. Again, all reactions were entropy-driven. The ΔH values were also positive for the mutant except for TPV.

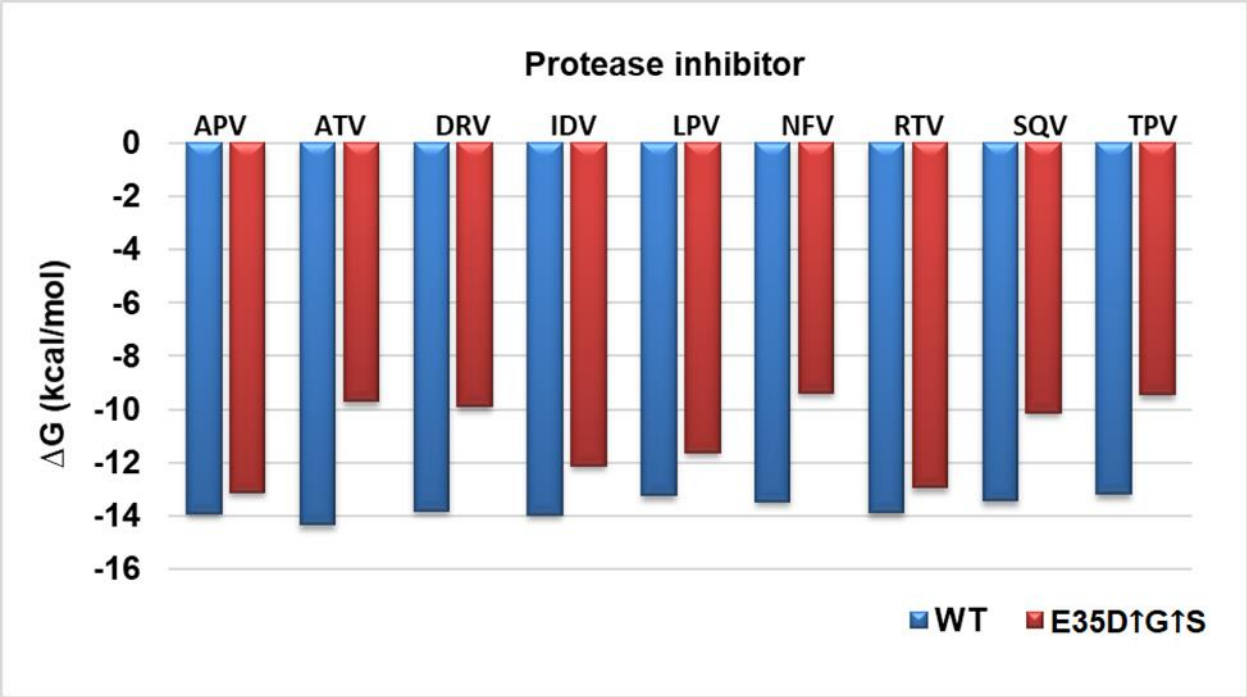

Figure 4: Gibbs free binding free energy of the E35D↑G↑S protease and the wild type C-SA HIV protease. The wild type is represented in blue whilst the E35D↑G↑S is in red.

To compare the effect of the mutations in the binding of PIs with the wildtype ΔΔG, ΔΔH and -TΔΔS values were calculated and are presented in Table 2. The values are the difference between the wild type and the mutant (mutant–wild type). From the table, it is seen that there was an overall decrease in the binding energies against the mutant. APV and RTV showed less change in the binding with ΔΔG values of 0.80 and 0.93 kcal/mol respectively. NFV and TPV showed the most decrease in binding with ΔΔG values of 4.63 and 4.10 respectively. There was no observable trend in the ΔΔH and -TΔΔS values. The K_i ratios in Table 2 show that the nine drugs had weaker binding to the mutant.

Table 2. A comparison of the difference (mutant-wildtype) between the inhibition constants and thermodynamic parameters of the wild type (C-SA) and the mutant (E35D↑G↑S).

Inhibitor	K_i Ratio	ΔΔG	ΔΔH	-TΔΔS
APV	4	0.80	12.9	12.1
ATV	1828	4.6	3.1	-1.5
DRV	560	3.9	2.1	-1.8
IDV	20	1.9	-0.1	1.8
LPV	12	1.6	-13.1	14.7
NFV	532	4.1	2.3	-1.8
RTV	5	0.9	6.8	5.8
SQV	215	3.3	2.9	0.4
TPV	292	3.7	3.2	-7.1

3 Discussion

The hinge region (residues 35-42 and 57-61) of the HIV-1 protease is closely associated with stability and movement of the flap region [15]. The flap region undergoes substantial movement allowing for substrate/inhibitor (open conformation) and form key interactions during binding of substrate/inhibitor (closed conformation) [16]. The flaps are required to display flexibility. However, increased flexibility may reduce substrate processing and binding of PIs. From the kinetic data (Figure 1), it was observed that the variant had a low affinity for substrate and reduced catalytic efficiency. This observation is in contrast with what was observed in the I36T↑T mutant we recently reported[17]. The I36T↑T mutant showed increased affinity for substrate and increased catalytic activity [17]. Both mutants (I36T↑T and E35D↑G↑S) are in the hinge region but they show different properties. E35 in HIV-PR maintains long range interactions within the PR polypeptide chain [18]. A study by Naicker *et al.* showed that the E35-R57 salt bridge (ion pair) is absent in both monomers of the C-SA HIV PR [15]. They further showed that the R57 in C-SA PR adopts a different rotamer from that of R57 in the subtype B PRs, resulting in the absence of a salt bridge. Interestingly the mutant studied here, also experience an E35D mutation, suggesting that it also does not have an E35-R57 salt bridge. The salt bridge controls movement and decrease the flexibility of the flaps [18]. The E35D mutation was reported to induce reduced binding affinities to PIs [8, 15]. The mutant being studied here showed reduced affinity for the nine FDA approved PIs as seen from the K_i and thermodynamic data. Interestingly the wild type was still susceptible to the PIs. The behaviour of the mutant could be caused by the E35D mutation. The mutant in this study though having different properties when compared to the previously reported mutant (I36T↑T) [17], they both showed weaker binding to PIs.

M36I (present in the wild type) is reported to regulate the size of the binding cavity of the protease and influence the shape of the active site [19]. This mutation is related to NFV and other PIs by complementing other mutations [19, 20]. The wild type only contains only the M36I polymorphism. The 36^{th} residue interact with residues located near the active site [19]. Mutations in this position results in the change in conformation of the binding pocket [19]. This polymorphism does not cause resistance on its own. This explains why the drugs were still effective against the wild type. Binding of the nine protease inhibitors to the wild type in this study was in the same range for reported other non-C HIV-1 proteases. The variant we are studying contain an I36G mutation and showed weaker binding to NFV and had the worst IC_{50} result (Table 2 and Figure 4) with respect to this drug. Overall, the mutant showed reduced binding to all the nine drugs. We propose that I36G together with the other mutations in E35D↑G↑S caused the reduced binding energies of the PIs.

4 Conclusion

The effect of the insertions and mutations in the C-SA HIV-PR was studied. The mutant (E35D↑G↑S) showed decreased affinity for the substrate. Binding to the nine FDA approved inhibitors was also significantly reduced for the mutant. APV and RTV can still be prescribed for patients with this mutant as their IC_{50} values are less 10 nM. The other seven drugs are much less effective. Further studies need to be done to further explain why the variant exhibit reduced binding affinities.

5 Materials and Method

5.1 Protein expression and purification

Protein expression was performed as reported previously[13]. Briefly C-SA HIV protease and mutant E35D↑G↑S were cloned in pGEX-6P-1 and expressed in *E. coli* BL21 (DE3) pLysS. Cells were harvested 4 hours after IPTG induction by centrifugation (8 000 *x g*). Cells were then re-suspended in ice cold buffer A (10 mM Tris HCl, 5mM EDTA, 1mM PMSF) ruptured by sonication and lysate was spun at 14 000 *x g*. Pellet was washed with buffer A with 1 % triton and again spun at same speed for 20 min. Pellet containing inclusion bodies was re-suspended in buffer B (10 mM Tris-HCl, 5 mM EDTA, 8 M urea, 5 mM DTT) and kept at room temperature for 1 hour. Presence of GST tagged protein was verified by SDS-PAGE and western blot using GST antibodies. Protein purification was carried out using AKTA 100-950 (GE Health Care). Partial purification was carried out using a Hitrap QFF cation exchange column (5 mL GE Health care) and the protein of interest was eluted using a NaCl gradient (0 - 1 M NaCl). Eluted samples were then desalted with using a Hitrap desalting column. Further purification was then carried using a GSTrap affinity column. GST tag was the removed by digestion with prescission protease overnight at 4 °C. All contents were then loaded back on a GSTrap affinity column and HIV protease was collected in the flow through, refolded and stored at -70 °C until further use. The purified proteases were confirmed by SDS-PAGE, Western blot and LC-MS-TOF (Central Analytical Facility, University of Stellenbosch).

5.2 Kinetic parameters

Enzymatic activity of the HIV-1 C-SA and mutant (E35D↑G↑S) protease was measured by following the hydrolysis of the HIV-PR chromogenic substrate, Lys-Ala-Arg-Val-Nle-nPhe-Glu-Ala-Nle-NH_2 as reported before [13, 17]. The substrate resembles the conserved protease cleavage site, KARVL/AEAM [8] between the capsid protein and the nucleocapsid p2 in the Gag-polyprotein precursor. Hydrolysis of the HIV chromogenic substrate was characterised by the decrease in absorbance at 300 nm. Catalytic properties such as the K_m, k_{cat}, and k_{cat}/K_m of the proteases were determined [8]. All catalytic activity assays were performed using a Jasco V-630 spectrophotometer.

5.3 Inhibition studies

Inhibition constants, K_i, for the inhibitors (Amprenavir, APV; Atazanavir, ATV; Darunavir, DRV, Indinavir, IDV; Nelfinavir, NFV; Lopinavir, LPV; Ritonavir, RTV; Saquinavir, SQV; Tipranavir, TPV) against E35D↑G↑S were obtained at 37 °C. This was done by monitoring the rate of chromogenic substrate hydrolysis using 2 µM protease in 50 mM sodium acetate, 0.1 M NaCl, pH 5, and (0 - 250 µM) substrate in increasing amounts of inhibitor (0 - 10nM).

5.4 Vitality

For comparing the relative selective advantage of a given protease mutant over the wild type in the presence of an inhibitor, the catalytic efficiency of the mutant must be included in the calculations. This is done by introducing the term ‘vitality’ which is a measure of

resistance. Vitality, v, is defined as $v = (K_i/K_{cat}/K_m)_{MUT}/(K_i/K_{cat}/K_m)_{WT}$ and predicts the therapeutic effect of a given protease inhibitor.

5.5 Quenching and Thermodynamics

Quenching experiments were performed according to the method reported by Maseko *et al* [17]. Spectrofluorometry was used to determine structural changes induced in HIV protease by the interaction of the inhibitors with the purified enzymes using Jasco V-630 spectrofluorometer (Jasco International co., LTD, Japan). The excitation wavelength was fixed at 295 nm, the wavelength at which tryptophan absorbs and the emission wavelength measured was at 482 nm. The change in fluorescence of a solution was monitored over 10 minutes, as increasing concentrations of inhibitors were added to a reaction mixture of HIV protease in 50 mM sodium acetate, 1 M NaCl, pH 5 in a final volume of 100 μL. All fluorescence quenching experiments were performed at 4 different temperatures (293 K, 298 K, 303K, 310K). The following equations are applicable [21].

$$\mathbf{F_0/F = 1 + K_{sv}Q} \qquad \textbf{(Equation 1)}$$

$$\mathbf{\ln K_{sv} = -(\Delta H/RT) + (\Delta S/R)} \qquad \textbf{(Equation 2)}$$

Where F_0 and F are the florescence in the absence and presence of quencher, K_{sv} is the Stern Volmer constant, Q is the quencher (drug), ΔH is the enthalpy, ΔS is entropy, R is the gas constant and T is the experimental temperature.

$$\mathbf{\Delta G = RT\ln K_i} \qquad \textbf{(Equation 3)}$$

5.6 Statistical analysis

Experiments were done in triplicates and results were presented as the mean ± standard deviation. Significance was set to 0.05 and the data was analysed using unpaired t-test. GraphPad Prism 7 software program was used [22].

CONFLICT OF INTEREST

The authors declare that they have no competing interests.

ACKNOWLEDGEMENTS

We thank the NRF, University of KwaZulu-Natal, University of the Witwatersrand, Aspen Pharmacare and MRC (SA) for financial support. The protease sequence was supplied by Professor Lynn Morris (Head: HIV Research, National Institute for Communicable Diseases, South Africa)

6 References

1. Behbahani, M. and E. Mohammadi, *Construction of pseudotyped human immunodeficiency virus for evaluation of anti-HIV drugs.* Research in Pharmaceutical Sciences, 2012. **7**(5): p. S427.
2. Palella Jr, F.J., et al., *Declining morbidity and mortality among patients with advanced human immunodeficiency virus infection.* New England Journal of Medicine, 1998. **338**(13): p. 853-860.
3. Arts, E.J. and D.J. Hazuda, *HIV-1 antiretroviral drug therapy.* Cold Spring Harbor perspectives in medicine, 2012. **2**(4): p. a007161.
4. Ghosh, A.K., Z.L. Dawson, and H. Mitsuya, *Darunavir, a conceptually new HIV-1 protease inhibitor for the treatment of drug-resistant HIV.* Bioorganic & medicinal chemistry, 2007. **15**(24): p. 7576-7580.
5. Ali, A., et al., *Molecular basis for drug resistance in HIV-1 protease.* Viruses, 2010. **2**(11): p. 2509-2535.
6. Konvalinka, J., H.-G. Kräusslich, and B. Müller, *Retroviral proteases and their roles in virion maturation.* Virology, 2015. **479–480**: p. 403-417.
7. Pokorná, J., et al., *Current and novel inhibitors of HIV protease.* Viruses, 2009. **1**(3): p. 1209-1239.
8. Velazquez-Campoy, A., Y. Kiso, and E. Freire, *The binding energetics of first-and second-generation HIV-1 protease inhibitors: implications for drug design.* Archives of Biochemistry and Biophysics, 2001. **390**(2): p. 169-175.
9. Crepaz, N., T.A. Hart, and G. Marks, *Highly active antiretroviral therapy and sexual risk behavior: a meta-analytic review.* Jama, 2004. **292**(2): p. 224-236.
10. Muzammil, S., P. Ross, and E. Freire, *A major role for a set of non-active site mutations in the development of HIV-1 protease drug resistance.* Biochemistry, 2003. **42**(3): p. 631-638.
11. Ghosh, A.K., et al., *Design of HIV protease inhibitors targeting protein backbone: an effective strategy for combating drug resistance.* Accounts of chemical research, 2007. **41**(1): p. 78-86.
12. Hou, T. and R. Yu, *Molecular dynamics and free energy studies on the wild-type and double mutant HIV-1 protease complexed with amprenavir and two amprenavir-related inhibitors: mechanism for binding and drug resistance.* Journal of medicinal chemistry, 2007. **50**(6): p. 1177-1188.
13. Maseko, S.B., et al., *Purification and characterization of naturally occurring HIV-1 (South African subtype C) protease mutants from inclusion bodies.* Protein expression and purification, 2016. **122**: p. 90-96.
14. Lockhat, H.A., et al., *Binding free energy calculations of nine FDA-approved protease inhibitors against HIV-1 subtype C I36T↑ T containing 100 amino acids per monomer.* Chemical biology & drug design, 2016. **87**(4): p. 487-498.
15. Naicker, P., et al., *Structural insights into the South African HIV-1 subtype C protease: impact of hinge region dynamics and flap flexibility in drug resistance.* Journal of Biomolecular Structure and Dynamics, 2013. **31**(12): p. 1370-1380.
16. Gustchina, A. and I.T. Weber, *Comparison of inhibitor binding in HIV-1 protease and in non-viral aspartic proteases: the role of the flap.* FEBS letters, 1990. **269**(1): p. 269-272.

17. Maseko, S.B., et al., *I36T↑ T mutation in South African subtype C (C-SA) HIV-1 protease significantly alters protease-drug interactions.* Biological Chemistry, 2017.
18. Swairjo, M.A., et al., *Structural role of the 30's loop in determining the ligand specificity of the human immunodeficiency virus protease.* Biochemistry, 1998. **37**(31): p. 10928-10936.
19. Ode, H., et al., *Computational characterization of structural role of the non-active site mutation M36I of human immunodeficiency virus type 1 protease.* Journal of molecular biology, 2007. **370**(3): p. 598-607.
20. Kaldor, S.W., et al., *Viracept (nelfinavir mesylate, AG1343): a potent, orally bioavailable inhibitor of HIV-1 protease.* Journal of medicinal chemistry, 1997. **40**(24): p. 3979-3985.
21. Kožíšek, M., et al., *Molecular analysis of the HIV-1 resistance development: enzymatic activities, crystal structures, and thermodynamics of nelfinavir-resistant HIV protease mutants.* Journal of molecular biology, 2007. **374**(4): p. 1005-1016.
22. Motulsky, H., *Analyzing data with GraphPad prism*. 1999: GraphPad Software Incorporated.

CHAPTER FIVE

Crystallization and ^{15}N labelling of the Wildtype and two Mutant HIV-1 Proteases for Structural Studies

1 Brief Introduction

This short chapter reports cloning of the inactive form of the wild type HIV PR and the two mutants. As the quantitative (enzyme kinetics and inhibition) data of the proteases is now available it would be interesting to understand structurally how the drugs interact with the specific residues in the enzyme. The active site (Asp 25) was replaced with asparagine, and a mutation was employed [1]. The mutations do not affect the overall structure of the enzyme [1]. As crystallography and NMR studies take a significant period of time, the mutations, particularly D25N, help avoid autocatalysis [2]. The proteins were then purified in bulk for crystal growth and ^{15}N labelled for future NMR studies.

2 Materials and Methods

2.1 Proteins expression

Synthetic genes encoding the 99,100 and 101 amino acids for the inactive wild type and inactive mutants $^{WT}PR_{D25N}$, $^{I36T\uparrow T}PR_{D25N}$ and $^{E35D\uparrow G\uparrow S}PR_{D25N}$ were obtained from Genescript (USA). A TEV site was added in the N-terminus to facilitate His-tag removal and cloned in pET302 Champion vector (Thermo Scientific) flanked by EcoRI and XhoI sites, and transformed into *E. coli* BL-21 DE3 [3]. Expression was performed in Luria Bertani medium or in minimal medium for isotope labelling using IPTG induction. ^{15}N ammonium chloride was used as the sole nitrogen source for isotopic labelling in M9 minimal media [4].

2.2 Protein purification

The expressed proteins were purified using affinity chromatography. Briefly, the cells from 1 L of culture were harvested by centrifugation at 8000 *x g*. The cell pellet was then the dissolved in ice cold buffer A (50 mM Tris, pH 8, 1.0 mM TCEP, 1 mM PMSF) and then sonicated in ice. The mixture was then clarified by centrifugation at 14 000 *x g*. About 40 % of the HIV-1 protease was found in the soluble fraction, thus the supernatant was used to purify the enzymes. The crude supernatant was loaded to a His trap cobalt 5 column connected to the AKTA system (GE Health Care, Sweden) previously equilibrated with 5 column volumes of buffer B (50 mM Na_2PO_4, pH 7.4, 5 mM imidazole,300 mM NaCl. The column was then washed with two column volumes of the same buffer to remove unbound proteins. Bound proteins were using a liner imidazole (0 - 150 mM) gradient in buffer C (50 mM Na_2PO_4, pH 7.4, 150 imidazole, 300 mM NaCl). The proteins were then dialyzed to remove imidazole, the His tag was removed by TEV digestion. The cleavage mixture was then loaded back on to the column to remove the TEV and His tag. Pure tag-protease was collected from the flow through.

2.3 Far-UV circular dichroism of the $^{WT}PR_{D25N}$, $^{I36T\uparrow T}PR_{D25N}$ and $^{E35D\uparrow G\uparrow S}PR_{D25N}$ HIV-1 proteases

Far-UV (250 - 190 nm) CD spectra arising from peptide bond absorption was used to give information about the backbone secondary structures of the wild-type and mutant proteins. The experiments were performed using 10 µM protein concentrations in 10 mM sodium acetate buffer, pH 5 (Figure 1). CD spectra for $^{WT}PR_{D25N}$, $^{I36T\uparrow T}PR_{D25N}$ and $^{E35D\uparrow G\uparrow S}PR_{D25N}$ variant proteins were recorded from a Jasco model J-810

spectropolarimeter using a cuvette of 2 mm path length at 20 °C. Replicate scans were obtained at a 0.1 nm data pitch, 0.1 nm bandwidth and a scan speed of 50 nm/min. Spectra were averages of 10 scans with the baseline or buffer control subtracted from 250 to 190 nm in 0.1 nm increments [5].

2.4 Crystallization of protein.

A total of four crystallization screens from Molecular dimension™ were used to determine conditions for crystal growth [6]. Each screen contains 96 conditions. The screens were, (1) PACT, a pH, Anion, Cation crystallization trial devised to test pH within a PEG/Ion screen, (2) Index, (3) MIDAS, a Modern Intelligent Dynamic Alternative Screen and is based on alternative polymeric precipitants, (4) ProPlex, formulated for the crystallization of **Pro**tein com**Ple**xes [7]. Equal volume (0.1 µL of protein (4 mg/ml in 10 mM sodium acetate containing 1 mM TCEP) and reservoir solution from each screen in a 96 well plate format was mixed, and the plates were then sealed and kept at 16 °C in a crystallization robot. Crystal growth was monitored daily. Crystals started appearing after 4 - 7 days (Figure 2). These were then used as seeds for growing crystals in a bigger volume using the hanging drop method.

3 Results

3.1 Far UV-CD

Circular dichroism was used as a probe to compare the secondary structure of the proteins. Far-UV CD (250 - 190 nm) spectra is shown in Figure 1 and it is shown that the proteins exhibited a minimum of about 216 nm, typical for predominantly β-sheet content.

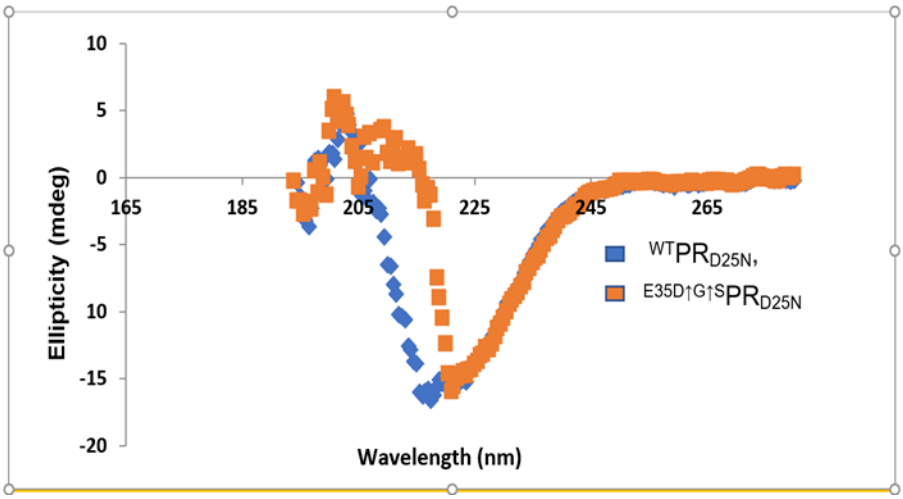

Figure 10: Far-UV circular dichroism spectra of the $^{WT}PR_{D25N}$ and $^{E35D\uparrow G\uparrow S}PR_{D25N}$ HIV-1 proteases. The data from 10 runs were collected from 250 nm to 200 nm and averaged. Experiments were performed in 10 mM sodium acetate buffer, pH 5, containing 10 µM protein solutions.

3.2 Protein crystallization

Out of the four screens performed, crystals were obtained from only one (INDEX) condition number 30, which contains a solution of 0.1 M sodium chloride, 0.1 M Bis Tris pH 6.5 and 1.5 M ammonium sulfate. An image of the solution and crystals are shown in Figure 2.

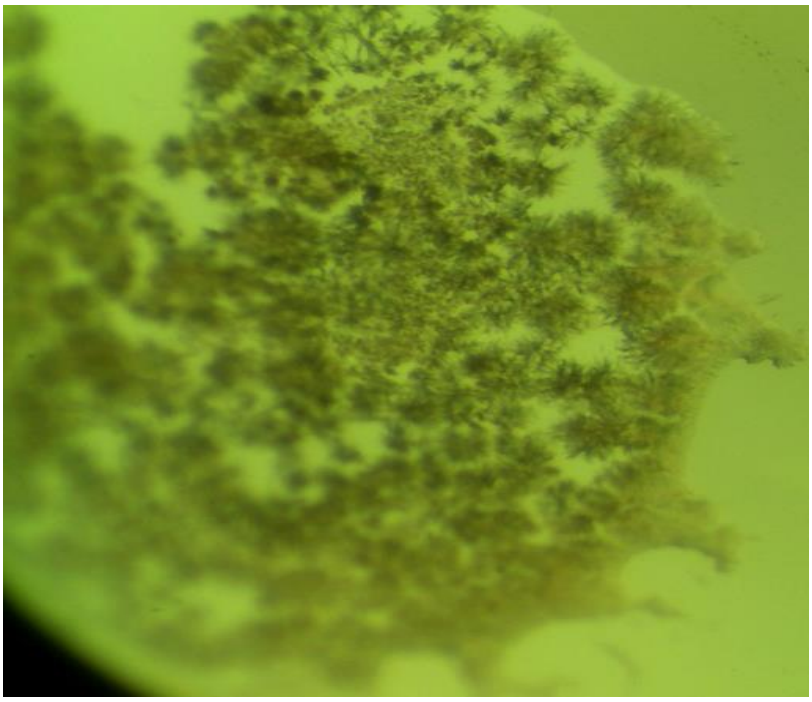

Figure 2: Crystals obtained from of the C-SA HIV-1 protease. Crystals appeared in 7 to 10 days in the INDEX screen which has a solution of 0.1 M sodium chloride, 0.1 M Bis Tris pH 6.5 and 1.5 M ammonium sulfate.

4 Future Perspective

In future, these crystals will be optimized, harvested and taken for three-dimensional structural determination of the variants. This will hopefully give a deeper understanding of the interactions involved between the C-SA proteins and inhibitors.

5 References

1. Sayer, J.M., et al., *Effect of the active-site D25N mutation on the structure, stability and ligand binding of the mature HIV-1 protease.* Journal of Biological Chemistry, 2008.
2. Agniswamy, J., et al., *Structural studies of a rationally selected multi-drug resistant HIV-1 protease reveal synergistic effect of distal mutations on flap dynamics.* PloS one, 2016. **11**(12): p. e0168616.
3. Coleman, A.S. and U. Pal, *BBK07, a dominant in vivo antigen of Borrelia burgdorferi, is a potential marker for serodiagnosis of Lyme disease.* Clinical and Vaccine Immunology, 2009. **16**(11): p. 1569-1575.
4. Kilpatrick, E.L., et al., *Expression and characterization of 15N-labeled human C-reactive protein in Escherichia coli and Pichia pastoris for use in isotope-dilution mass spectrometry.* Protein expression and purification, 2012. **85**(1): p. 94-99.
5. Naicker, P., et al., *Structural insights into the South African HIV-1 subtype C protease: impact of hinge region dynamics and flap flexibility in drug resistance.* Journal of Biomolecular Structure and Dynamics, 2013. **31**(12): p. 1370-1380.
6. Newman, J., et al., *Towards rationalization of crystallization screening for small-to medium-sized academic laboratories: the PACT/JCSG+ strategy.* Acta Crystallographica Section D: Biological Crystallography, 2005. **61**(10): p. 1426-1431.
7. Gatreddi, S., S. Are, and I.A. Qureshi, *Ribokinase from Leishmania donovani: purification, characterization and X-ray crystallographic analysis.* Acta Crystallographica Section F: Structural Biology Communications, 2018. **74**(2): p. 99-104.

CHAPTER SIX

Overall conclusion of the research outcome

1. Conclusion

HIV-1 is one of the highly studied viral infections worldwide [1, 2]. Many of these studies are based on the molecular understanding of the virus and are aimed at improving drug design to help reduce the spread of the virus within its host. HIV reverse transcriptase, integrase and protease are important HIV enzymes and also the predominant drug targets [3, 4]. The design of drugs inhibiting these enzymes is necessary for blocking the replication of the virus and has formed part of the mainstream research for over two decades [5]. As mentioned previously, the protease is responsible for the proteolytic cleavage of the Gag and Gag-Pol polyproteins, required for the development of mature virion proteins [6]. So therefore, blocking or inhibiting this enzyme stops the replication of the virus, and studies on this enzyme date back to over two decades [7].

In this chapter the summation of the thesis is presented. Provided in the first chapter is a general background review and the life cycle of HIV-1. It also brings forth more on the problem statement and emphasis was placed on HIV protease inhibition and resistance. The chapter also highlights briefly a new highly potent HIV-1 drug that targets the viral capsid offering 95 % inhibition for up to 10 weeks, as well as an overview of quantitative and molecular techniques used in enzymology.

Chapter 2 reports an efficient procedure for recovering of HIV-1 protease from inclusion bodies. It also provides solutions to the difficulties that are often faced by researchers

when expressing this enzyme. The HIV-1 protease was cloned into seven vectors containing fusion tags to optimize expression and solubility. Expression of the PR with larger fusion tags is key (GST, TRX) as it resulted in better expression compared to untagged or using His-tag only. Though GST had greater expression, the recovery yield was low due to high aggregation, with only about 0.2 mg/L of active PR recovered. Trx was the best fusion tag to recover the enzyme with about 5 mg/L of culture with a high specific activity.

The next phase of this study (Chapter 3) was aimed at investigating the effect of I36T↑T insertion mutation in the protease on the efficacy of nine FDA approved inhibitors. The mutant showed a higher affinity to the natural substrate as seen from the lower K_M. Generally, the nine inhibitors showed weaker binding to the mutant as compared to the wild type. The thermodynamics data revealed a reduction in Gibb's energy, meaning the mutant enzyme binding to inhibitors was less favourable, indicating that in a clinical environment the efficacy of currently available PIs would be significantly reduced. This data is consistent with our computational studies as the theoretical binding of inhibitors followed the same trend [8]. With respect to the I36T↑T mutant, APV, LPV and RTV can still be prescribed to patients harbouring this mutant as they are more effective inhibitors.

Chapter 4 reports on the interaction between the double insertion mutation (E35D↑G↑S) and the nine FDA approved inhibitors. Interestingly this mutant had shown slightly lower affinity for the natural substrate (high K_M) compared to the wildtype enzyme. Binding of the nine PIs was significantly reduced for the mutant compared to the wildtype. Nelfinavir and atazanavir were the weakest inhibitors against the variant as seen from the IC_{50}, with

values of 1401±3.0 and 685±3.0 nM respectively. For patients harbouring this mutant APV and RTV can still be prescribed as they rendered the best inhibition.

Chapter five provides necessary information on the conditions required to crystalize these proteins. The crystal appeared after 7- 10 days of incubation in a solution of 0.1 M sodium chloride, 0.1 M Bis Tris pH 6.5 and 1.5 M ammonium sulfate. The expression of the proteases was also optimized in ^{15}N minimal media for future NMR studies.

Future studies will involve optimization of crystal growth for diffraction and structure elucidation. These will be done in both the absence and presence of protease inhibitors. The crystallography data will be supplemented with NMR studies of the ^{15}N labelled proteins. It will give a deeper insight on how the two mutants interact with specific residues within the protease molecule. The information will be used for designing new inhibitors for these mutants. Again, mutants that are resistant to most PIs could prove to be an excellent prototype to design inhibitors that overcome drug resistance induced by distal mutations.

2 References

1. Cohen, M.S., et al., *Antiretroviral therapy for the prevention of HIV-1 transmission.* New England Journal of Medicine, 2016. **375**(9): p. 830-839.
2. Sallam, M., et al., *Genetic characterization of human immunodeficiency virus type 1 transmission in the Middle East and North Africa.* Heliyon, 2017. **3**(7): p. e00352.
3. Mehellou, Y. and E. De Clercq, *Twenty-six years of anti-HIV drug discovery: where do we stand and where do we go?* J. Med. Chem, 2010. **53**(2): p. 521-538.
4. Wensing, A.M., et al., *2017 Update of the Drug Resistance Mutations in HIV-1.* Topics in antiviral medicine, 2017. **24**(4): p. 132-133.
5. Saladini, F., et al., *Agreement between an in-house replication competent and a reference replication defective recombinant virus assay for measuring phenotypic resistance to HIV-1 protease, reverse transcriptase, and integrase inhibitors.* Journal of clinical laboratory analysis, 2018. **32**(1).
6. Maseko, S.B., et al., *Purification and characterization of naturally occurring HIV-1 (South African subtype C) protease mutants from inclusion bodies.* Protein expression and purification, 2016. **122**: p. 90-96.
7. Wensing, A.M., N.M. van Maarseveen, and M. Nijhuis, *Fifteen years of HIV Protease Inhibitors: raising the barrier to resistance.* Antiviral research, 2010. **85**(1): p. 59-74.
8. Lockhat, H.A., et al., *Binding free energy calculations of nine FDA-approved protease inhibitors against HIV-1 subtype C I36T↑ T containing 100 amino acids per monomer.* Chemical biology & drug design, 2016. **87**(4): p. 487-498.

APPENDIX

1 Supplementary Information for Chapter Two

Optimized procedure for recovering HIV-1 protease (C-SA) from inclusion bodies

Sibusiso B Maseko[a], Deidre Govender[a], Thavendran Govender[a], Tricia Naicker[a], Johnson Lin[b], Glenn E.M. Maguire[ac], Gert Kruger[a. *]

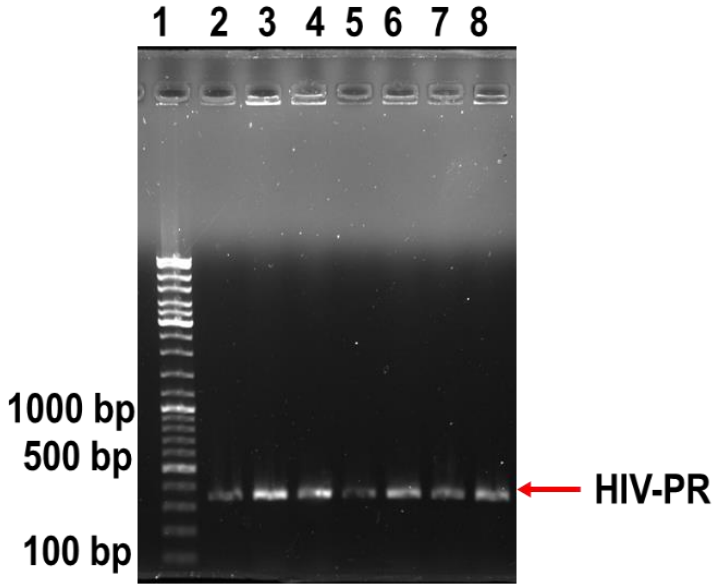

Figure S1: Agarose gel electrophoresis of amplified HIV-PR gene. Each band correspond to an amplification of the HIV-PR gene using vector specific primers.

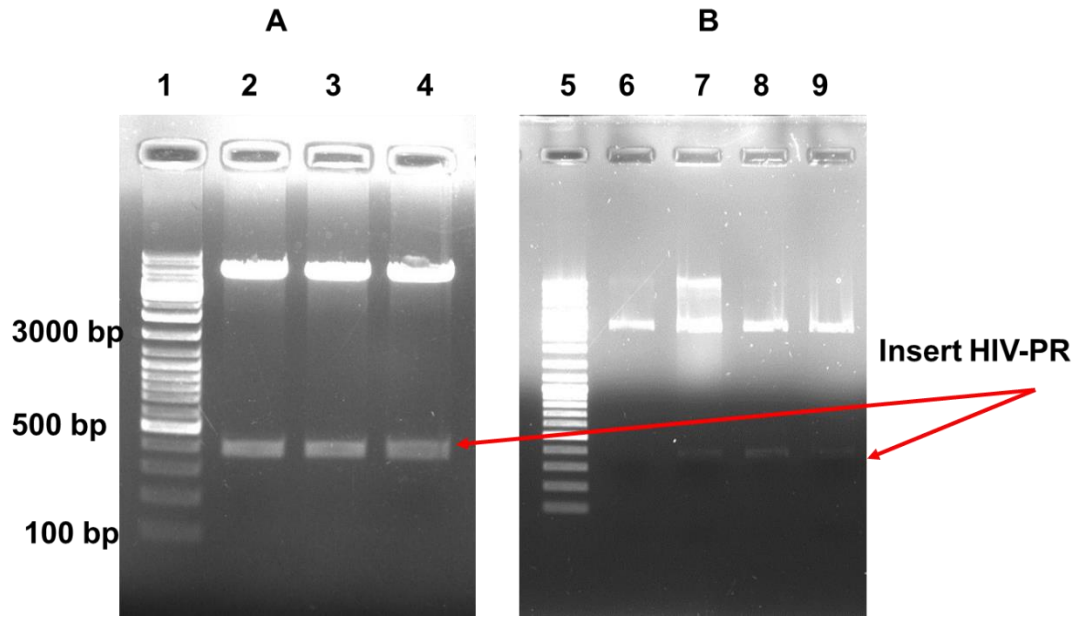

Figure S2: Confirmation of clones from each of the seven vectors used. Plasmid from each of the clones were isolated and restricted to with the specific restriction enzymes.

```
HIV-PR          ------------------------------------------------------CCGCAG    6
T7promoter      AGCCATCATCATCATCATCACAGCAGCGGCCTGGTGCCGCGCGGCAGCCATATGCCGCAG    120
                                                                      ******

HIV-PR          ATCACTCTGTGGAAACGTCCGCTGGTATCCATCAAAGTCGGTGGTCAGATCAAAGAAGCT    66
T7promoter      ATCACTCTGTGGAAACGTCCGCTGGTATCCATCAAAGTCGGTGGTCAGATCAAAGAAGCT    180
                ************************************************************

HIV-PR          CTGCTGGACACTGGCGCTGACGACACTGTTCTGGAAGAAATCAATCTGCCGGGTAAATGG    126
T7promoter      CTGCTGGACACTGGCGCTGACGACACTGTTCTGGAAGAAATCAATCTGCCGGGTAAATGG    240
                ************************************************************

HIV-PR          AAGCCGAAAATGATCGGTGGCATCGGCGGTTTTATCAAAGTTCGTCAGTATGATCAGATC    186
T7promoter      AAGCCGAAAATGATCGGTGGCATCGGCGGTTTTATCAAAGTTCGTCAGTATGATCAGATC    300
                ************************************************************

HIV-PR          CTGATCGAAATCTGCGGTAAAAAAGCTATCGGTACCGTTCTGGTTGGTCCGACTCCGGTT    246
T7promoter      CTGATCGAAATCTGCGGTAAAAAAGCTATCGGTACCGTTCTGGTTGGTCCGACTCCGGTT    360
                ************************************************************

HIV-PR          AACATCATCGGCCGTAACATGCTGACTCAGCTGGGTTGCACTTTGAACTTC---------    297
T7promoter      AACATCATCGGCCGTAACATGCTGACTCAGCTGGGTTGCACTTTGAACTTCGGATCCGAA    420
                *************************************************
```

Figure S3: Sequence alignment of HIV-PR gene with sequencing data. T7 promoter primers were used to sequence the multiple cloning site in order to confirm successful cloning.

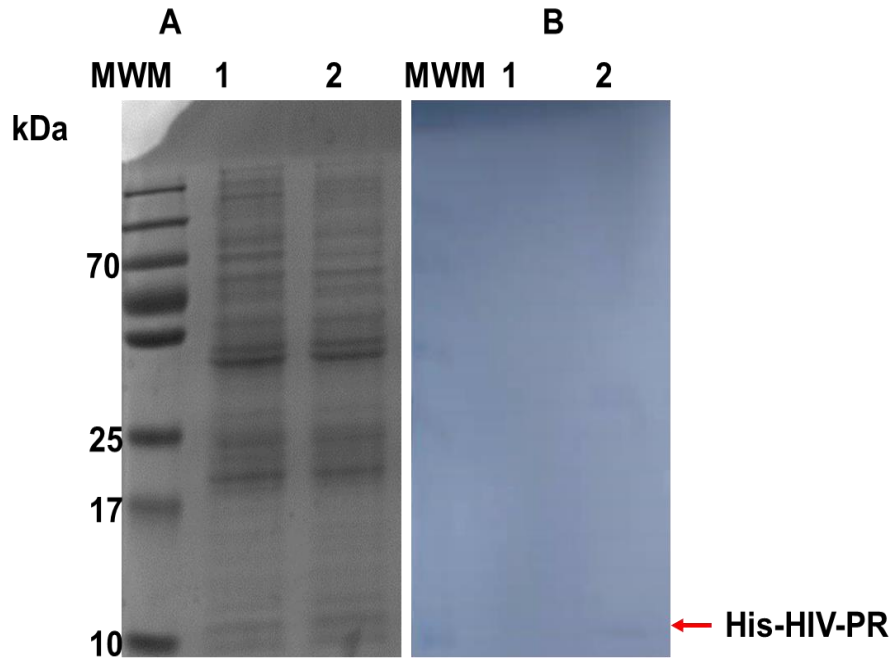

Figure S4: SDS PAGE and western blot confirming expression in pET28a. A, SDS-PAGE, B western blot, MWM, Molecular weight marker 1, induced sample and 2 uninduced sample

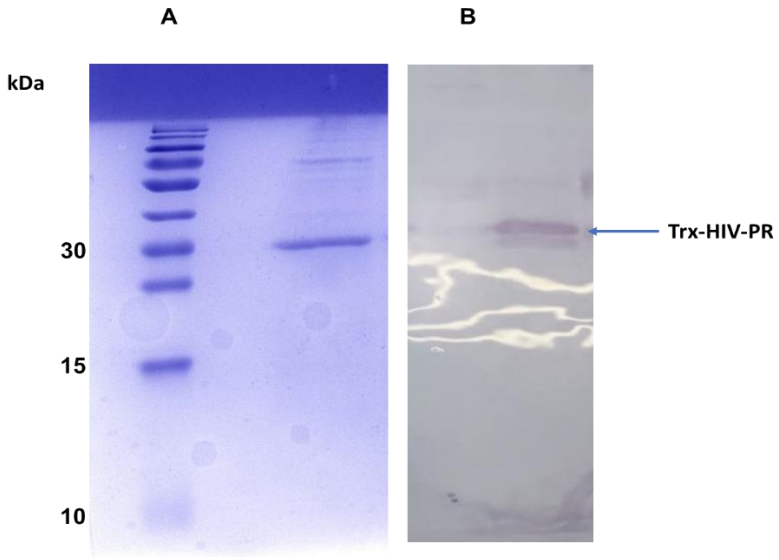

Figure S5: SDS PAGE and western blot confirming expression in pET32a. A, SDS-PAGE, B western blot,

Table S1: Protein fragments obtained from LC-MS-TOF

	Protein Fragments from sequencing		
Accession Number	**Description**	**Score**	**Molecular Weight(kDa)**
Q73368	Gag-Pol polyprotein	744	161.4
Q75002	Gag-Pol polyprotein	196	162.1
B3CJR9	Protease and reverse transcriptase	587	67.3
H6SH68	Polyprotein	498	56.9
V6BSA8	Protease and reverse transcriptase	573	65.6

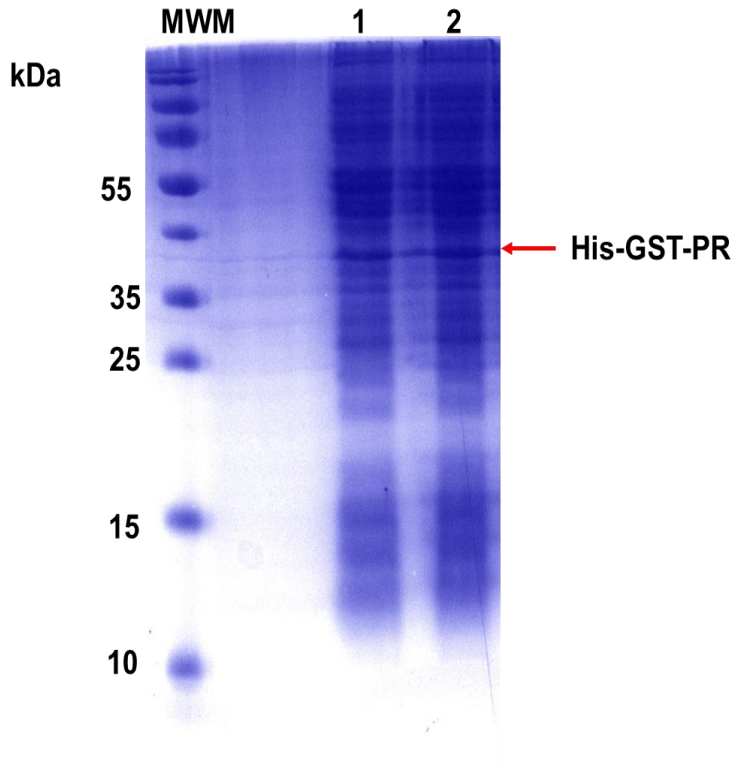

Figure S6: SDS-PAGE showing protein expression in pET41b. MWM, molecular weight marker, 1 uninduced sample,2 induced sample

2 Supplementary Information for Chapter Three

I36T↑T Mutation in South African Subtype C (C-SA) HIV-1 Protease Significantly Alters Protease-Drug Interactions

Sibusiso B Maseko[a], Eden Padayachee[a], Thavendran Govender[a], Yasein Sayed[b], Gert Kruger[a*], Glenn E.M Maguire[ac], Johnson Lin[d.]

The figure below shows the positions of the tryptophan within the HIV-1 C-SA protease

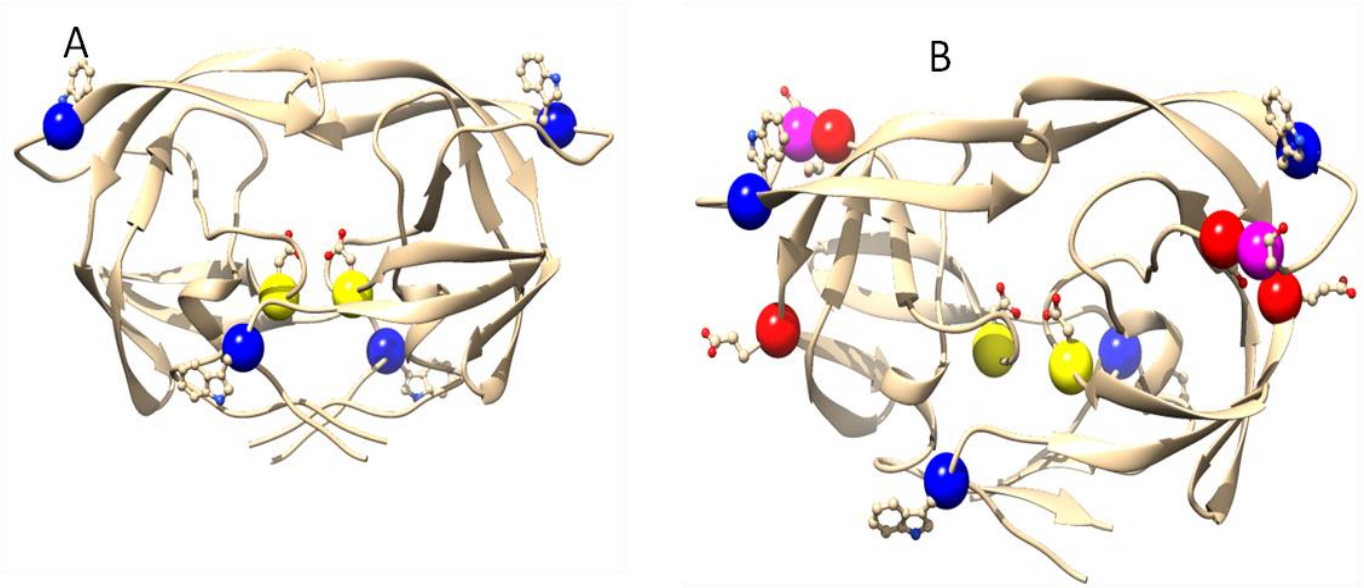

Figure S1. Figure 1. A ribbon presentation of Wild type C-SA HIV protease (A) and I36T↑T mutant (B). Shown in yellow is the aspartic residues (Asp 25.25') Insertion mutations are shown in pink. The red spheres are amino acid mutations. Tryptophan 3 residues are shown in blue (created using UCSF Chimera version 1).

Inhibition studies

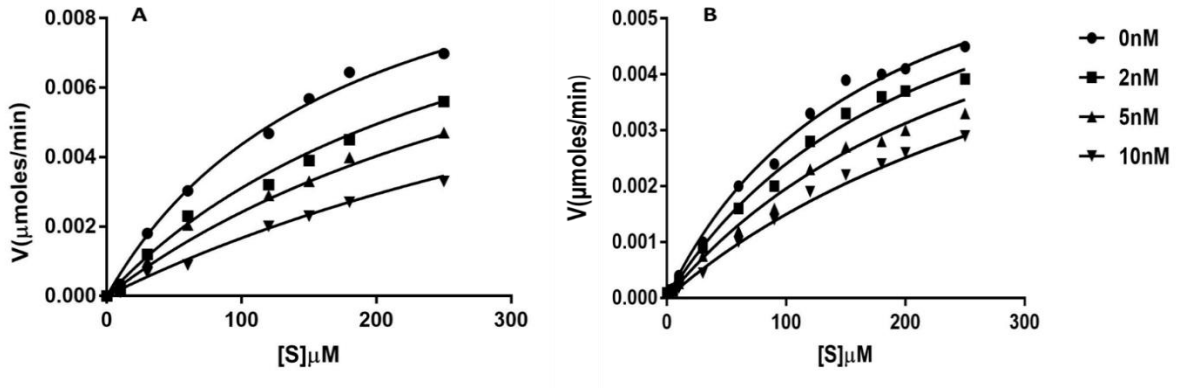

Figure S2: Inhibition (K_i) of the protease activities of wild type [A] and I36T↑T [B] by APV. The reaction mix contained an increasing substrate concentration (0 - 250 μM); Protease enzyme (50 nM), protease inhibitor (0 - 10 nM) in a 96-well plate with a total volume of 100 μL (n = 3).

Table 3: Stern Volmer quenching constants (K_{sv}) at different temperatures for both wild type (WT) and mutant (36T↑T)

Temp.	293 K	298 K	303 K	310 K		293 K	298 K	303 K	310 K
APV	K_{sv} (nM^{-1})				ATV	K_{sv} (nM^{-1})			
WT	0.0436 ±0.0042	0.0867±0.002	0.08724 ±0.0091	0.0885 ±0.0426	WT	0.1040 ±0.0066	0.1140 ±0.0021	0.1420 ±0.0037	0.1720 ±0.0311
I36T↑T	0.0217 ±0.0050	0.0805±0.0018	0.08514 ±0.0055	0.0861 ±0.0199	I36T↑T	0.0454 ±0.0074	0.0704 ±0.0227	0.1400 ±0.0354	0.1820 ±0.0021
DRV	293 K	298 K	303 K	310 K	IDV	293 K	298 K	303 K	310 K
WT	0.0287 ±0.0075	0.0822±0.0094	0.0813 ±0.0028	0.1490 ±0.0060	WT	0.0067 ±0.0237	00.0949±0.087	0.0933 ±0.0154	0.1090 ±0.0220
I36T↑T	0.0484 ±0.0038	0.0508±0.0028	0.0648 ±0.0036	0.0683 ±0.0033	I36T↑T	0.0450 ±0.0107	0.0747±0.0021	0.0605 ±0.0166	0.0883 ±0.0164
LPV	293 K	298 K	303 K	310 K	RTV	293 K	298 K	303 K	310 K
WT	0.0384 ±0.0161	0.0572±0.0121	0.1490 ±0.0216	0.1700 ±0.0158	WT	0.0805 ±0.0086	0.0828±0.001	0.1072 ±0.0015	0.1730 ±0.0364
I36T↑T	0.0208 ±0.0282	0.0287±0.0086	0.1390 ±0.0272	0.1730 ±0.0147	I36T↑T	0.0356 ±0.0085	0.041±0.001	0.0795 ±0.0200	0.1030 ±0.0021
TPV	293	298	303	310	SQV	293 K	298 K	303 K	310 K
WT	0.0384±0.01	00.0484±0.01	0.1072 ±0.0015	0.1730 ±0.0364	WT	0.0408 ±0.0017	0.0686±0.0042	0.0669 ±0.0120	0.0819 ±0.0011
I36T↑T	0.0156 ±0.0085	0.0366±0.0004	0.0795 ±0.0200	0.1030 ±0.0021	I36T↑T	0.0106 ±0.0033	00.0217±0.005	0.0711 ±0.0033	0.0933 ±0.0018
NFV	293	298	303	310	NFV	293K	298K	303K	310K
I36T↑T	0.0484 ±0.0038	0.0561±0.002	0.0648 ±0.0036	0.0683 ±0.0033	WT	0.0450 ±0.0107	0.0759±0.002	0.0605 ±0.0166	0.0883 ±0.0164

3 Supplementary Information for Chapter Four

Kinetic and Thermodynamic Characterization of HIV-Protease inhibitors against E35D↑G↑Smutant in the South Africa HIV-1 Subtype C Protease.

Sibusiso B Maseko[a], Eden Padayachee[a], Thavendran Govender[a], Yasien Sayed[b],Glenn EM Maguire[ac], Johnson Lin[d] ,Hendrik G Kruger[a*]

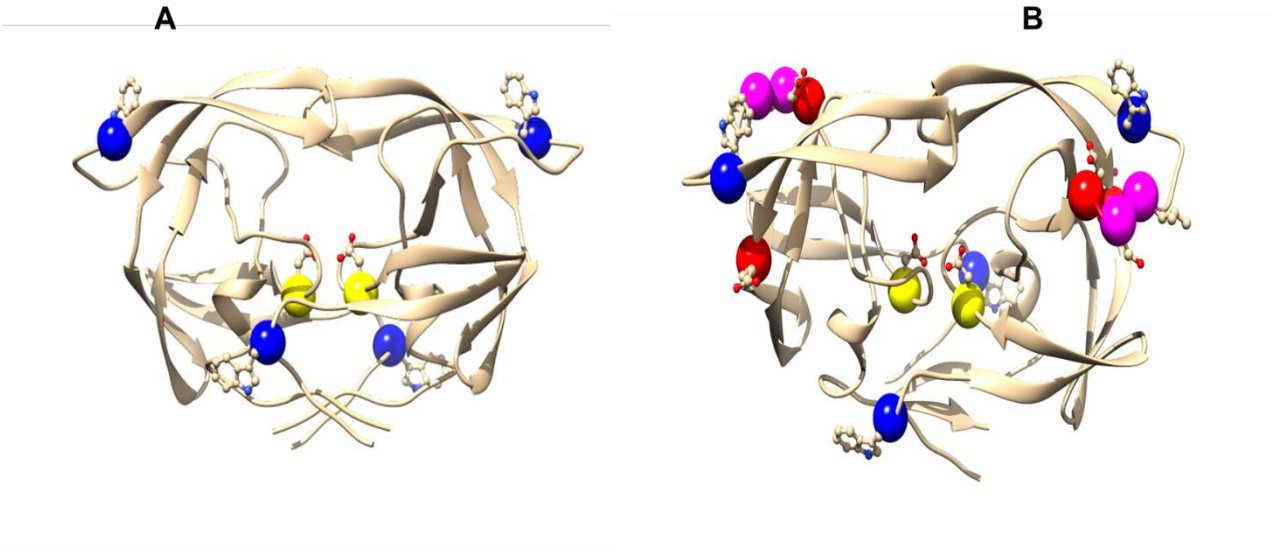

Figure S1. A ribbon representation of the wild type C-SA HIV protease (A) and E35D↑G↑Svariant (B). Shown in yellow is the aspartic residues (Asp 25/25'). The insertions are shown in pink and tryptophan in blue. The red spheres are other amino acid mutations found in this variant protease. The figures were created using UCSF Chimera version 1.9 [1].

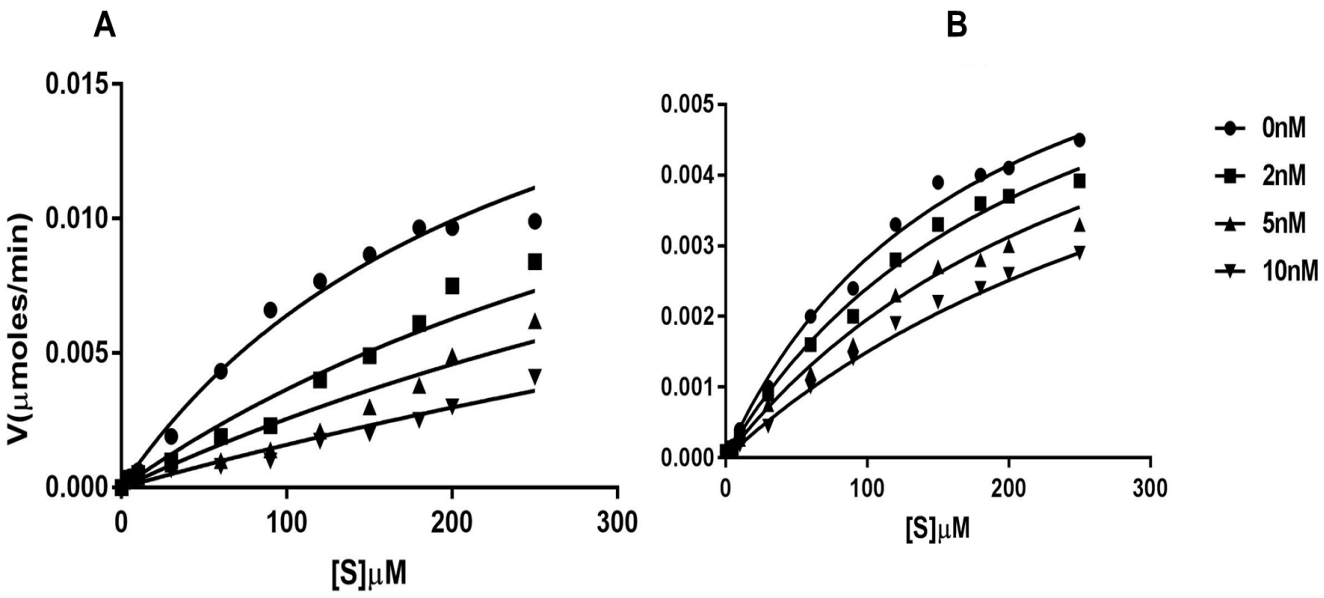

Figure S2: Inhibition (K_i) of the protease activities of wild type[A] and E35D↑G↑S[B] by RTV The reaction mix contained an increasing substrate concentration (0-250 μM); Protease enzyme (50 nM), protease inhibitor (0-10 nM) in a 96-well plate with a total volume of 100 μL (n = 3).

The K_i values were estimated using a competitive inhibition equation (Equation 1) according to Williams et al. [2].

$$V = \frac{\mathbf{Vmax}[S]}{\boldsymbol{K}\mathbf{m}\left(\mathbf{1}+\frac{[\mathbf{I}]}{\boldsymbol{K}\boldsymbol{i}}\right)+[\mathbf{S}]} \qquad \textbf{(Equation S1)}$$

[I] is the inhibitor concentration, K_m is the Michaelis constant, K_i is the inhibition constant, V and V_{max} are the velocity and the maximum velocity of the enzyme, respectively.

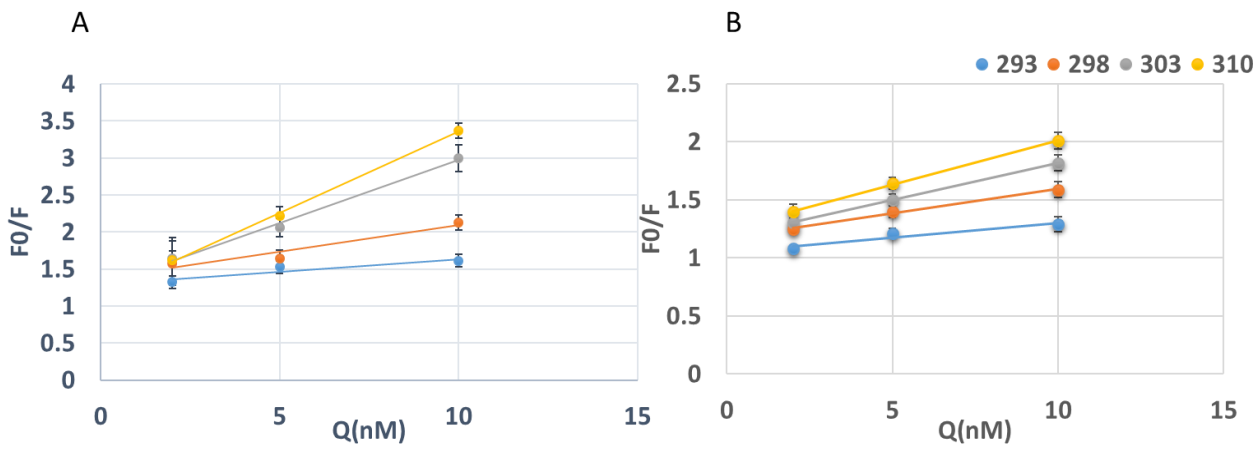

Figure S3: Examples of Stern Volmer plots for fluorescence quenching of WT (A) and the mutant E35D↑G↑Sin 50 mM Sodium Acetate buffer (pH 5) containing NaCl (1M) in a final volume (100 µl) when treated with Ritonavir at different temperatures (n = 3).

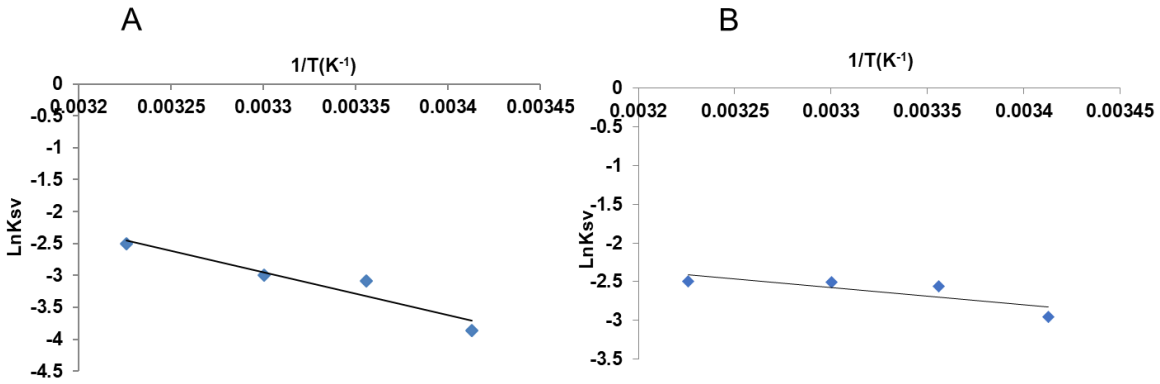

Figure S4: Van't Hoff plots for the determination of thermodynamic data (ΔH and ΔS) for the interaction of the protease inhibitor, Ritonavir with HIV protease at different temperatures. (A) Wild Type (B) Mutant E35D↑G↑S (n = 3).

References

1. Pettersen, E.F., et al., *UCSF Chimera--a visualization system for exploratory research and analysis.* J Comput Chem, 2004. **25**(13): p. 1605-12.
2. Kožíšek, M., et al., *Characterisation of mutated proteinases derived from HIV-positive patients: enzyme activity, vitality and inhibition.* Collection of Czechoslovak chemical communications, 2004. **69**(3): p. 703-714.